UNIVERSITY OF SOUTHAMPTON

The Effect of Nano Size Fillers on Electrical Performance of Epoxy Resin

By

Qi Wang

A thesis submitted for the degree of Doctor of Philosophy

Project Supervisor:

Prof. George Chen

In the
Faculty of Physical and Applied Sciences,
University of Southampton,
United Kingdom.

May 2012

UNIVERSITY OF SOUTHAMPTON

ABSTRACT

FACULTY OF PHYSICAL AND APPLIED SCIENCES
SCHOOL OF ELECTRONICS AND COMPUTER SCIENCE

Doctor of Philosophy

The EFFECT OF NANO SIZE FILLERS ON ELECTRICAL PERFORMANCE OF EPOXY RESIN

By Qi Wang

Epoxy resin is widely used in high voltage apparatus as insulation due to its excellent mechanical, electrical and chemical properties. Fillers are often added to epoxy resin to enhance its mechanical, thermal and chemical properties. With the new development in nanotechnology, it has been widely anticipated that the combination of nanoparticles with traditional resin systems may create nanocomposite materials with enhanced electrical, thermal and mechanical properties. The project aims to improve the overall electrical performance by adding nanoparticles into epoxy resin.

In the present thesis a detailed study on dielectric permittivity, AC breakdown strength and space charge behaviour of epoxy resin/nanocomposites with nano-fillers of SiO_2 and Al_2O_3 has been carried out. The epoxy resin/nanocomposite thin film samples were prepared and tests were carried out to measure their dielectric permittivity and tan delta value in frequency range of 1Hz- 1MHz. The space charge behaviours were also observed by using the pulse electroacoustic (PEA) technique. The influence of filler type, filler size and filler concentration on nanocomposites ac breakdown strength were also examined. In addition, traditional epoxy resin microcomposites were also prepared and tested and the results were compared with those obtained from epoxy resin/nanocomposites.

The present results indicate that the presence of nano-sized fillers enhances the insulation properties of the epoxy resin and the dielectric properties are strongly influenced by the interfacial region between epoxy and nano particles. It is the key factor that affects the electrical performance of epoxy nanocomposites. The multi core model has been applied to explain the effects of such interfacial region on the electrical performance epoxy nanocomposites. A new phenomenon of space charge accumulation at higher nano size filler loading concentration has been observed at a filler loading concentration above 3wt%. This phenomenon is a result of the formation of electrical double layer surrounding the nano particles.

A comparison study between epoxy nanocomposites loaded with both surface treated and non-surface treated nano particles has also been carried out. The results indicate that nano particle dispersion rate is an important factor in determine the electrical performance epoxy nanocomposites. Surface functionalisation on nano size fillers by using silane as a coupling agent could help avoiding the formation of large agglomerations resulting in better insulating performance. In addition, it has also been found that the presence of water inside epoxy nanocomposites also leads to the reduction in dielectric properties due to the formation of water layers surrounding the nano particles. Those water layers could act as a conductive path to help charge carriers travelling through the bulk of the materials.

CONTENT

List of Figures

List of Tables

List of Terminology

3D	Three dimensional
AC	Alternating current
ASTM	American society for testing and materials
BD	Breakdown
CDF	Cumulative distribution function
CFRP	Carbon fibre reinforced plastics
DGEBA	Diglycidyl ether of bisphenol-A type epoxy resin
DSC	Differential scanning calorimetry
EDL	Electrical double layer
ESR	Equivalent series resistance
Free volume	Volume of cage that a given molecule is free to wander
MLE	Maximum likelihood estimation
MQT	Macroscopic quantum tunnelling effect
PD	Partial discharge
PDF	Probability density function
PE	Polyethylene
PEA	Pulse electroacoustic technique
SC	Space charge
SCLC	Space charge limited current
SEM	Scanning electron microscope
Specific surface	Total surface area per unit of mass
Surface atom	Atoms on the surface of particle
TEM	Transmission electron microscopy
Tg	Glass transition temperature
Volume fraction	Volume concentration

Publications

Article：

1) Q. Wang and G. Chen. "*Effect of Nanofillers on the Dielectric Properties of Epoxy Nanocomposites", Advances in Materials Research, An International Journal*, Vol. 1, pp. 93-107, 2012.

2) Q. Wang and G. Chen. "*Effect of Pre-treatment of Nanofillers on the Dielectric Properties of Epoxy Nanocomposites",* Submitted.

Conference Item：

3) Q. Wang, G. Chen and A. S. Alghamdi, "*Influence of Nanofillers on Electrical Characteristics of Epoxy Resins Insulation*" *10th IEEE International Conference on Solid Dielectrics*, 4-9 July 2010, Potsdam, Germany.

4) Q. Wang, P. Curtis and G. Chen, "*Effect of Nano-Fillers on Electrical Breakdown Behavior of Epoxy Resin*" *IEEE Conference on Electrical Insulation and Dielectric Phenomena*, 17-20 October 2010, West Lafayette, Indiana, USA.

5) Q. Wang and G. Chen, "*The Influence of Nano-fillers on the Insulation Properties of Epoxy Resin*" *19th Annual International Conference on Composites or Nano Engineering*, 24-30 July 2011, Shanghai, China.

Acknowledgements

I would like to thank my supervisor, Dr George Chen for his continuous supports, guidance, expertise, ideas and valuable suggestions. He gave endless encouragement and patience with me during the progress of my PhD study.

My special thanks go to my colleagues, Mr. Junwei Zhao for his advice and support through my research. I would also like to give my thanks to Dr Abdulsalam S. Alghamdi for spending hours training me up on preparing thin film epoxy sample used in this project; Dr. Chris Green for showing my how to perform breakdown test with the breakdown kits in HV lab; Nuriziani Hussin for training me up on measuring the dielectric properties of film sample.

I would also like to thanks Mr. Michael Smith, Mr. Brian Rogers and Mr. Neil Palmer in Tony Davies High Voltage Lab for their support through my project.

Finally, I would like to thanks my family for their support and understanding during my studies.

1 Introduction

1.1 Background

Epoxy resin is a thermosetting epoxide polymer that contains two or more epoxide groups. It is one of the most commonly used thermosetting macromolecular synthetic materials. Epoxy resin has properties of excellent adhesiveness, mechanical property, dielectric property and chemical stability [1]. It also has advantages such as low contraction percentage, low cost and easy shaping etc. It is widely used in application areas such as dielectric materials, anti corrosion materials, cementation between metals and non-metals and manufacture of composite materials. Epoxy resin has an important impact on electrical, electronic, mechanical manufacturing, chemical anticorrosion, aerospace, shipping， coating materials and other industrial areas, and becomes one of the essential materials for industrial applications.

In recent years, research on epoxy resin modification has been carried out ceaselessly. In the past, the modification research on epoxy resin was limited with rubber. However, as the research on epoxy resin increases, new methods of epoxy resin modification such as using liquid crystal and nano particles have been introduced. Especially the method of using nano particles to improve the properties of epoxy resin has become a hot spot of epoxy resin modification research in recent years.

In order to widen the application areas of epoxy resin, it is important to improve epoxy resins' properties. Therefore, researchers start to look for new methods of epoxy resin modification. Because of its special structures and properties, nano particles have become one of the most possible choices. In recent years, a large amount of studies have been carried out on the application of nano reinforced technology of epoxy resin and the research has shown that epoxy resins' properties such as thermal property, mechanical property, physical property and dielectric property can be enhanced significantly by

mixing them with a small amount of nano filler (normally 1%-10%). Nano materials have a bright future on reinforcing epoxy resin and it is important to study the influence of nano additives on the electrical performance of resultant epoxy nanocomposites. It is predictable that as the development of nano reinforcement technology and the predictable appearance of low cost nano particles, the epoxy nanocomposites will tend to be industrialisation and commercialisation step by step.

1.2 Motivation

Nanometer is a length unit, which is defined as 10^{-9} meter. Nanotechnology is the technology that studies the properties and applications of materials that have a structure size between 1 and 100 nm. The research about nano material is initially started from areas such as ceramics and metal powder. Nowadays, more and more peoples start to look at the nano technology. Figure 1 shows the summary of journal papers about polymer nanocomposites and epoxy nanocomposites being published in last 10 years. It can be seen that the amount of publications increases rapidly in last few years. This is because nanomaterial has many new physical and chemical properties that many ordinary macroscopic bodies do not have. When materials reach nano-size, they will gain completely different properties comparing with the bulk materials. The key factor is that nano-particles have large specific surface area even under a small loading concentration due to their small size [2, 3]. The interfacial characteristics between nano particles and base polymer materials play an important role in determining the electrical properties due to the presence of such large surface area [4]. Moreover, the changes in morphology due to the large surface area might also affect the trap depth and its density as well. Since the nano size particles have extremely large surface area, it is expected that even polymer materials loaded with a relative small amount of nano fillers lead to a strong effect on dielectric properties of the resultant composites [5, 6]. Consequently, polymer nanocomposites could have unique properties compared with ordinary polymer composites.

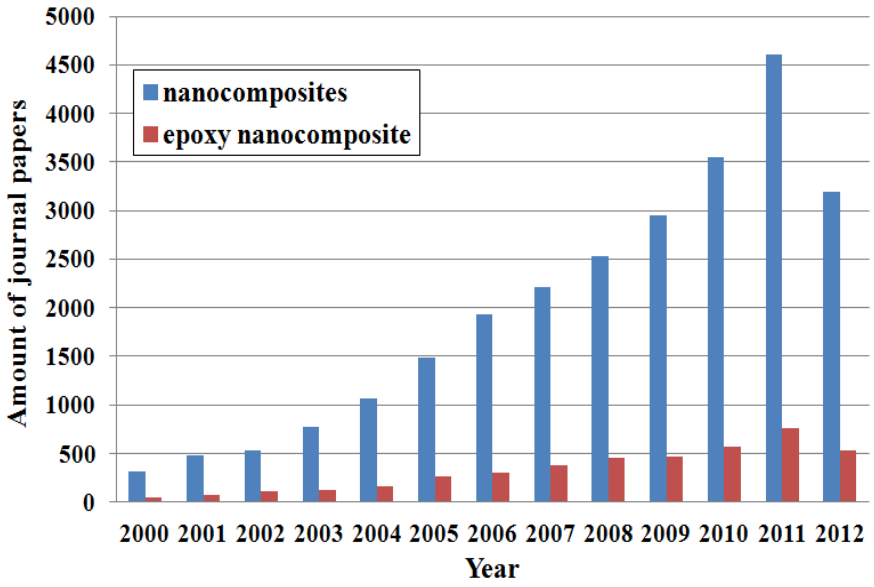

Figure 1 Amount of journal papers published in last 10 years

Although nano reinforced epoxy resin technology have a bright future, It is also need to be aware that, nano reinforced epoxy resin technology is still a relatively young field. Due to the complex structure of nanocomposites and its quantum effect and surface effect, it is difficult to understand the mechanisms that affect nanocomposites' properties. Currently, there are only limited amount of studies in this area. Thus it is important to have a top-down research that examines how the overall properties of nanocomposites can be affected by different kind of nano particles.

1.3 Objectives and Aims

As epoxy resin/nano-composites have shown much improved properties, the subject of epoxy resin modification using nano-scale fillers has become increasingly important. However, the studies about nano-composites are still immature. It is necessary to have a systematic approach. The main objectives of this project are to study how nano-scale fillers influence epoxy resins/nano-composites' dielectric properties, to find out effect of interfacial region between the epoxy resin and nano-scale fillers on the insulating performance of epoxy nanocomposites. In this thesis the effect of inorganic nano particles on the dielectric properties has been studied in term of filler type, filler size and various filler loading concentration. The interfacial characteristic between the epoxy and the nano particles has also been investigated. The diglycidyl ether of

bisphenol-A (DGEBA) epoxy resin (LY556) commonly used in power apparatus was used in this project. Silane was used as a coupling agent to surface treat the nano particles. The epoxy resin nanocomposites thin film samples were prepared and tests were carried out to measure their dielectric permittivity and tan delta value in a frequency range of 1Hz- 1MHz. The space charge behaviours were also observed by using the pulse electroacoustic (PEA) technique. The differential scanning Calorimetry (DSC) measurements were carried out at a ramp rate of 10℃/min. In addition, traditional epoxy resin/microcomposites were also prepared and tested and the test results were compared with those obtained from epoxy resin/nanocomposites. By investigating the interfacial condition between epoxy matrix and nano particles, it is hoped that not only a comprehensive study of the effects of inorganic nano size particles on the result epoxy nanocomposites can be provided, but also give important information about how to engineer the dielectric properties of epoxy resin to the desirable characteristics in industrial applications.

1.4 Contribution of the Thesis

This project contributes to the scientific research in the field of epoxy nanocomposite insulation. In this project, the following contributions have been made:

1) A detailed study on the dielectric properties of epoxy nanocomposites loaded with different concentration of nano size fillers has been carried out. The effect of inorganic nano particles on the dielectric properties has been studied in term of filler type, filler size and various filler loading concentration.

2) Space charge properties in epoxy nanocomposite thin film were successfully studied. The influence of nano size filler on the space charge accumulation has also been discussed. The presence of nano size filler will reduce the amount of total charge in general. However, a new phenomenon of space charge accumulation at higher nano size filler loading concentration has been observed where space charge begins to

accumulate in the middle of material bulk rather than near the electrodes after the nano size filler loading concentration increases to a certain value.

3) The role of interfacial area between epoxy matrix and inorganic nano particles has been discussed. The experiment results indicate that those interfacial areas are the key factor that affects the electrical performance of epoxy nanocomposites. The experiment results show that the interfacial area has a significant effect on the dielectric properties of epoxy nanocomposites. The multi core model has been used to explain the effects of interfacial region on the dielectric properties and the space charge accumulation observed in epoxy nanocomposites.

4) A comparison study between epoxy nanocomposites loaded with both surface treated and non-surface treated nano particles has also been carried out to give a better understanding on the effects of interfacial regions on the dielectric properties of epoxy nanocomposites.

5) The effect of water absorption on the dielectric properties of epoxy nanocomposites has also been investigated. The result indicates that a water layer may form surrounding the nano particles and the presence of such water layer has a negative effect on the dielectric properties of epoxy nanocomposites.

1.5 Outline of the Thesis

This thesis concentrates on the measurement and analysis of the influence of nano size additives on the dielectric properties of epoxy resin. It has been divided into the following chapters. Chapter 2 gives a brief introduction about the epoxy resin and polymer nanocomposites. The importance of filler dispersion and surface treatment technology is also discussed in this chapter. In addition, the interfacial characteristic and the models used to explain the

insulating performance of polymer nanocomposites are also introduced. Chapter 3 describes the epoxy nanocomposite sample manufacturing technology together with the dielectric spectroscopy, AC breakdown, space charge measurement and DSC technology. In chapter 4, a brief on epoxy nanocomposite sample characterization using SEM and DSC has been performed and the results are present in this chapter. A brief background of dielectric permittivity is given in chapter 5 and the detailed measurement results of dielectric permittivity and tan delta value using dielectric spectroscopy are presented. The effect of nano size filler on the dielectric permittivity of resulting nanocomposites has been examined and discussed. Chapter 6 contains the AC breakdown measurement results of epoxy nanocomposites loaded with different concentration of nano size fillers. The space charge measurement technique is described in chapter 7. The pulsed electric acoustic (PEA) method is used to measure the space charge accumulation inside the thin film sample and the measurement results are presented and discussed. In chapter 8, the effects of surface treatment on nano particles and the influence of water absorption on resulting epoxy nanocomposites has been examed. DSC, dielectric spectroscopy, AC breakdown and space charge measurement results are presented and discussed. Chapter 9 gives a brief conclusion of this project and some further directions are also suggested.

2 Literature Review

2.1 The Concept of Epoxy Resin

Epoxy resin belongs to the epoxy oligomer class. It is able to react with a curing agent or hardener to form a three-dimensional net structure thermosetting plastic. Various properties over a wide range at an acceptable cost could be achieved depend on the type of epoxy and hardener used. The epoxy resin has excellent adhesion, chemical and heat resistance, mechanical properties and insulating properties. It is also possible to improve epoxy resins' properties by choosing different epoxy oligomer and hardener or suitable modification method. Therefore it has become one of the most popular thermosetting resins in industrial applications.

2.1.1 Definitions and Classification of Epoxy Resin

Rings formed by two carbon atoms and one oxygen atom are called epoxy or epoxy group (as shown in figure 2). A compound that contains such rings is called epoxide. The simplest epoxide compound is ethylene epoxide. Ethylene epoxide is able to form thermosetting polyethylene oxide through ionic polymerization. Such polyethylene oxide is known as epoxy resin.

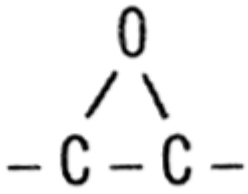

Figure 2 Illustration diagram of epoxy group

Epoxy resin is the collective name for compounds that contain two or more epoxy groups in its molecules and is able to form three-dimensional net structure solidifying under suitable chemical reagent [7]. In order to distinguish from their solidified products, sometimes epoxy resins are also called epoxy

oligomer as their molecular weight belongs to oligomer. The main characteristic of epoxy resins' chemical structure is that there are epoxy groups within epoxy resins' molecular chain. However, by using different raw materials and synthesis methods, the resulting epoxy resins are different. Thus those epoxy resins can be applied to variety of situation with different properties requirements.

Epoxy resins can be divided into glycidyl epoxy resins and non-glycidyl epoxy resins, according to their synthesis methods. The glycidyl epoxy resins are formed by a condensation reaction of appropriate dihydroxy compound, dibasic acid or a diamine and epichlorohydrin, whereas the non-glycidyl epoxy resins are prepared by peroxidation of olefinic double bond. According to the synthesis methods, glcidyl ether resin, glycidyl ester resin and glycidyl amine resin belong to glycidyl resins, whereas alicyclic epoxy resin and aliphatic epoxy resin are classified into non-glycidyl epoxy resins.

Moreover, glycidyl ether epoxy resin can be further divided into dyiglycidyl ether of bisphenol-A (DGEBA) and novolac epoxy resin. Both of DGEBA and novolac epoxy resins are the most commonly used resins in industrial applications. DGEBA epoxy resins are produced from reactions between epichlorohydrin and bisphenol-A. The property of molecular structure of this epoxy resin is that the molecular chain contains active epoxy groups. Because there are active epoxy groups in the molecular chain, the epoxy resin is able to have cross linking reactions with hardeners to form 3D crosslinked polymer net. The molecular structure of bisphenol-A type epoxy resin and 3D crosslinked polymer net formed from reactions between epoxy resin and hardeners are shown in figures 3 and 4:

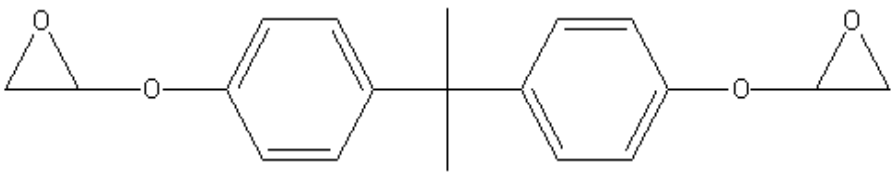

Figure 3 Molecular structure of bisphenol-A type epoxy resin

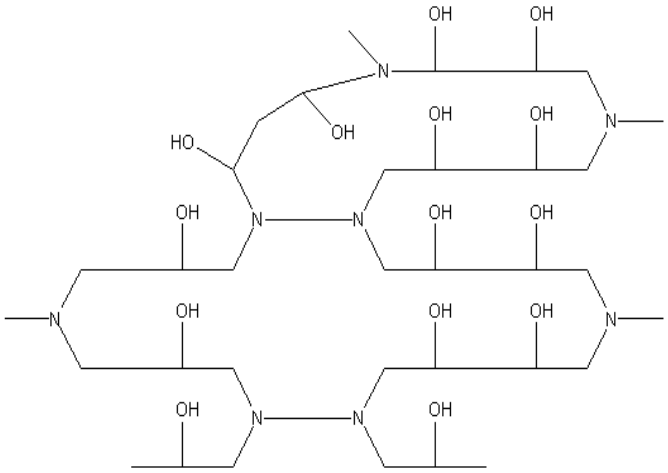

Figure 4 3D crosslinked polymer net

Novolac epoxy resins are formed under a reaction between phenolic novolac resin and epichlorohydrin. The molecular structure of novolac epoxy resins is shown in figure 5. Comparing with DGEBA, novolac epoxy resins contain more than two epoxy groups in its molecular structure. Thus its curing products have larger cross linking density, better thermal stability, mechanical properties, dielectric properties, and water and corrosion resistance. As a result they are widely used to make microelectronic moulding compounds.

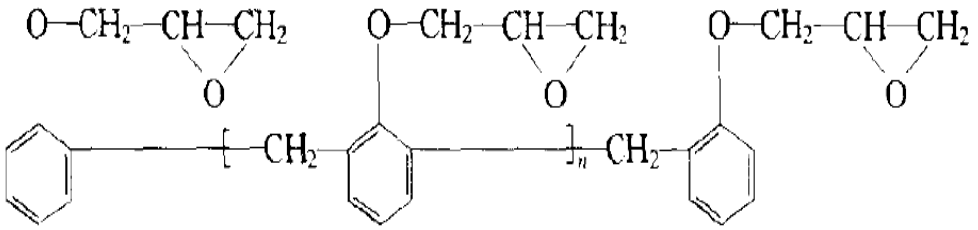

Figure 5 Molecular structures of novolac epoxy resins

Glycidyl ester resins have better dielectric properties and weather resistance. Their viscosity is normally lower than other epoxy resins. Glycidyl ester resins are more adhesive than other epoxy resins, thus their condensates have better mechanical properties. Moreover, they also have good resistance to very low temperature, which means that their adhesive strength is still higher than other epoxy resins at very low temperature.

Glycidyl amine resins, on the other hand, have high epoxide equivalent, big cross-linking density and higher thermal resistance. Thus they have been used to manufacture carbon fibre reinforced plastics (CFRP).

Alicyclic epoxy resins are prepared by epoxidation of alicyclic alkene's double bond, and their molecular structure has a large difference comparing with DGEBA and other epoxy resins [1]. This is because DGEBA and other epoxy resins' epoxy group are directly connected on their alicyclic ring, whereas alicyclic epoxy resins' epoxy groups are connected on aliphatic hydrocarbon or benzene nucleus. Alicyclic epoxy resins' curing products have high compressive and tensile strength. Moreover, the alicyclic epoxy resin could remain good mechanical properties at high temperature for long term.

2.1.2 Curing of Epoxy Resin

The epoxy resins before curing are only a sticky liquid and do not have any practical values. It needs to be cured into a three dimensional cross linking network structure before being put into use. Such curing process is a reaction between the epoxy group and the curing agent (also called hardener). The reaction between epoxy groups and hardeners is able to form a three dimensional cross linking network structure and therefore the epoxy resin is able to cure into solid materials which are firm and infusible.

Epoxy resins are always easily cured under certain circumstance and curing agent. Most of the epoxy resins, for example, bisphenol-A type epoxy resin, have strong temperature stabilities. The bisphenol-A type epoxy resin is able to remain unchanged even at 200 ^{o}C. However, epoxy resins have a strong reactivity as well. Thus they are able to react under certain curing agents. However, different epoxy resins have different curing requirements. Some epoxy resins are able to cure under low temperature or room temperature, whereas others need to cure under high temperature. To some extent, the resulting curing products' properties are also being influenced by the curing agent.

As the curing agent is able to influence epoxy resins' properties significantly, it is also necessary to consider the curing agents used. There are many types of curing agent, so it is necessary to choose those curing agents according to the epoxy resins' properties and curing process requirements. For example, some of the hardeners are able to react with epoxy resin under room temperature quickly, whereas most of the hardeners require higher temperature and longer times. The glass state temperature (Tg) and curing kinetics are also decided by the hardeners. It is also necessary to add accelerant to reduce the curing temperatures.

Hardeners can be generally divided into addition polymerization type hardener and catalytic type hardener. The addition polymerization type hardener is able to cause the addition polymerization reaction with the epoxy groups inside the epoxy resin. Because all compounds containing two or more active hydrogens that can be used as addition polymerization type hardener, the amount of hardener type is large. As the hardener itself will react with epoxy groups during addition polymerization reaction to form the three dimensional cross linking network structures, the amount of hardeners used is also important. If the amount of hardener added is not enough, there will be un-reacted epoxy groups inside the curing products, which will affect the resulting products' properties. For addition polymerization type hardener, it is also necessary to consider the amount to use during the curing process. Catalytic type hardener, on the other hand, only offers positive or negative ion during the addition polymerization process of the epoxy groups. Thus the amount of catalytic type hardener used only affects the addition polymerization reaction's speed. The resulting curing products' properties are not affected by its amount. The addition polymerization type hardener includes polyamine based hardeners, anhydride based hardeners, polyphenol based hardeners and polythiol based hardeners. Polyamine base hardeners and anhydride based hardeners are the most commonly used hardeners for epoxy resin curing. Especially polyamine based hardeners hold 71% of total hardener. Catalytic type hardener is also divided into positive ion type and negative ion type.

There is a huge difference for hardeners in term of curing temperature. Generally speaking, hardeners with higher curing temperatures always cause the curing product having better thermal resistance. For addition polymerization type hardeners, the curing products using anhydride type hardener generally have higher thermal resistance than the curing products using polyamine based hardeners.

The curing temperature is also one of the important parameters that need to be considered when selecting hardeners. Because the curing process is a kind of chemical reaction, the increase in curing temperature will also increase the reaction speed and reduce the time taken for curing. However, it is also necessary to notice that if the curing temperature is too high, the epoxy resin may be heated unevenly. The resulting curing products' cross linking density will become asymmetric as well, which may reduce the resultant products' properties. Therefore, it is necessary to consider the curing temperature's up limit during the curing process and make a balance between the curing time and resulting curing products' overall properties.

2.1.3 Epoxy Microcomposites

Epoxy resins' properties can also be improved by adding fillers. In order to gain good modification results, it is important to consider the adhesiveness between epoxy resin and fillers when using fillers to modify epoxy resin. It is also a good idea to surface treat the fillers with coupling agent to improve its adhesiveness. By using surface treated silicon fillers, the resulting dielectric properties of epoxy microcomposites improve significantly. Sometimes the use of single fillers may result in worsening epoxy resins' curing products' dielectric properties. For examples, when using aluminium hydroxide fillers to improve epoxy resins' mechanical properties, the resulting curing products' dielectric properties are reduced at the same time. Thus, in order to gain a satisfied result, it is important to choose fillers according to the specific requirements. Silica and alumina fillers are commonly used fillers. Silica has better insulation properties, good dielectric properties and low thermal

expansion coefficient. It is commonly used as filler within high voltage applications. On the other hand, alumina filler is able to improve materials' mechanical properties, dielectric properties, hardness and thermal resistance. The researches on epoxy microcomposites also show that as the amount of fillers increases, materials' arc resistance increases sharply. The fillers' size also influences materials' arc resistance as well. Z. Yu has studied the application of natural powder quartz in epoxy encapsulation materials [8]. The results show that after adding fillers, the epoxy encapsulation materials' breakdown strength increases. The maximum increase in breakdown strength has been observed at a filler loading concentration of 3wt% and the rate of increases is around 10%. Further increasing the filler loading concentration will lead to a reduction in breakdown strength.

2.2 The Concept of Nanocomposites

When materials reach nano size, the properties of materials change. Those materials always have unique optical, mechanical, thermal, magnetic and electrical properties which are different from ordinary materials. Those materials are known as nano materials. In 1984, German scientist H. Gleiter successfully produced nano size metal powders. Following this the nanometer sized materials were also introduced [9]. Because of their extremely different properties comparing with the ordinary materials, nanometer size materials and nano structures have become the most attractive area in the advanced materials researches.

In recent years, as the development of nano technology, researchers try using nano size fillers to modify epoxy resins. The nano particle reinforced epoxy resins show huge improvements on their properties due to the unique characters of nano size fillers [10, 11]. Currently people believe that the improvements of epoxy resins' properties are the result of nano size particles' surface effect, quantum size effect and macroscopic quantum tunnelling effect (MQT) [2, 3]. Because of the high viscidity of epoxy resin, it is hard to mix nano size fillers uniformly into epoxy resins. So it is also necessary to consider the manufacture process.

The word “nanocomposites” is put forward by Roy and Komarneni in 1984 [12]. The definition of nanocomposites is shown below [13]:

> *“A nanocomposite can be defined as a multiphase solid material where one of the phases has one, two or three dimensions of less than 100 nanometers (nm), or structures having nano-scale repeat distances between the different phases that make up the material”*

Because the inorganic nano particles have large surface area, the interface area between the inorganic nano particles and polymers is large as well. The interface stresses will reduce significantly. As a result, the problem of unmatched thermal expansion coefficient of inorganic nano particles and polymer base material has been solved. Thus it is easy to make full use of the excellent mechanical properties and heat resistance property of the inorganic nano particles and the flexibility and process ability of the polymer. The physical properties of polymer/inorganic nanocomposites are much better than the ordinary composites. In recent years, studies on nanocomposites also achieved significant results [14, 15].

The surface areas of spherical particles are proportionately to the square of particles’ diameter. The particles’ volume is proportionately to the cube of diameter. The specific surface of particle is inversely proportional to the particle’s diameter, as shown in figure 6(a). Thus the specific surface will increase as the diameter of particle decreases. Particles that contain high percentage of surface atom have quite high activity and extremely unstable. Such particles will tend to show some unique characteristics. For particles with average diameter larger than 0.1mm, the surface effect is negligible. However, for particles with average diameter less than 0.1mm, it is important to consider the surface effect.

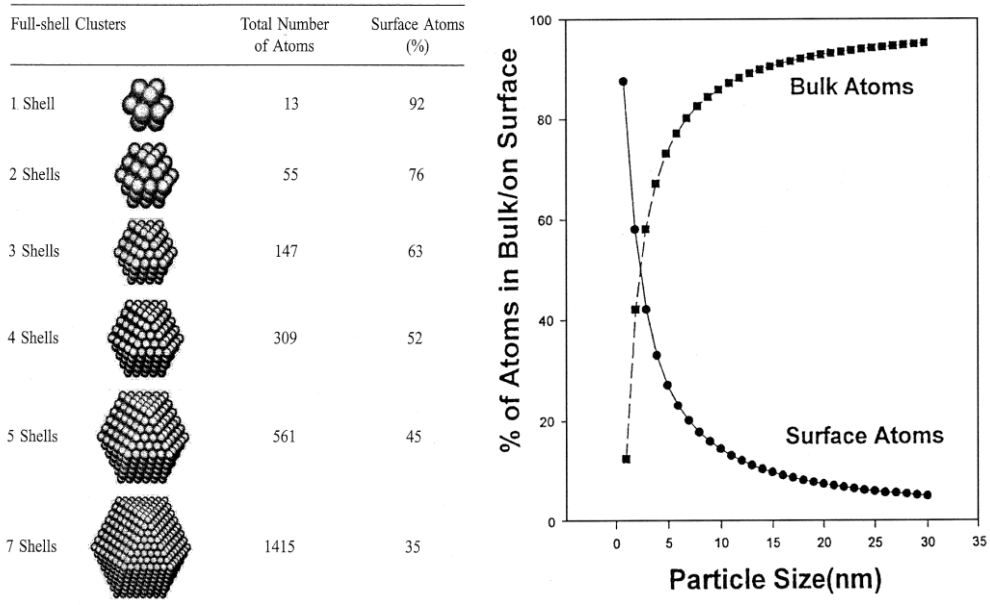

(a) (b)

Figure 6 Large specific surface areas of nano particles [16]

For nanocomposites, as the size of particle decreases to nano scale, the percentage of surface atom increases sharply. For example, for nano particles which have a diameter of 10nm, the percentage of surface atom is 20%. When the particles' diameter reduces to 1nm, the percentage of surface atom will increase to 99%, as shown in figure 6(b). At this stage, almost all atoms of the particle are distributed at the surface of the particle. Those surface atoms are highly instauration and easy to combine with other atoms. Consequently the nano material will show high chemical activity. In conclusion, as the diameter of particle decreases, the nano materials' surface area, surface energy and surface binding energy increase sharply.

2.3 Particle Dispersion and Surface Treatment

2.3.1 Particle Dispersion

When the nano size fillers are dispersed into the epoxy resin to form composites, the nano particles tend to agglomerated with each other as a result of the interactions between nano particles. Poor dispersion was frequently observed in epoxy nanocomposites. The result epoxy nanocomposites tend to lose their unique characteristics as a result of agglomeration of nano particles.

Thus it is a great challenge to achieve a uniform and stable dispersion of nano particles in the base resin. The Van der Waals force and the columbic force between nano particles are part of the reasons to form the agglomeration. Such agglomerations caused by the interaction force can be dispersed under mechanical forces and chemical reactions. The presence of chemical bounds could also lead to particle agglomerations. To help producing polymer nanocomposites with consistent and high qualities, it is necessary to understand the factors that influence the particle dispersion in base resin.

The interaction forces between nano size particles are the key factors that affect the formation of nano agglomerations. When dispersing nano particles into base resin, the nano particles tend to move randomly due to the collision between particles and epoxy matrix. There is a possibility for particles to collision with each other during Brownian motion. It is known that the electrons from different nano particles start moving to avoid collision with each other. Therefore the charge density in the nano particles is non-uniformly distributed along the particles. The formation of such molecules is known as the instantaneous dipoles. Under the effect of Van der Waals force, those instantaneous dipoles tend to attract with each other. As a result, nano particles tend to agglomerate together to form large size particles. The columbic force, which is also known as the electrostatic force, on the other hand, could act as a repulsion force. When the nano particles are placed in liquid medium, the surface of nano particles could be charged as a result of surface group dissociation or charge adsorption. The charged particles will attract charges with opposites sign from the surrounding. The region that surrounds the surface of charge is known as the electrical double layer (EDL), as shown in figure 7 [4]. The interactions between those EDL will act as a repulsion force between nano particles. The combination effect of both the Van der Waals attraction force and the columbic repulsion force which depends on the distance between nano particles is the key factor that determines the stabilization of nano particle dispersion.

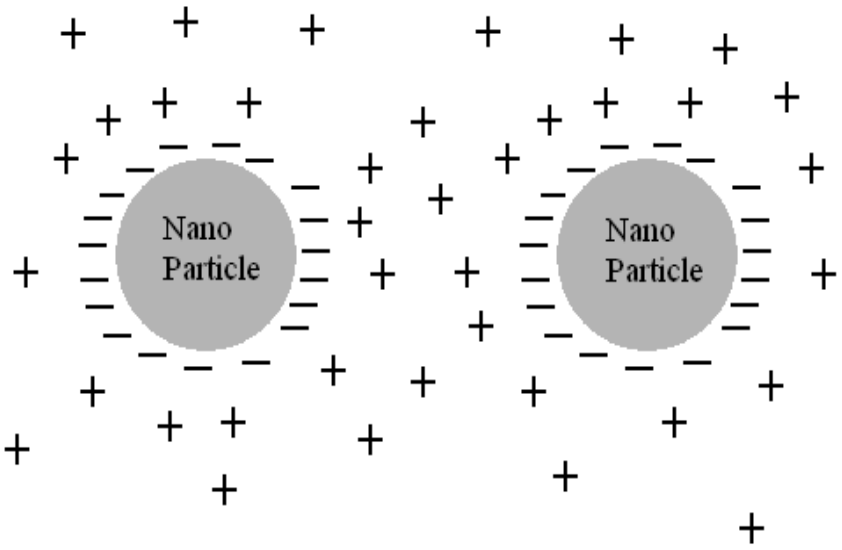

Figure 7 Electrical double layer between nano particles

The interactions between nano particles and polymer matrix could also result in agglomeration of fillers. As discussed in chapter 2.2, the percentage of surface atom increases sharply as the size of nano particle decreases. Such increase in surface atom will result in properties changes, known as the surface effect of nano particles. The presence of such high percentage of surface atoms leads to high surface energy. When the nano particles are dispersed into epoxy resin, the resulting composites could be treated as a non-solvent system that contains a low ionic concentration. So the columbic repulsion force is weak due to this low ionic concentration. Those surface atoms are more likely to interact with other atoms to form agglomerations. Moreover, for epoxy nanocomposites, interfacial regions are formed when the nano particles are dispersed into epoxy. The interfacial region is a short region surrounds the surface of the particles that contains epoxy matrix and harder molecular. As the size of nano particle is only about tens of nanometers. The inter-particle distance between particles is small, especially at higher loading concentrations, it is also necessary to consider the effect of interfacial region on nano particle dispersion. A uniform dispersion could be achieved if the interaction force between nano particles and the polymer matrix are strong enough. The dispersion has a strong influence on the insulating

performance of epoxy nanocomposites. In order to obtain good insulating properties, a strongly interfacial interaction between nano particles and polymer matrix is required. However, the compatibility between nano particles and polymer matrix is not good enough due to the large surface area of nano particles that surround with silanol group. Instead of the polymer matrix, the nano particles are more likely to attract with each other through hydrogen bonding to form aggregations. As a result of such agglomerations, the epoxy nanocomposites exhibit a reduction in insulating properties.

2.3.2 Surface Treatment with Silane Solution

To obtain better particle dispersion, different methods based on mechanical and chemical methods have been developed to solve the agglomeration of nano particles. The mechanical methods aim to break the interaction force between nano particle agglomerations and modify the surface structure of nano particles by applying mechanical stress. The most frequently and simply used mechanical methods are high speed mixture method and ultrasonic dispersion method. Especially the ultrasonic dispersion method becomes more popular in recent years. By applying the ultrasonic waves to the mixture, the agglomeration of nano particles could be broken and a uniform dispersion of nano particles can be obtained. However, it is also necessary to notice that the surface activity of nano particles could be increased due to the high energy of ultrasonic wave. Long time ultrasonic wave leads to a high possibility of collision between nano particles and results in the formation of new agglomerations.

The surface treatment on nano particles is another way to achieve better particle dispersion in polymer nanocomposites. The surface treatment with silane as a coupling agent is the most popular chemical method to modify the surface structure of nano SiO_2 and Al_2O_3 particles and it is widely used in nowadays. The silane coupling agent contains functional groups that could react with both inorganic fillers and organic polymer matrix. The silane coupling agent normally contains two types of groups, as shown in figure 8.

Silanol molecule chains are able to form oligomer structures and form hydrogen bonds to the surface of inorganic nano size fillers. Moreover, additional condensation reactions will also occur between the coupling agent, silanol groups and the surface hydroxyls of inorganic fillers. Further condensation and dehydration reactions can also be obtained by drying the nano fillers after surface treatment with silane. The inorganic nano size fillers with organic functional groups that attach to their surface by strong chemical bounds can be finally obtained, as shown in figure 9 [18].

Figure 8 Chemical structure of silane coupling agent [121]

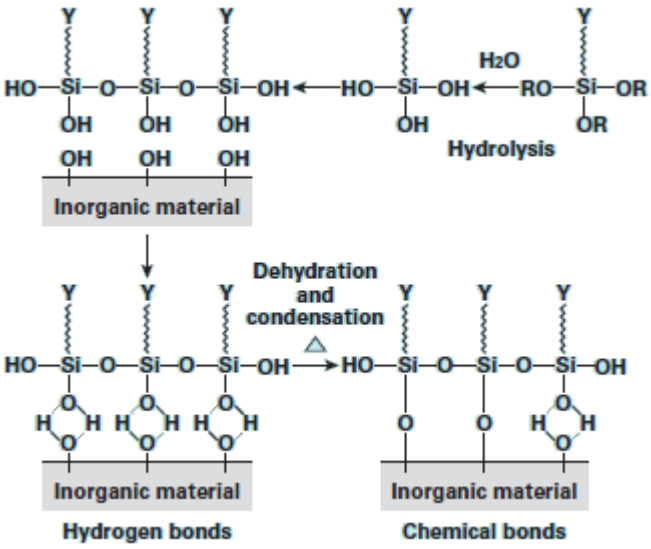

Figure 9 Mechanism of silane surface treatment [121]

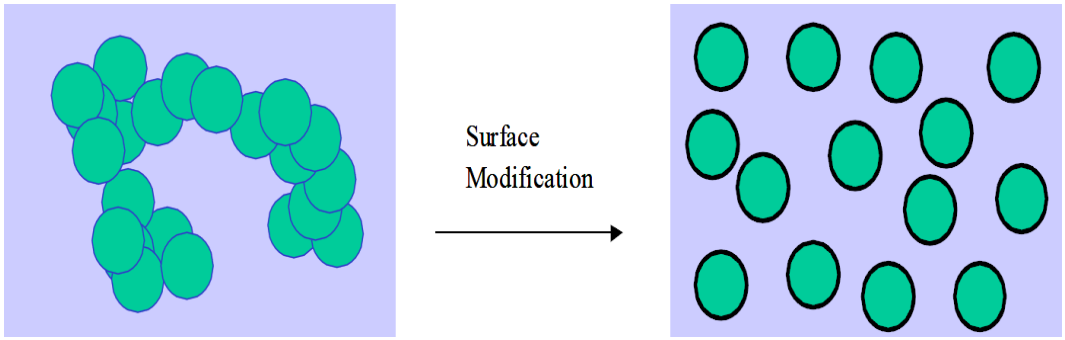

Figure 10 The dispersion of nano particles before and after silane surface treatment [20]

The compatibility between nano particles with silane surface treatment and polymer matrix is better compared with the nano particles without silane surface treatment. The presences of hydrogen bonds increase the surface tension of inorganic nano particles [17], a more uniform dispersion of nano particles in the epoxy nanocomposites can be achieved, as illustrated in figure 10. Recent studies show that the nano particle dispersion has strong effects on the insulating behaviours of resulting polymer nanocomposites. The dielectric properties of polymer nanocomposites could be enhanced by surface treatment methods [18, 19] as the use of coupling agent will result in an increase in interfacial interactions. There are many factors which may affect the effectiveness of surface treatment, such as the type of coupling agent chosen, the coupling agent concentration, the time used for treatment and the dispersion method. In order to obtain a better dispersion, the process of surface treatment also needs to be taken into consideration [20].

2.4 Interfacial Characteristic

2.4.1 Inter-particle Distance and Surface Area

As discussed in chapter 2.2, the enhancement of insulating properties in polymer nanocomposites is mainly due to the increases in specific surface area or the decrease in inter-particle distance. In polymer nanocomposites, by assuming that the spherical nano particles are uniformly dispersed in the base

material, the inter-particle distance between any two nano particles is proportional to the particle diameter and the surface area is inversely proportional to the particle diameter. Both of the inter-particle distance and the surface area have been calculated using the equation given by Tanaka et al [21].

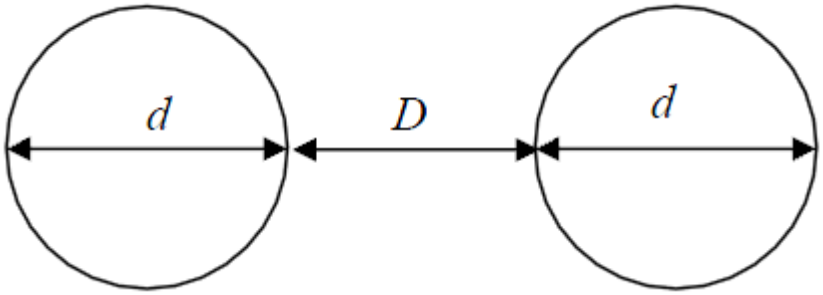

Figure 11 Schematic diagram for inter-particle distance and surface area calculation

The inter-particle distance D as a function of particle diameter d is described as

$$D = [\left(\frac{\pi\sqrt{2}}{6V_f}\right)^{\frac{1}{3}} - 1]d \quad (1)$$

Where V_f is the volume fraction of the nano particles in the base material. The surface area per unit volume S of the particles is shown as

$$S = 6V_f/d \quad (2)$$

The above two formula can also be expressed based on the weight percentage of the nano particles, as shown below

$$D = [\{\frac{\pi}{6}(\frac{\rho_n}{\rho_m})\frac{100}{wt\%}[1 - \frac{wt\%}{100}(1 - \frac{\rho_m}{\rho_n})]\}^{\frac{1}{3}} - 1]d \quad (3)$$

$$s = \frac{\pi d^2}{(D+d)^3} = \pi(\frac{d}{D+d})^2\frac{1}{D+d} \quad (4)$$

Where ρ_m and ρ_n are the specific gravity for the polymer matrix and the nano particles respectively. Base on the equations above, the inter-particle distance and the surface area of nano particles can be worked out. For a typical epoxy nanocomposite that contains 5wt% nano particles with a diameter of 40nm, the inter-particle distance is 46.7nm and the surface area per unit volume is 10.8 km^2/m^3. In comparison, the inter-particle distance between 100 μm particles is 117 μm and the surface area per unit volume is 0.0043 km^2/m^3. It can be seen that the nano particles have extremely large surface area. It is necessary to consider the influence of interfacial region between nano particles and polymer

matrix on the dielectric properties of nanocomposites as the area of interfacial region is associated with the surface area of nano particle.

When the nano particles are dispersed into polymer materials, the nano particles tends to be in equilibrate with each other in the polymer nanocomposites as an effect of the interaction forces, as discussed in section 2.3. Those forces are essentially constant with each particle although they might vary with the inter-particle distance between particles [14, 22]. The surrounding area of nano particles is increasingly modified by the nano particles. Those surrounding areas that have different force compared with the base polymer materials are defined as the interface between nano particles and the polymer matrix. The interface regions have different mechanical, chemical, thermal and insulating properties compared with the bulk materials and have a great influence on the overall properties of the polymer nanocomposites [23]. Moreover, particles with smaller size tend to have thicker interface region resulting in a greater effect on the resulting nanocomposites. As discussed in section 2.2. The specific surface area of particles increases sharply as the diameter of these particles reduces to a sufficient low value. The high specific surface area results in a large interface region and high surface defects.

In polymer nanocomposites, if the nano particles are uniformly dispersed in the base polymer materials, the inter-particle distance tends to be distributed according to the Poisson distribution [24]. In this case, for spherical nano particles uniformly distribute in polymer materials, the probability for the interface region surrounding a nano particle to overlap with another nearby interface region can be given by the following equation

$$P = 1 - exp\{-\frac{2t}{d}\} \quad (5)$$

Where P is the probability of overlapping, t is the thickness of interface region and d is the inter-particle distance. For a given filler loading concentration, the probability of interface overlapping as a function of interface thickness over inter-particle distance is shown in figure 12. Thus for nano particles with an average inter-particle distance of 40nm, there is a 50% possibility for its

interface region to overlap with a nearby interface if the thickness of interface is 14nm.

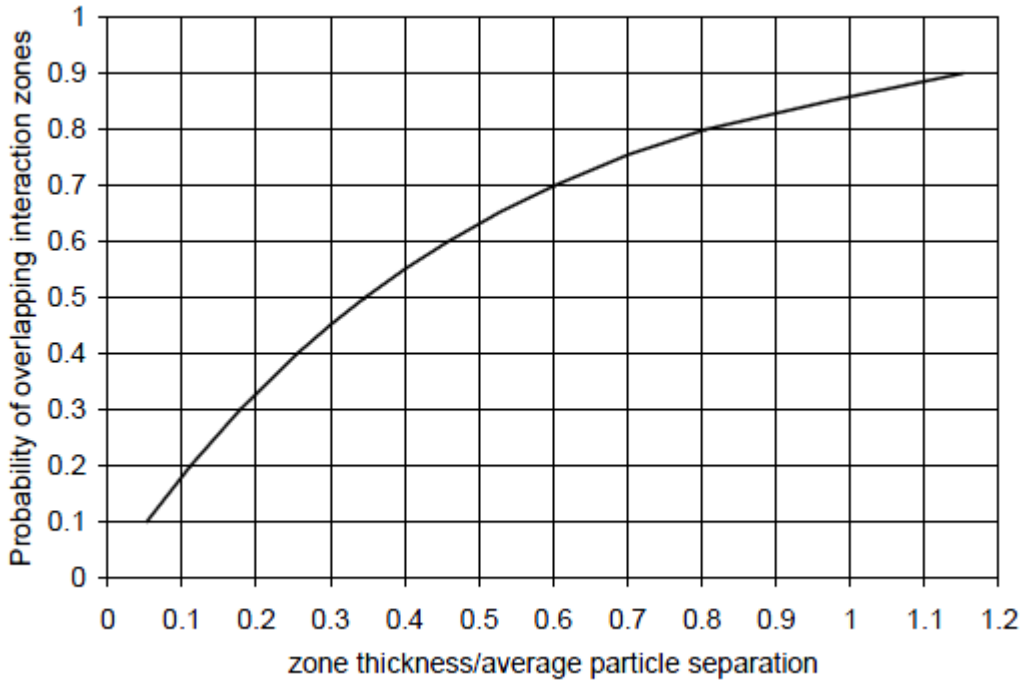

Figure 12 Probability of interface region overlapping [24]

2.4.2 Models for Polymer Nanocomposites

2.4.2.1 Dual Layer Model

As the interfacial region has properties that differ from both nano particles and the polymer matrix due to the interaction between the two phases, a dual layer model has been proposed by Tsagarapoulos et al [25] to help understanding the behaviors of polymer nanocomposites. A schematic diagram of the dual layer model is shown in figure 13. In this model the interfacial area between nano particles and the polymer matrix has been divided into two different layers [25, 26]. The inner layer that surrounds the surface of nano particles is assumed to be a tightly bound layer where the polymer chains are tightly bounded to the surface of nano particles and those polymer chains are highly restricted. There is also another layer that surrounds the inner layer where the polymer chains are loosely bound. The outer layer is named as loosely bound layer and the

thickness of this layer is slightly greater than the tightly bound layer. The polymer chains tend to have higher mobility in the loosely bound layer. It is also easier for charge carriers to move in the loosely layer.

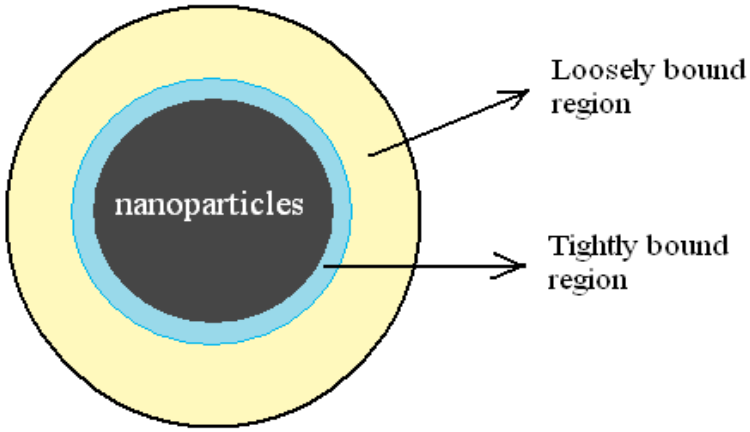

Figure 13 Schematic diagram of dual layer model

2.4.2.1 Multi-core Model

Base on the idea discussed by Lewis [4], Tanaka has proposed a multi-core model, as illustrated in figure 14. In this model, it is assumed the spherical nano particles are uniformly distributed in the base polymer materials, the interface area between nano particles and polymer matrix can be classified into three different layers [21]. The first layer which is closest to the surface of nano particles is a bonded layer that tightly bound to both the surface of nano particles and polymer by coupling agents such as silane. The second layer is a bound layer that contains polymer chains which are strongly bound to the first layer and the nano particle surface. This bound layer is more tightly bound compared with the base polymer matrix. The third layer is a loose layer that is loosely bound to the second layer. Because of the surface tension effect, the loose layer has high free volume compared with the base polymer matrix. Moreover, an electric double layer, which is also known as the Gouy-Chapman diffuse layer, is also formed in the interface region. As the effect of this electric double layer, the charge carriers with opposite sign are diffused outward from the interface region to the Debye shielding length.

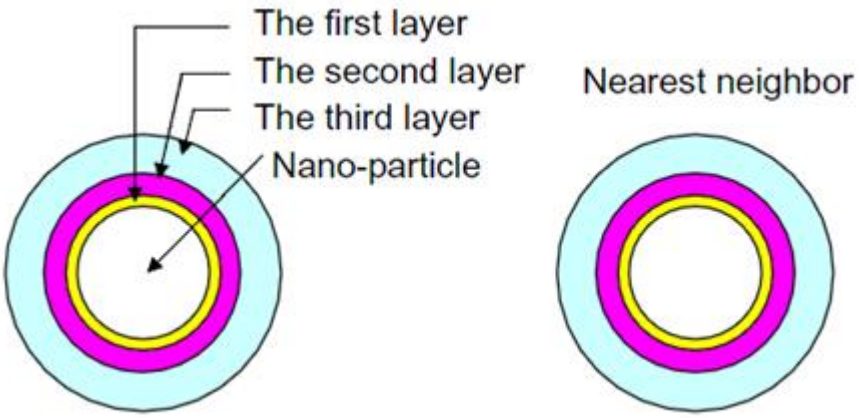

Figure 14 Schematic diagram of multi-core model [21]

The multi-core model can provide an understanding of many dielectric phenomena observed in polymer nanocomposites. Generally speaking, the bound layer and the loose layer are the main regions that affect the dielectric performance of the polymer nanocomposites. The presence of both bonded layer and the bound layer is believed to restrict the mobility of polymer chains and leads to an increase in permittivity and the glass transition temperature etc. On the other hand, the third layer with large free volume is responsible for the reduction in both permittivity and the glass transition temperature. The increase in mobility observed in some studies is also believed to be due to the presence of shallower traps in the loose layer.

3 Experiment Procedure

3.1 Materials

The materials used in this project are Bisphenol-A type epoxy resin (araldite LY556) along with methyl tetrahydrophthalic anhydride hardener (aradur HY917) and accelerator (DY070) supplied by Huntsman Advanced Materials. The resin was selected because of its excellent mechanical, dynamic and thermal properties along with low room temperature viscosity. Moreover, it also has good chemical resistance, especially to acids at temperature up to 80℃. Thus this practical system is widely used by electric power industries. The product data of araldite LY556, hardener HY917 and accelerator DY070 are shown in table 1, table 2 and table 3 below:

Bisphenol A epoxy resin			
Colour	Clear, pale yellow liquid		
Density at 25℃	ISO 1675		
Viscosity at 25℃	DIN 53015	g/cm^3	1.15－1.20
Epoxy content	ISO 3001	mPa s	10000－12000

Table 1 Product data for araldite LY556

Anhydride curing agent			
Colour	Clear liquid		
Density at 25℃	ISO 1675		
Viscosity at 25℃	DIN 53015	g/cm^3	1.20－1.25

Table 2 Product data for hardener HY917

Heterocyclic amine			
Colour	Clear liquid		
Density at 25℃	ISO 1675	g/cm^3	0.95－1.05
Viscosity at 25℃	DIN 53015	mPa s	≦50

Table 3 Product data for accelerator DY070

3.2 Sample Preparation

The epoxy resin system of araldite LY556 with hardener HY917 and accelerator DY070 is a low-viscosity, solvent-free system based on the Bisphenol-A epoxy resin and an anhydride curing agent. The content reactivity is able to be adapted to suit the processing and curing conditions by varying the DY070 accelerator. This resin system is especially suitable for wet filament winding, pultrusion and resin transfer moulding as its low room temperature viscosity and long pot life. It also shows good fibre impregnation properties and is easy to process. The cured system exhibits excellent mechanical, dynamic and thermal properties and good chemical resistance. The mix ratio of this epoxy resin system is shown in table 4 below:

	Parts by weight (pbw)	Parts by volume (pbv)
Araldite LY556	100	100
Hardener HY917	90	86
Accelerator DY070	0.5-2	0.6-2.4

Table 4 Mix ratio of epoxy resin system

3.2.1 Surface Treatment of Nano Particles

To improve the nano particle dispersion, 3-glycidoxypropyltrimethoxysilane was used as a coupling agent. The surface treatment of SiO_2 nano particles with silance coupling agent has been carried out by using method which is reported by Ash [55]. The detail process is listed below:

1) Nano SiO_2 particles (5g) are dispersed into 100ml ethanol solution by using ultrasonic mixing method for 1 hour.
2) A mixture solution that contains 95% ethanol and 5%of water is adjusted to a pH value between 4.5 and 5.5 by using acetic acid.
3) 50ml of Silane solution is added into the mixture solution by magnetic stirring for 15 minutes.
4) The mixture solution is then added into the ethanol solution that contains nano SiO_2 particles to form silanol group.
5) The mixture is then mixed for another 48 hours to wet the particles with silanol group.
6) The mixture is then separated by using a centrifuge.
7) The particles is washed in hexane solution and then separated by using a centrifuge.
8) Repeat step 7 twice and the nano particles with surface treatment can be observed.

3.2.2 Preparation of Epoxy Nanocomposites

The mould used for preparing epoxy resin composites film was initially designed by Dr. Steve Dodd from the University of Leicester. This practical design of the mould was, according to his experience on how to prepare good epoxy resin samples, an efficient way to prepare samples. This mould contains two metal plates, one flexible plastic plate and one rigid plastic plate. Both the shape of upper and lower plates is shown in figure 15. There are two slots on both sides of the upper plates. The slots are used for fill epoxy resin before they are injected into the mould. Before preparing samples, a plastic film with the middle part cut away also needs to be prepared. The plastic film is positioned between the two plates (as shown in figure 16) and the two plates will be tightened by screws. The thickness of resulting epoxy resin film is equal to the thickness of the plastic film. The mould release agent QZ13 is used as a release agent to help release the resulting sample from the mould.

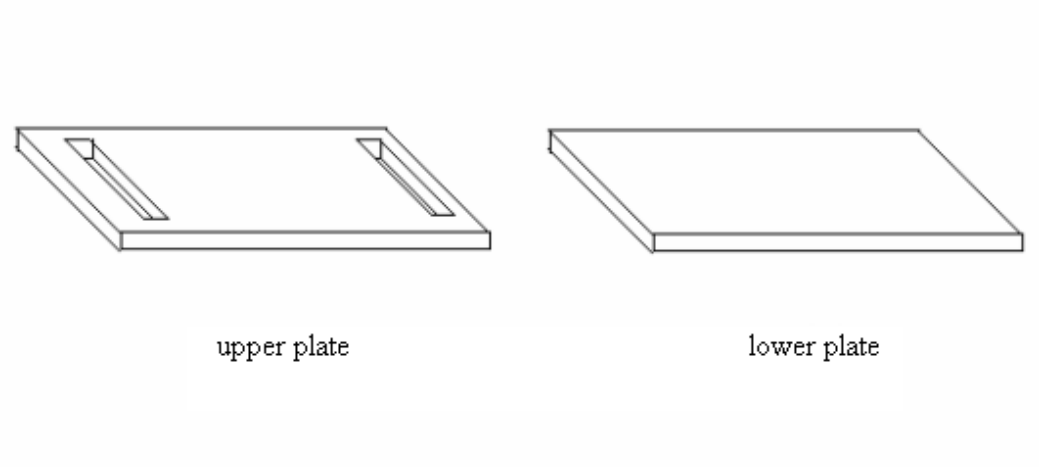

Figure 15 Plate-mould

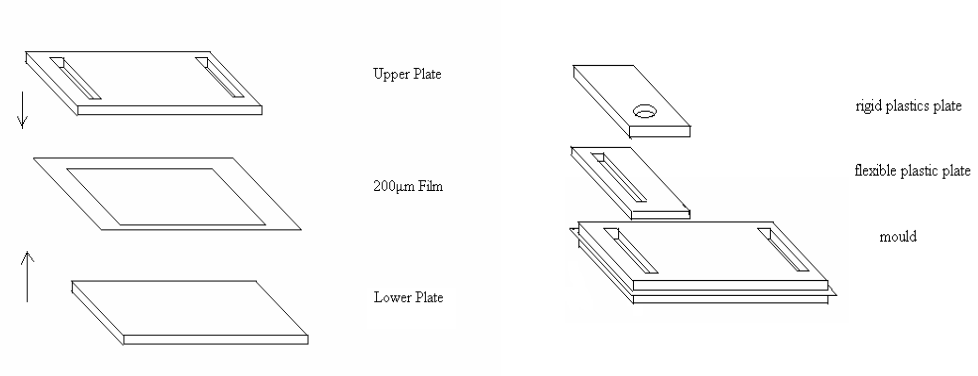

Figure 16 Mould

The fillers that will be tested within this project include micro silicon fillers, nano size silicon dioxide and aluminum oxide. Based on the methods described in the literature review chapter, the heat blending method has been selected to prepare the epoxy resin sample. The detail process is listed below:

1) The epoxy resin is pre-heated to 40°C to reduce its viscosity.
2) Appropriate amount of epoxy resin and hardener is degassed separately by using vacuum oven (10^3Pa, 40°C) for half an hour. The amount of epoxy resin and hardener used follows the mixing ratio of this epoxy resin system shown in table 4.
3) The resin, hardener, accelerator and fillers (both micro and nano) are then mixed together by using magnetic stirring (600rpm, 40°C) for 1 hour.
4) In case of nano size fillers, the mixture solution is then further mixed by using ultrasonic for another half an hour at 40°C.
5) The mixture solution is degassed again by using vacuum oven (10^3Pa, 40°C) for another 10 minutes.
6) The mixture solution is then filled into one of the slots in the mould.
7) The flexible plastic plate and rigid plastic plate will be positioned on the top of the mould respectively as shown in figure 16.
8) The nitrogen gas is then applied to the mould through the hole on rigid plastic plate to press the mixture solution flow through the inner space between two metal plates of the mould.
9) The mould is then placed in an oven at 80°C for 4 hours.
10) Then increase the temperature inside oven to 120°C and wait for another 8 hours.
11) Release the sample form mould and it is ready for use.

3.3 Sample Coding

As the amount of samples used in this project is large, it is necessary to code the samples with different numbers to help reading. The base epoxy resin used in this project can be abbreviated as EP. The nano Al_2O_3 filler can be abbreviated as A, followed by a number which represented the filler loading

concentration. For example, the epoxy nanocomposites loaded with 0.3wt% and 3wt of nano Al_2O_3 fillers can be then abbreviated as EPA03 and EPA3 instead. As both nano SiO_2 filler with an average diameter of 20nm and 80nm have been used in this project, they can be abbreviated as 2S and 8S respectively. Moreover, T and S are used to represent the nano particles with surface treatment and saturated epoxy nanocomposite samples. Some examples of sample coding are shown in table 5.

Sample code	**Type of particle**	**Size of particle**	**Particle wt%**	**Surface treatment**	**Water absorption condition**
EP0	-	-	-	-	Dried
EP2S1	SiO_2	20nm	1	N	Dried
EP8S5	SiO_2	80nm	5	N	Dried
EPA03	Al_2O_3	30nm	0.3	N	Dried
EPA3	Al_2O_3	30nm	3	N	Dried
T-EP2S1	SiO_2	20nm	1	Y	Dried
S-EP2S1	SiO_2	20nm	1	N	Saturated

Table 5 Example of sample coding

3.4 Dielectric Properties Measurements

Epoxy resin are widely used as dielectric materials, it is necessary to study its dielectric properties when investigating the epoxy resin/nanocomposites' properties. In this section, the techniques that are used to measure dielectric permittivity, space charge performance and breakdown strength of epoxy resin/nanocomposites will be introduced.

3.4.1 Dielectric Spectroscopy Measurement

3.4.1.1 Dielectric Polarization Principles

The dielectric spectroscopy measurement is the method to measure the materials' dielectric properties as a function of frequency [27, 28], the applied

electric filed and temperature also can be variables in the measurements. The dielectric spectroscopy is based upon the interaction of the electric dipole moments within the sample and the applied filed, and provides the dielectric properties of materials, such as relative permittivity and loss factor. By testing the sample's dielectric properties, the information about mobility of polymers can be provided. Researches on dielectric spectroscopy measurement have been widely carried out to study material structure. A schematic diagram for dielectric spectroscopy measurement is shown in figure 17 below.

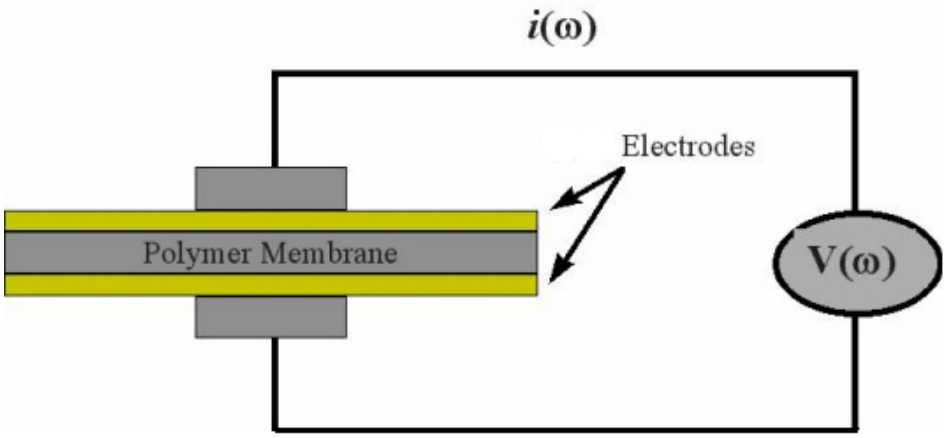

Figure 17 Schematic diagram for dielectric spectroscopy measurement

A SI 1260 impedance/Gain-phase analyzer with solarton 1296 dielectric interface was used to perform the dielectric spectroscopy measurements (as shown in figure 18). Both the permittivity and tan delta values of the epoxy resin composites' dielectric permittivity over a range of 0.1Hz to 1MHz were measured. The sample was cut into circle with 25mm in diameter and the thickness of the sample was 200μm. The applied voltage was set to 1V and the resulting relative permittivity and its loss characteristics (tanδ value) are measured.

Figure 18 Dielectric spectroscopy measurement kits

3.4.1.3 Gold Coating

In order to increase the surface conductance, the thin film samples was coated with gold before dielectric spectroscopy. For dielectric spectroscopy, both side of samples need to be coated. Figure 19 shows the schematic diagram of gold coater.

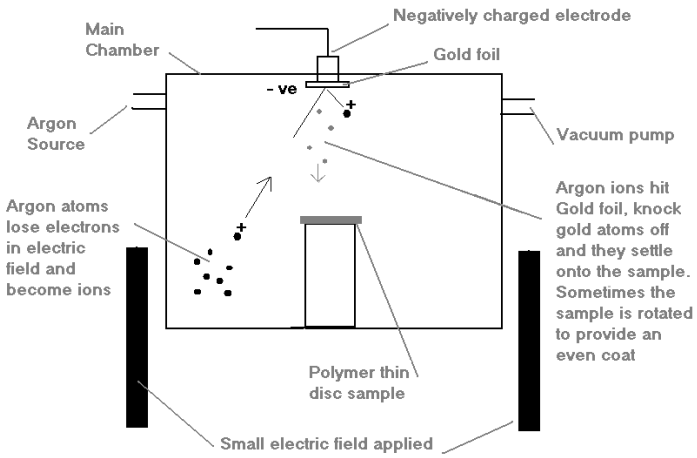

Figure 19 Schematic diagram of gold coater

Before coating, the film epoxy sample is placed into the coater and held by a columnar holder. Then the gold coater is sealed and vacuumized. The argon gas is injected into the gold coater and the negative charges are injected from

the top electrode which is above the sample. Then a small electric field is applied across the gold coater. As the presence of the electric field across the coater, positive ions are generated due to the ionization of argon atoms inside the coater. Those positive ions are then moved towards the negative electrode, with an accelerated speed due to the applied field, knocking gold atoms off from the gold foil. The gold atoms are then injected and deposited on the surface of the sample. An example of gold coated sample and the samples prepared for this project are shown in figure 20.

Figure 20 Example gold coated sample

The Emitech K550X sputter coater is used to coat the sample films. K550X sputter coater is designed to coat the sample for SEM microscopy. But it can be also used for coating in case of the dielectric properties measurements. A guide for the deposition rate of the K550X sputter coater when using gold has been given in the user manual as shown in figure 21

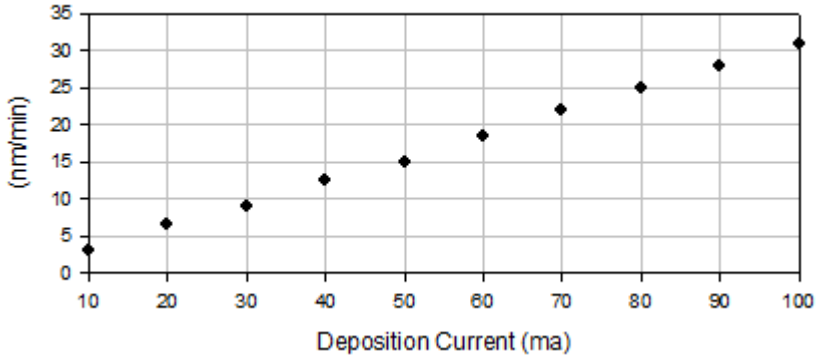

Figure 21 Deposition rate given in manual

A previous measurement test for coating with varies of current and time setting and the corresponding surface resistance has been carried out by Dr. Reading to decide the time and current setting that is used for the gold coating the result is list in table 6 below [29]

Sample	Time /mins	Current /mA	Resistance /Ohms
A	2	20	27.2
B	2	30	14.9
C	2	40	11.1
D	2.5	20	12.7
E	2.5	30	7.4 *
F	2.5	40	6 *
G	3	20	11
H	3	30	7.8 *
I	3	40	5.3 *
J	3.5	20	10.7
K	3.5	30	6.1 *
L	3.5	40	5.3 *
M	4	20	7.5 *
N	4	30	4.9 *
O	4	40	4.3 *

* = sample is of acceptable resistance

Table 6. Test gold coat samples, varying time and current

It can be seen from the table above that the thickness of gold layer will increase as the applied time and current increase resulting in a reduction in surface resistance. It is believed that the values in the middle range of allowance should be chosen for both time and current. 3 minutes and 30 mA have been selected for this study which will give a resistance of around 7.8 ohms.

3.4.2 Space Charge Measurement

3.4.2.1 Pulse Electroacoustic Technique (PEA)

PEA is used to measure the space charge distribution and displacement in the samples [30]. The idea of PEA measurement is to apply a short pulse voltage

across the sample and therefore observe its charge distribution. Its basic principle is given in figure22.

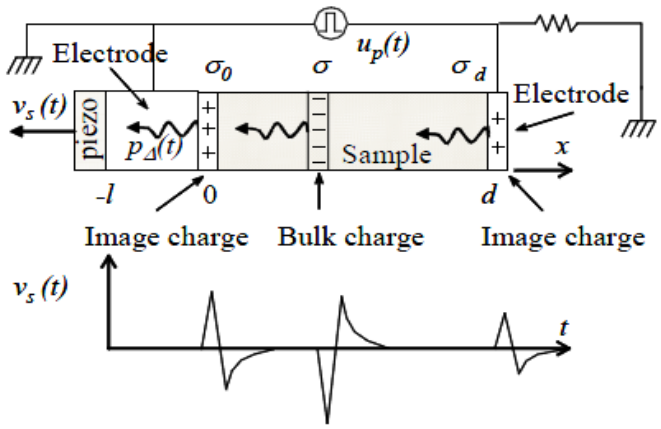

Figure 22 Principle of PEA method [30]

In PEA measurements, the dielectric sample is placed between two electrodes. Because of the difference in the acoustic impedance between the electrode and samples and to fill the gap between sample and electrode, silicone oil has been applied to the surface of both electrodes to avoid the formation of acoustical interface between the electrode and samples. Then a short pulse voltage *Up(t)* is applied to the sample to produce an electric field impulse. The pulse voltage will cause the space charge inside the sample (if there is any) to experience a pulse force which travels between the two electrodes, resulting in a displacement under the Coulomb force.

$$\vec{F} = q\vec{E} \qquad (6)$$

The acoustic wave with amplitude proportional to the local charge density inside the sample will be able to be detected by a piezoelectric sensor which is positioned under the other electrode. The piezoelectric sensor will transform the acoustic wave into electric signals. The signal will be transferred and recorded in an oscilloscope as a function of time. Figures 23 and 24 shows the schematic diagram of PEA system for film sample and the PEA system used in this project respectively. Figure 25 shows a calibrated result of PEA system.

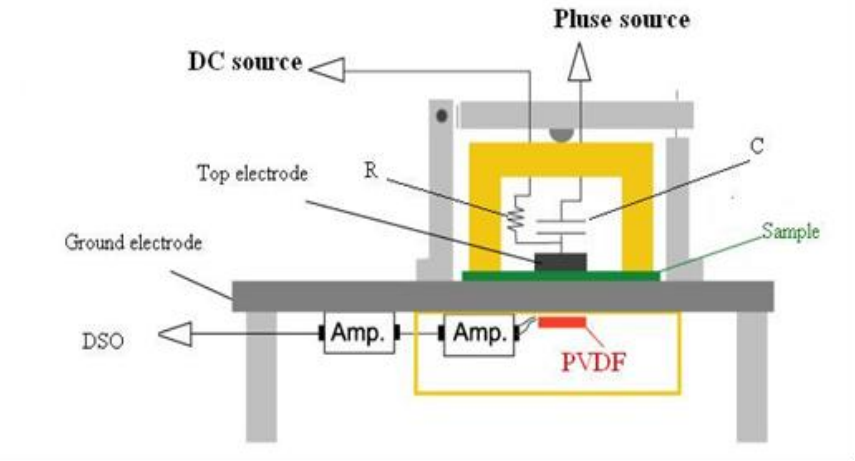

Figure 23 Pulsed electro-acoustic (PEA) system for film sample

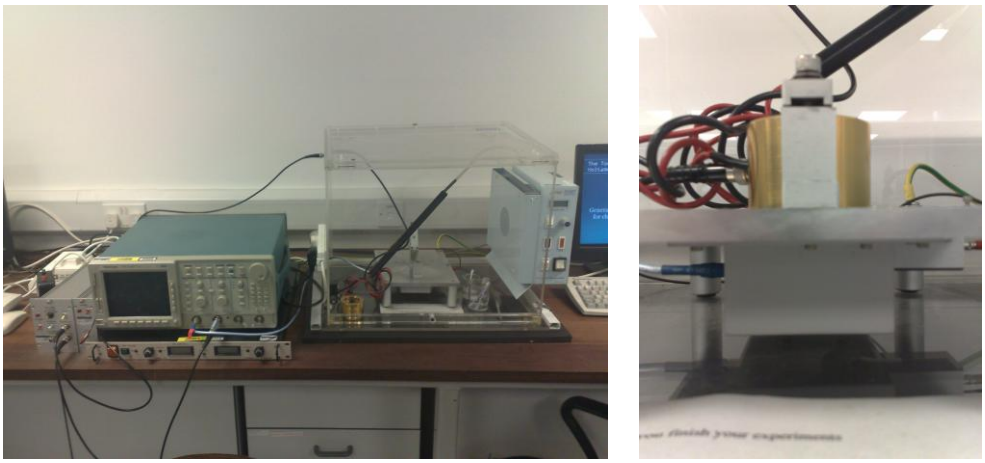

Figure 24 PEA system used in this project

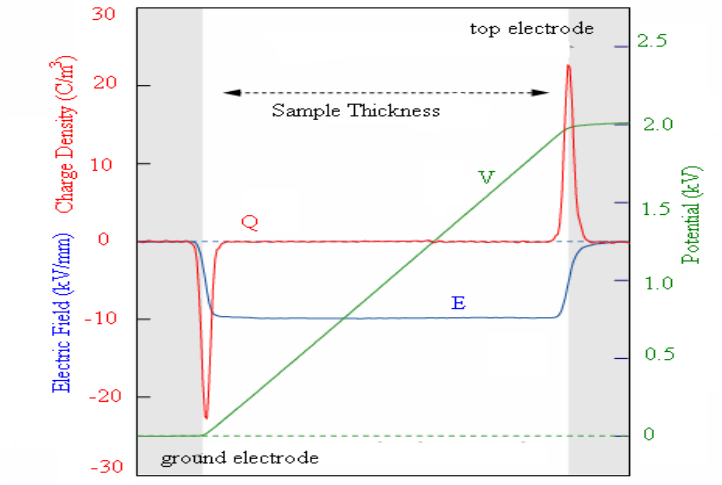

Figure 25 A calibrated result of PEA

For ideal samples, there should be no charges inside the sample. However, the PEA signal of the sample is not always zero as a result of the system response after the pulse voltage is applied to the sample. Therefore, it is necessary to remove the influence of system response on the measurement results. The calibration of the PEA signal can be done by taking reference measurements.

In order to investigate how the presence of inorganic filler influences the base resins' space charge behaviours, the space charge measurements will focus on the ionisation of impurities (both micro and nano size fillers in this project) inside base resin. Other mechanisms are ignored as all the other variables such as temperature, electrodes used and the applied voltage remain constant.

3.4.3 AC Breakdown

3.4.3.1 Experimental Set-up

The breakdown strength of epoxy resin is an important factor for the industrial applications. It is necessary to study how the presence of nano filler influences the epoxy resin/nanocomposites' breakdown strength. The AC breakdown test was performed with a purpose-built kit based on ASTM standard D149-87. The schematic diagram of this kit is shown in figure 26. The breakdown kits used in this project is also shown in figure 27. The ramp testing method has been used to test the breakdown strength of epoxy samples. The process is simply applying a linearly increased voltage to the tested sample, until the breakdown occurs. With this purpose-built kit, both of the breakdown voltage, V_{bd}, and time taken for breakdown to happen can be recorded down. The breakdown strength, E, of the epoxy resin film can be work out with the following function:

$$E = V_{bd}/d \qquad (7)$$

where d is the sample thickness.

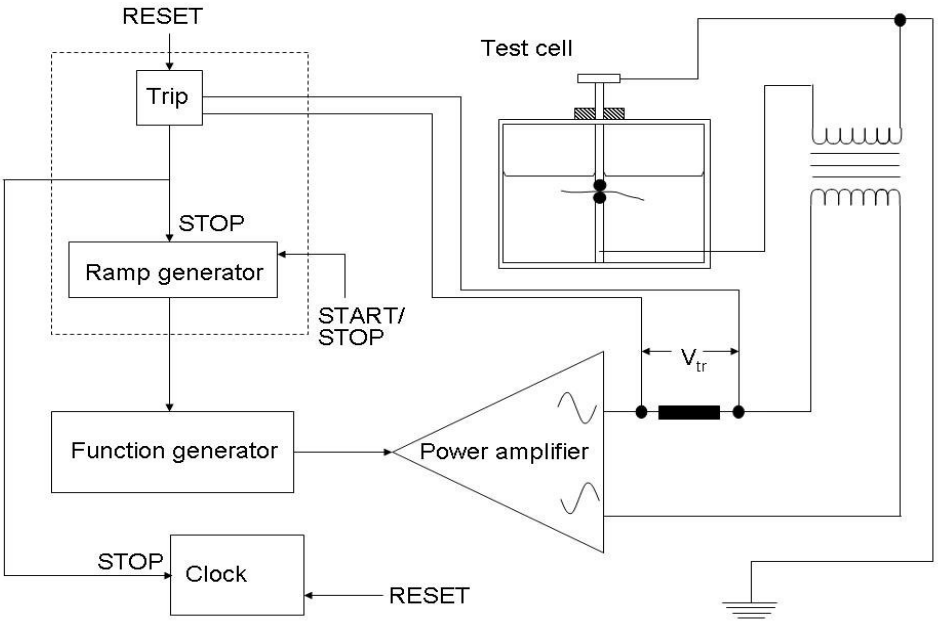

Figure 26 Schematic diagram of AC dielectric breakdown kit

Figure 27 AC dielectric breakdown kit used in this project

Due to the upper limit of the kit, samples with 200μm thickness cannot breakdown. Thinner samples have to be produced. The 100μm epoxy resin film has been used in the test. It needs to be noticed that the thickness of each sample film needs to be measured before the breakdown test as epoxy sample films may have a small difference in thickness. The sample film is immersed in silicone oil, with two steel ball bearings with a diameter of 0.25cm at each side. It has been found that about 15 breakdown will cause pitting on electrodes. During the test, the ball bearings were changed after every 10 breakdown tests.

In this project, the investigations about epoxy resin/nanocomposites' breakdown strength are mainly focused on how inorganic nano size fillers and space charge behaviours affect the breakdown strength. The experiment temperature is set to room temperature so the effect of temperature on the dielectric breakdown strength can be ignored.

3.4.3.2 Weibull Distribution

During the test process, a ramp increasing voltage is applied to the sample with the breakdown voltage, *V*, and time to breakdown, *t*, are recorded. Then the average breakdown strength can be worked out. Therefore, the Weibull 7++ software package (Supplied by Reliasoft) has been used to analyse the results. The Weibull distribution is a continuous probability distribution that is used to describe breakdown distribution. It was firstly introduced by Weibull in 1951. It is the most commonly used probability distribution in breakdown studies due to its flexibility. It is also the IEEE recommends standard probability distribution.

The Weibull distribution allows either one, two or three parameters being used to describe the breakdown distribution [31, 32]. The previous studies by C. Green show that the one parameter Weibull is unable to approaching the experimental date accurately. Three parameter Weibull, on the other hand, introduces one more extra parameter but does not show big improvements, compared with two parameter Weibull [33]. The two parameter Weibull has the best overall performance and it is also widely used in analysing breakdown date. In this project, two parameter Weibull is selected to analyse the breakdown results. The equation of two parameter Weibull is shown as:

$$P_f(x) = 1 - \exp\left[-\frac{(x - x_t)}{\alpha}\right]^{\beta} \tag{8}$$

Where $P_f(x)$ is the cumulative probability of failure at time *x*, x_t is a threshold time, which means that before time x_t, no failures can occur. Both α and β are

known as location (the average of *x*) and shape parameters (describe the separation of result data) respectively.

To help understanding the probability distributions, both the probability density function (PDF) and the cumulative distribution function (CDF) can be used when analysing life data. Example plot graphs of both PDF [34] and CDF [33, 35] functions of Weibull (2-Parameter) with location parameter λ=1 and various shape parameter k are shown in figures 28 and 29 respectively. The PDF is used to describe the probability of breakdown occurs at a certain value, whereas the CDF is used to describe probability of breakdown occurs before a certain value.

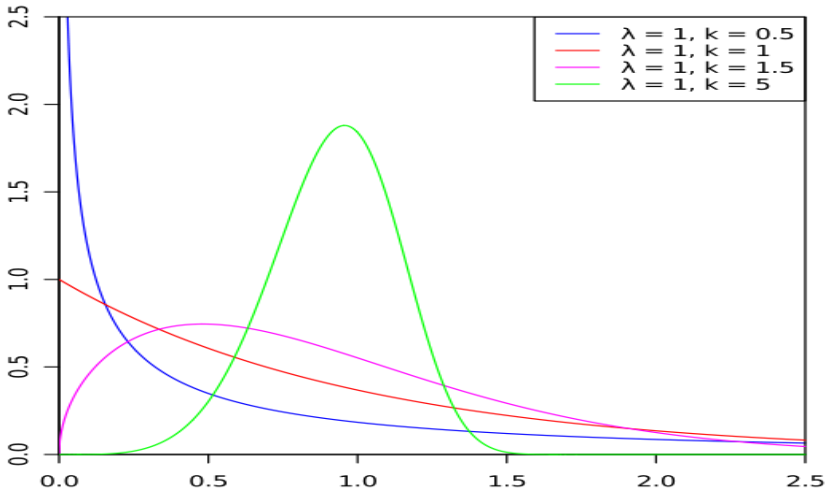

Figure 28 Probability density function of Weibull (2-Parameter) with the location parameter λ=1 and different shape parameter k

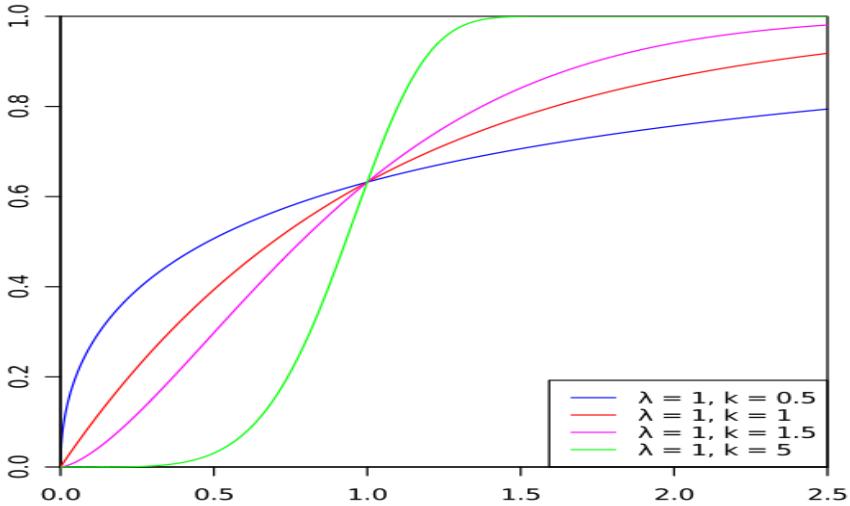

Figure 29 Cumulative distribution function of Weibull (2-Parameter) with the location parameter λ=1 and different shape parameter k

Figure 30 is a PDF described by two parameters a and b. The function can be written as

$$P(a \leq x \leq b) = \int f(x)ds \qquad (9)$$

Where the probability for a value x that positions between the lower bound *a* and upper bound *b* is the area in between.

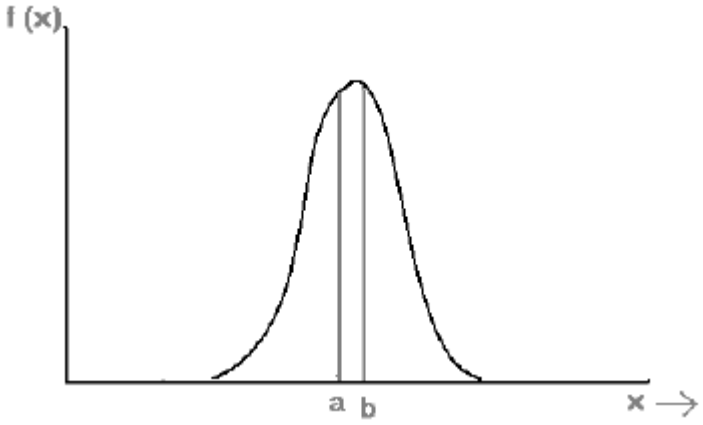

Figure 30 Probability density function (PDF)

On the other hand, The CDF can be described as

$$F(x) = P(X \leq x) = \int_0^x f(s)ds \qquad (10)$$

Where *F(x)* is the probability of obtained value *X* that is less or equal to a given value *x*.

The spread of result data can be worked out if a function is applied to the result data. By using the upper and lower confidence bounds, the results can be described more accurately [36], as shown in figure 31.

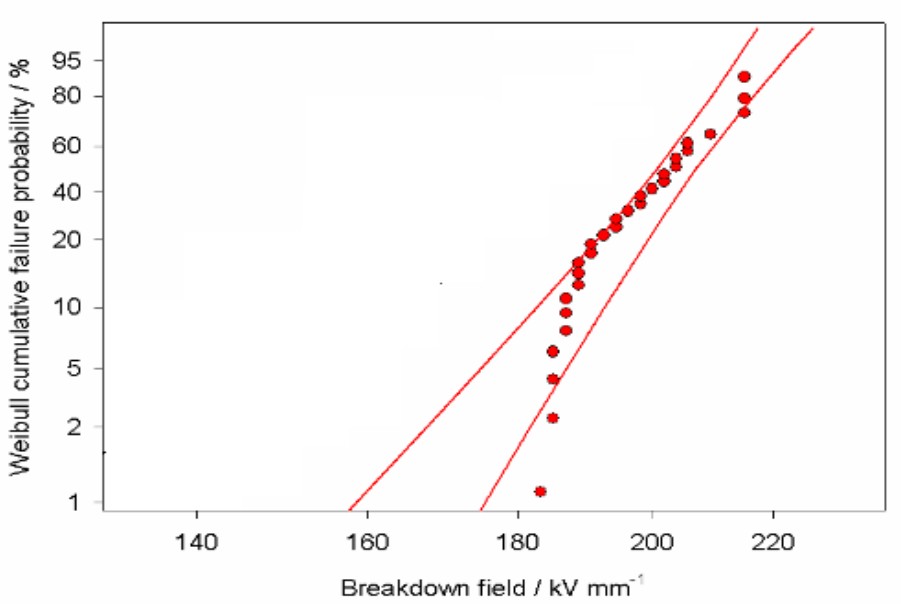

Figure 31 Example of breakdown distribution with confidence bound

It can be seen that by applying the upper and lower bounds, an area with certain percentage of data has been picked out [37]. The above figure shows a set of data with a confidence bound of 90%.

3.4.4 Differential Scanning Calorimetry (DSC)

For the DSC measurements, the Perkin-Elmer DSC7 together with the Perkin-Elmer Pyris software has been used. Samples with a small mass of around 5mg (between 4.8 mg and 5.4 mg) has been selected and sealed in an aluminium can. Then the sealed can was placed in the DSC together with an empty reference aluminium can separately. The difference in heat flow between the two cans was measured as a function of temperature. The basic principle of the measurement is to maintain the equal temperature between two cans and measure the difference in power.

An indium sample has been used to calibrate the DSC measurements. The melting temperature of the indium sample is known at 156.6 ℃, so before the measurement start, the indium sample was always being tested first to calibrate the temperature axis. During the measurements, the effects of temperature increase/decrease rate also need to be considered as the rate of temperature changes will affect the accuracy. In this project, a rate of 10 ℃ /min has been

selected for all the DSC measurements. During the measurements, the temperature was hold at 40 ℃ for 1 minute. Then the temperature was increased from 40 ℃ to 170 ℃ with a rate of 10 ℃/min. As given in the datasheet, the glass transition temperature of epoxy used in this project is around 140 ℃. So the temperature range 40 ℃ to 170 ℃ had been selected. A peak is usually observed near the T_g, as shown in figure 32. This is believed due to the enthalpy relaxation of the material that is due to incomplete curing or ageing.

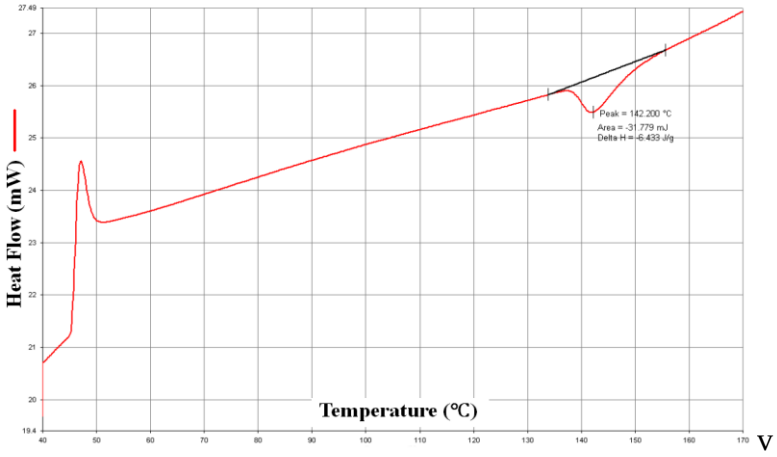

Figure 32 DSC measurements result (1st time)

In order to get rid of the unexpected drop, a repeating measurement has been performed immediately after the first measurement as the enthalpy history will be removed during the first measurement. It can be seen from figure 33 that the peak was disappeared. Instead, there is a step increase that refers to the glass transition temperature range.

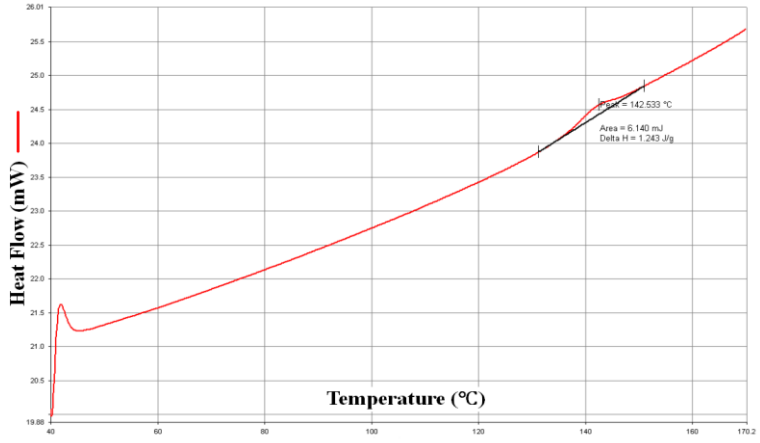

Figure 33 DSC measurements result (2nd time)

3.4.5 Humidity

As the water absorption has a huge effect on polymer dielectric materials' insulating properties, it is necessary to consider the effects of humidity on polymer dielectrics materials that are used as insulators [38, 39, 40]. In case of a humid situation, epoxy resin is able to absorb water from surrounding environment. The maximum amount of water that epoxy resin is able to absorb is up to several weight percent. The presence of water inside the epoxy resin will then result in a reduction of overall dielectric properties [40]. In case of the epoxy nanocomposites, the situation may determinate [41, 42]. As the nano-size fillers have sufficient high specific area of the particle surface, the water absorbed by epoxy nanocomposites will tend to locate in the interface between epoxy and nano-size filler. Although more detailed study needs to be carried out before the effect of humidity on epoxy resin can be well established, the recent studies already show that the presence of water absorption will cause weakness and therefore reduce the dielectric and mechanical properties of the composites [41, 42].

In this research, both dried samples and water-saturated samples (100% relative humidity) were tested for pure epoxy resin and epoxy resin loaded with nano size fillers. The epoxy sample with 100% relative humidity can be obtained by placing the sample into de-ionized water for two weeks at room temperature [43]. It needs to be noticed that the relative humidity may vary slightly with changing temperature, but with a given temperature and solution, it is able to decide epoxy samples' relative humidity. In addition, it is known that the nano size fillers can be modified into hydrophobic type by using the silane as a surface treatment agent.

4 Sample Characterization Using SEM and DSC

4.1 Scanning Electron Microscope (SEM)

It is known that the dielectric properties of polymer nanocomposites are strongly depended on nano filler dispersion. Therefore it is important the study the nano filler dispersion inside the base polymer materials. The most commonly used method for obtaining the dispersion of nano size fillers inside the base polymer materials is by using optical microscopy. High quality images of materials' surface structure could be observed and analyzed by focusing and magnification using light and lenses. Although the Transmission electron microscopy (TEM) is able to produce images with higher quality and larger magnification, the SEM is still widely used due to its simplicity of system and ease of use. It is enough to analysis the nano filler dispersion in polymer nanocomposites at such magnifications. Thus the SEM has been selected for this investigation.

SEM was introduced by Max Knoll [44] in 1935. It is able to observe the surface structure of materials down to the nanometer scale. It is frequently used in material investigations. By using SEM, the morphology (such as size and shape of particles) and composition of material can be observed. In SEM, an electron beam is created by the electron gun positioned at the top of the sample. The beam is focused onto the selected area of sample surface. The electrons could penetrate into the sample up to 1 μm and experience a multiple scattering, resulting in a subsequent interaction that can be detected. The interaction is usually secondary electrons that are able to escape from the upper 50nm of the sample (for polymer) due to their low energy (~30eV) and result in much higher resolution. The resulting image of secondary electrons is highly sensitive to the surface topology of materials, if the surface topography can be used to represent the internal morphology, the internal morphology of the material can be observed.

The Cambridge Stereoscan 360 high vacuum SEM was used in this project. To obtain high quality of images, the tungsten filament is set to 2.52A to produce electrons by thermionic emission. The gun voltage is set to 18kV with a 15mm working distance. During SEM test, it is also necessary to provide a path to earth for the beam electrons. Thus the samples need to be coated with gold before SEM test. The Emitech K550X sputter coater described in previous chapter is used to coat the sample

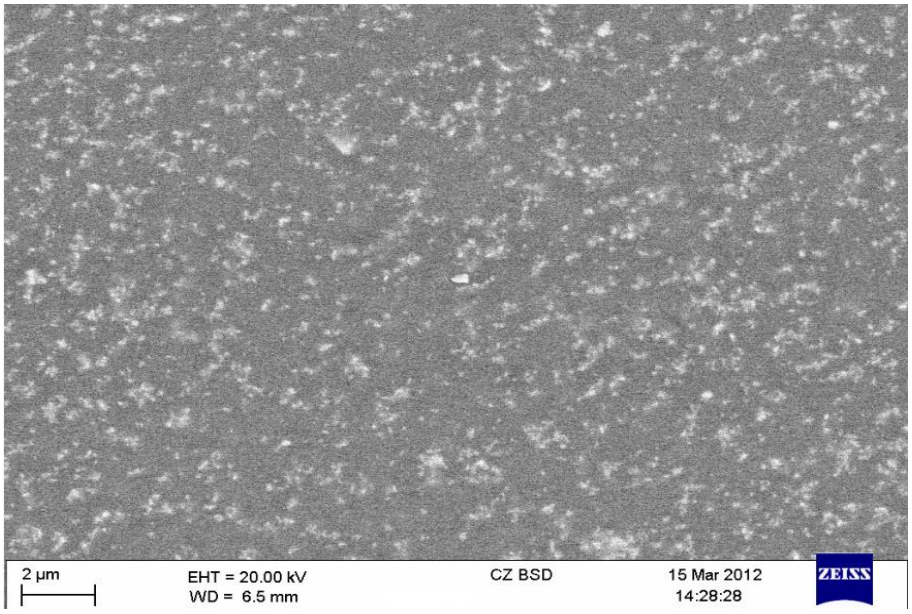

(a) With surface treatment

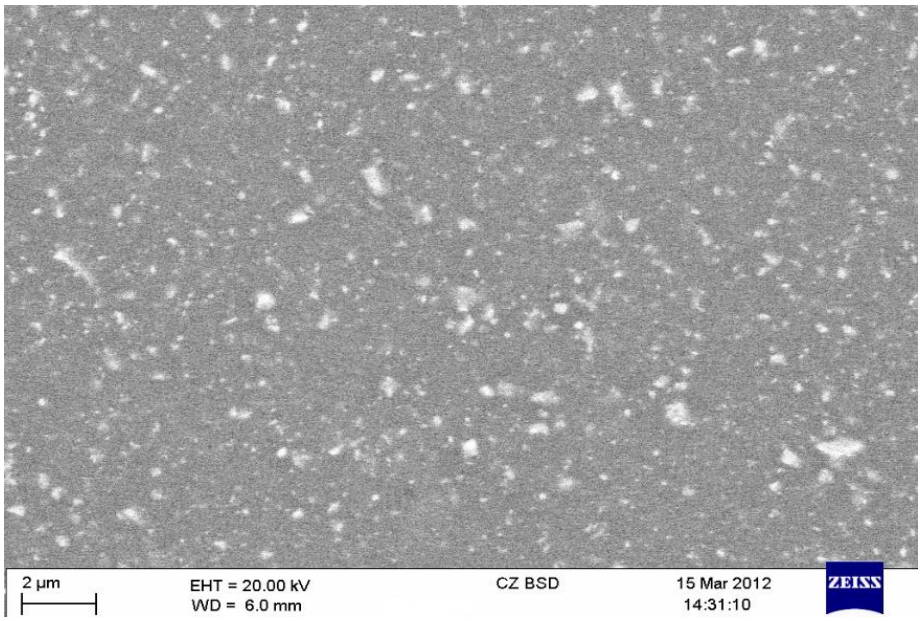

(b) Without surface treatment

Figure 34 SEM image of the epoxy–SiO_2 nanocomposite loaded with treated and untreated nano filler

The filler dispersion of the nano-size filler in the resin loaded with 3wt% of both treated and non-treated nano size fillers can be seen from figure 34. The SEM results show that no large agglomerations can be observed in both samples. However, some small agglomerations have been observed in epoxy nanocomposites loaded with non-treated nano fillers. To compare the difference in nano filler dispersion rate between treated and non-treated nano fillers, 60 random particles has been selected from both samples loaded with treated and non-treated nano size fillers and detailed dates are listed in Appendix A. The average diameter and standard deviation of those two set data has been worked out. The average diameter standard deviation of epoxy samples loaded with treated nano fillers are 97.2nm and 73.7nm respectively, whereas the average diameter standard deviation of epoxy samples loaded with treated nano fillers are 205.7nm and 155.8nm respectively. This suggests that the treated nano fillers have better dispersion compared with the untreated fillers.

4.2 Differential Scanning Calorimetry (DSC) Measurements

The term of glass transition is a reversible transition process that an amorphous polymer materials' physical state charges from a hard glass-like state into a rubber-like state. The glass transition temperature of materials can provide information about the thermal properties of the materials. The temperature where the glass transition occurs is known as the glass transition temperature (T_g). The T_g is the critical temperature that separates the glass-like and rubber-like behaviours of all amorphous solids. Many physical properties such as conductivity, thermal expansion coefficient, and thermal conductivity may experience a rapid change in the range of T_g. It is one of the most important parameters that describe the behaviours of amorphous materials as a function of temperature [45]. Below the T_g, the motion of large-size molecular in amorphous materials is almost impossible as the molecular are frozen. The materials are therefore in a hard, brittle and glassy state. But if the temperature is above T_g, the molecular will be able to move and the materials become rubbery. As the glass transition is very sensitive to the changes in molecular interaction, the material structures between different samples and the change of

structure in samples can be determined and characterized by measuring the T_g. The T_g of material can be obtained through thermal analysis. Figure 35 shows a specific heat capacity for a typical polymer in the region of glass transition [46]. As shown in figure 35, the curve 1 shows the cooling measurements, whereas the curve 2 shows the heating measurements immediately after cooling measurement.

The phase transitions of polymer materials under the effect of temperature usually result in changes in the overall properties of the materials such as heat flow and heat capacity. For example, when the epoxy resin is transited from glass-like state to the rubber-like state, there is an increase in both heat flow and heat capacity. The chain movements become easier as a result of the increase in heat capacity. The increase in heat flow and heat capacity can be measured by using differential scanning calorimetry (DSC) method [47].

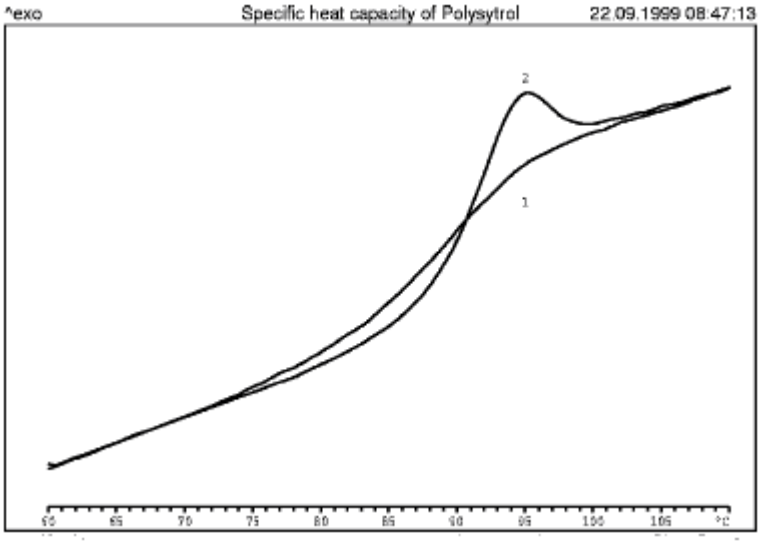

Figure 35 Specific heat capacity for a typical polymer in the region of glass transition

4.2.1 Differential Scanning Calorimetry Technique

For polymer dielectric materials, there is a significant change in the dielectric properties of materials around the temperature that the glass transition phenomena is about to occur. It is important to know the glass transition temperature (T_g) whenever a polymeric material is studied. The Differential Scanning Calorimetry (DSC) is one of the most popular methods that can be

used to study the thermal properties of polymer dielectrics, including the T_g. The enthalpies that is due to the change of materials' physical state such as crystallization, melting and glass transition phenomena can be measured by using DSC [48, 49].

The basic principle of DSC technique is the difference in the amount of heat flow between the sample and a reference as temperature increase or decrease is measured. If the sample experiences some change of physical states of material, more or less heat flow to the sample will be required to make sure the temperature of both sample and reference remains the same as the process is either exothermic or endothermic. One example is the melting temperature where the sample changes its state from solid state to liquid state. This is an endothermic process so more heat is required to flow to the sample to remove the difference between in temperature between sample and reference. As the difference in heat flow between the sample and the reference can be measured, the amount of heat absorbs or releases during certain process can be worked out by DSC. Figure 36 shows a schematic diagram of DSC.

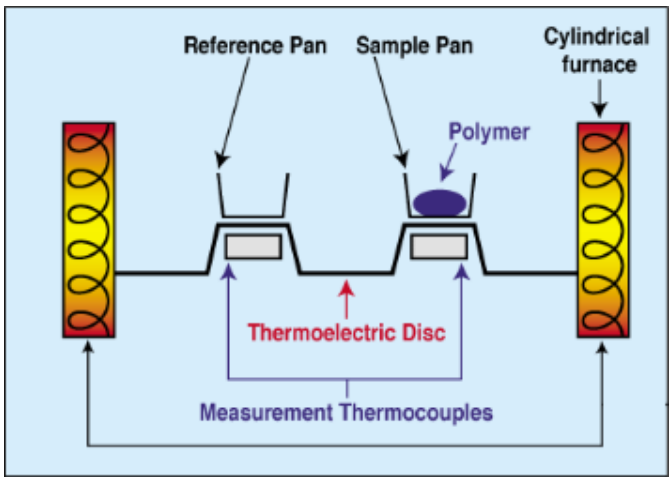

Figure 36 Schematic diagram of DSC

4.2.2 DSC Results

The glass transition temperature of epoxy samples with and without surface treatment and loaded with different loading concentrations have been measured

by DSC. Figure 37 shows the glass transition measurements result of pure epoxy resin sample by using the DSC. It can be seen in figure 37(a) that in the first measurement, an endothermic peak has been observed at the temperature around glass transition temperature (T_g). Such endothermic peak is believed to be caused by the enthalpy relaxation [50]. Most of the polymers start physical aging immediately after curing. If the aging time is long enough, or the aging temperature is sufficient high, the enthalpy will tend to reach the thermodynamic equilibrium state. Therefore when starting to scan from lower temperature by using DSC, an endothermic peak will be observed during measurement. This is because of the enthalpy of the epoxy is lower than the enthalpy of thermodynamic equilibrium state as the heating rate will result in a lower enthalpy changing rate compared with the equilibrium enthalpy it should have. So when the temperature reaches T_g, as the molecular chain becomes rubber like state, the molecular chains are able to return to their thermodynamic equilibrium state. Such changes require energy from the outside. Thus endothermic peak will be observed. In order to get rid of such enthalpy history, the sample needs to be heat up to a temperature that is higher than T_g, then cool the sample down at the same rate and finally heat it up again at the same rate. Figure 37(b) shows the second measurement result of epoxy resin sample. It can be seen that the endothermic peak has disappeared and a typical T_g curve with a step increase has been observed, indicating a change in the heat capacity of the polymer. In order to decide the T_g, extrapolate the sloping baseline before the glass transition forward and take the baseline of drastic change in heat flow. The value of T_g is measured at the cross point of two red lines shown in figure 37(b). It can be observed that the T_g of pure epoxy resin is around 137℃, which is similar to the T_g given in the data sheet about 140℃.

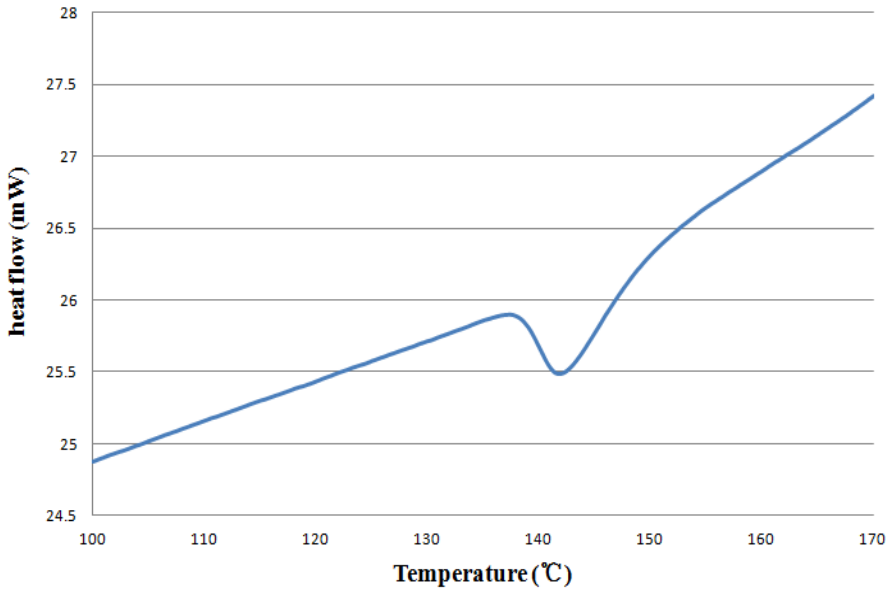

(a) First measurement

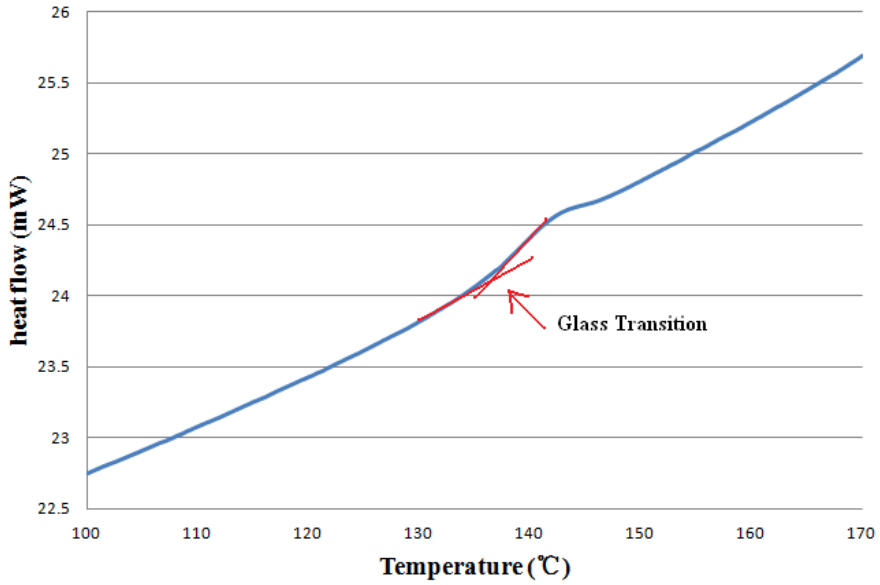

(b) Second measurement

Figure 37 First and second measurements of glass transition temperature of epoxy

The glass transition temperature for epoxy resin loaded with different loading concentration of nano SiO_2 and Al_2O_3 particles is given in figure 38 and the value of T_g is also given in table 8. It can be seen that the presence of nano size fillers seems to reduce the T_g. Compared with pure epoxy resin, EP2S01 seems to have a slightly lower T_g. As the loading concentration increases to 0.3wt%, there is a further reduction on T_g. However, the T_g of EP2S05 sample begins to increase. A further reduction has been observed as the nano filler loading concentration increases. The T_g of EP2S5 sample is around 117.5℃, which is

approximately 25℃ lower compared with the T_g of unfilled epoxy resin. Moreover, the changes of T_g in epoxy resin loaded with nano Al_2O_3 fillers seems to have similar tendency with those loaded with SiO_2 fillers.

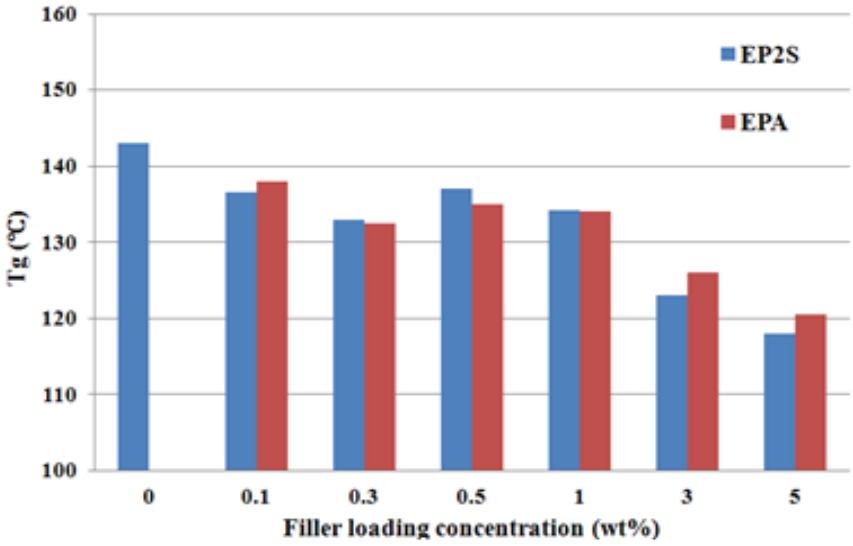

Figure 38 Glass transition temperatures of epoxy nanocomposites

Sample code	Weight percentage	Particle type	Tg (℃) ±2℃
EP0	-	-	142.5
EP2S01	0.1	SiO_2	136.7
EP2S03	0.3	SiO_2	133.0
EP2S05	0.5	SiO_2	136.5
EP2S1	1	SiO_2	133.4
EP2S3	3	SiO_2	122.8
EP2S5	5	SiO_2	117.5
EPA01	0.1	Al_2O_3	138.2
EPA03	0.3	Al_2O_3	132.7
EPA05	0.5	Al_2O_3	135.1
EPA1	1	Al_2O_3	133.3
EPA3	3	Al_2O_3	125.8
EPA5	5	Al_2O_3	120.4

Table 8: Glass transition temperature of samples

The T_g behaviours can be explained by the surface characteristics of nano filler and the interfacial region between nano filler and the polymer matrix. Early researches by Starr et al show that the interfacial region is the key factor that affects the T_g of polymer nanocomposites [51, 52]. Santanu and Thomas further developed the dual layer model to explain the behaviours of T_g observed [53, 54, 15]. In this model the interfacial region around the nano fillers is classified into a tightly bound layer and a loosely bound layer. The inner tightly bound region is believed to be tightly bound between nano fillers and polymer chain by weak hydrogen bounds and therefore restricts the chain mobility. The outer loosely bound layer, on the other hand, contains polymer chains that are loosely bound. The presence of loosely bound region acts as a mobile region and leads to a reduction in T_g. From T_g point of view, the two layers act in opposite senses. Reference to the early studies, a reduction of T_g has been reported when the nano filler is introduced [55, 51], where T_g increase trend has also been observed in a few case [14, 15], both at a filler loading concentration of around 3wt%. For EP2S01 samples, the amount of nano particles is less, and the tightly bound region is small. The presence of large mobile region leads to a reduction in T_g. The number of nano particles in EP2S03 is more than EP2S01 samples, but the inter-particle distance between each particle is still large, as shown in table 8. So the probability for the interfacial region to overlap is small. The interfacial area between epoxy and fillers increases significantly with the increase of filler loading concentration and results in the increase of free volume due to the loosened molecular packing of the chains. Such interfacial interaction will determine the T_g [25, 52, 51]. There is a further increase in free volume and leads to a further reduction in T_g. In EP2S05 samples, an increase in T_g has been observed. As the particle loading concentration increase to 0.5wt, the number of nano particles increase to a sufficient amount that the area of tightly bound region increases. The presences of the large tightly bound region will restrict the chain movement and result in a reduction in T_g. Moreover, as the inter-particle distance decreases, the free volume decease due to the overlapping of loosely bound region. It is also known that when the nano particles are dispersed into polymer

matrix, they are expecting to form cross-linking structures. As the filler loading concentrations increases further, another continuous decrease has been observed. In EP2S1 samples, as the inter-particle distance drops to 54.7nm, there is a possibility for the tight bound region to overlap with nearby interface region. Moreover, due to their high surface energy, the untreated nano particles tend to agglomerate with each other. Those large agglomerations of nano particles increase the free volume [21]. It is also shown that the dispersion and surface characteristic of nano size fillers will affect the relaxation of molecule chains and the polymer chain movement. As a result, the T_g of EP2S1 sample decreases. Further increase in filler loading leads to more interface overlapping and agglomeration of nano particles and therefore results in a further reduction in T_g [56].

Sample code	**Particle size (nm)**	**Inter-particle distance (nm)**	**Surface area (km^2/m^3)**
EP2S01	20	141.1	0.42
EP2S03	20	91.7	1.27
EP2S05	20	74.2	2.1
EP2S1	20	54.7	4.2
EP2S3	20	31.6	12.9
EP2S5	20	23.4	21.7
EPA01	30	211.4	0.4
EPA03	30	137.6	1.0
EPA05	30	110.7	1.7
EPA1	30	71.4	3.4
EPA3	30	47.5	10.3
EPA5	30	35.3	17.3

Table 9: Inter-particle distance and surface area of nano filler in epoxy nanocomposites

5 Dielectric Permittivity of Epoxy Nanocomposites

5.1 Sample under Study

In this chapter a comparative study on the dielectric permittivity of epoxy nanocomposites has been carried out. It is known that the epoxy microcomposites are widely used in the modern industrial applications due to their excellent mechanical and thermal properties [55]. However, there is a large reduction in insulating properties in epoxy microcomposites. Epoxy nanocomposites, on the other hands, are believed to enhance the insulating properties by introducing large surface areas. Early researches show that the presence of nano size particles has significant effect on various dielectric properties of polymer nanocomposites, either positively or negatively [56]. Those changes in dielectric properties are believed due to the large interface region between nano particles and polymer matrix. It is necessary to consider the effect of interfacial characteristic when study the insulating properties of polymer nanocomposites.

In order to study the effects of interface region in epoxy nanocomposites, both nanocomposites loaded with nano SiO_2 and Al_2O_3 particles have been prepared. Nano SiO_2 particles without surface treatment with an average diameter of both 20nm and 80nm have been used in this investigation. In comparison, epoxy resin loaded with nano Al_2O_3 particles with an average particle diameter of 30nm has also been prepared.

To help understanding effect of the inter-particle distance and interaction between interfacial regions on the dielectric properties of epoxy nanocomposites, the amount of nano particles dispersed into epoxy materials also need to be taken into considerations. Epoxy nanocomposites loaded with different weight percentage of nano particles have been prepared for both types of nano particles. Moreover, unfilled epoxy resin and the epoxy

microcomposites loaded with micro size SiO_2 particles are also prepared to give a comprehensive study of effect of nano size fillers on the insulating properties of resulting composites. A list of samples have been used in this chapter was shown in table 10.

Sample code	Particle wt%	Size of particle	Type of particle
EP0	0	-	-
EP2S01	0.1	20nm	SiO_2
EP2S03	0.3	20nm	SiO_2
EP2S05	0.5	20nm	SiO_2
EP2S1	1	20nm	SiO_2
EP2S3	3	20nm	SiO_2
EP2S5	5	20nm	SiO_2
EPA01	0.1	30nm	Al_2O_3
EPA03	0.3	30nm	Al_2O_3
EPA05	0.5	30nm	Al_2O_3
EPA1	1	30nm	Al_2O_3
EPA3	3	30nm	Al_2O_3
EPA5	5	30nm	Al_2O_3
EP8S03	0.3	80nm	SiO_2
EP8S05	0.5	80nm	SiO_2
EP8S1	1	80nm	SiO_2
EP8S3	3	80nm	SiO_2
EP8S5	5	80nm	SiO_2
EPM3	3	50μm	SiO_2
EPM5	5	50μm	SiO_2

Table 10: List of samples under study

5.2 Principle of Dielectric Spectroscopy Analysis

The dielectric spectroscopy measurement is the method to measure the materials' dielectric properties as a function of frequency [27], the applied electric field and temperature are also variables in the measurements. The dielectric spectroscopy measurement depends on the material polarization which is induced inside the material under the influence of external electric stress. The dielectric spectroscopy method has been widely used by experimenter to measure the dielectric properties of materials for many years [57]. For example, the dielectric spectroscopy measurements on water, has been investigated in 1980's. Dissado and Hill, investigated not only the dielectric spectroscopy performance on many materials, but also worked out a theory known as Dissado-Hill theory that was used to studies the dielectric response [58, 59, 60, 61]. The dielectric spectroscopy measurement result is able to provide the electrical properties of measured materials and the results can also be used to analyse some other material properties such as polymer molecule structure and so on [62]. It can be used to explore the internal structure of material by measuring the electrical response.

The first study on dielectric materials was presented by Debye in 1910's. Debye then introduced a theory which is based on the dielectric losses that related to both relaxation of electric dipoles and dielectric polarization. In this theory, Debye explains the dielectric performance by the free movement of non-interacting dipoles in a viscous medium. This model was developed from theory that used to explain the dilute solution. The later studies show that the model is not able to explain the solid materials [57]. Instead, Dissado- Hill theory has been developed to analyse the dielectric responds.

It is important to investigate the interaction between material and the applied electric field. In many investigations, the measurements results are shown in term of response to time-dependent signal as it helps to understand the result better, especially in the case of non-linear process [63]. But there is also another investigation method which is based on the response to harmonic

excitation such as sine waves [64]. Such studies are able to offer both theoretical and practical advantages.

For a given function of time *G(t)* which is based on the Fourier transformation, the mathematical expressions in term of frequency-dependent response that is written as Fourier transform [57]

$$F[G(t)] = \varphi(\omega) = 2\pi^{\frac{1}{2}} \int_{-\infty}^{\infty} G(t) \exp(-i\omega t)\, dt \qquad (11)$$

Where ψ (ω) is the frequency spectrum of the time-dependent function *G(t)*. The *i* included in the equation means that both real and imaginary parts are taken into account. In this case both the magnitude and phase behaviour of the material sample have been considered.

5.2.1 Field Depended Dielectric Response

When an external electric field is applied to the dielectric material, the bound charge will be separated slightly under the applied field. The dielectric displacement *D* under small electric field can be written as

$$D = \varepsilon * \varepsilon_0 E \qquad (14)$$

Where ε_0 is the permittivity of vacuum and ε^* is the complex relative permittivity [65]. For a periodic electric field which can be defined as

$$E(t) = E_0 exp\ (-i\omega t) \qquad (15)$$

Where E_0 is the amplitude of the applied field, ω is the angular frequency. As the electric displacement D and the applied electric field E have a phase difference δ, the electric displacement D can be shown as:

$$D = D_0\, cos(\omega t - \delta) \qquad (16)$$

where D_0 is the corresponding displacement. The electric displacement D can also be written as:

$$D = D_1\, cos\ \omega t + D_2\, sin\ \omega t \qquad (17)$$

Where:

$$D_1 = D_0\, cos\ \delta \qquad (18)$$

$$D_2 = D_0 \sin\delta \quad (19)$$

As D_0 is proportional to ε_0, and D_0/ε_0 is a function of ω, two relative permittivity $\varepsilon_1(\omega)$ and $\varepsilon_2(\omega)$ can be introduced:

$$D_1 = \varepsilon'(\omega)E_0 \quad (20)$$

$$D_2 = \varepsilon''(\omega)E_0 \quad (21)$$

Its complex relative permittivity ε^* can be written as

$$\varepsilon^*(\omega) = \varepsilon'(\omega) - j\varepsilon''(\omega) \quad (22)$$

Where $\varepsilon'(\omega)$ is the real part of complex relative permittivity which is the lossless permittivity and $\varepsilon''(\omega)$ the imaginary part of the complex relative permittivity due to bound charge and dipole relaxation phenomena, which results in energy loss.

The dielectric displacement, which is due to the response of dielectric materials under the external applied electric field only, is known as the polarization. The polarization P under the applied field can be written as

$$P = D - D_0 = (\varepsilon^* - 1)\varepsilon_0 E \quad (23)$$

The dielectric spectroscopy is used to measure the response of material under an external applied field with varying frequency. When an external AC field is applied to the materials, polarizations due to different mechanisms occur in the material. The direction of polarization changes as the applied filed changes. There is a delay between the change of the field and the change of polarization direction. Such phase-lag is known as the phase angle δ. The dielectric loss tangent, which can be defined as the ratio of energy loss, can be written as

$$\tan\delta = \varepsilon''/\varepsilon' \quad (24)$$

Figure 39 show that a real capacitor can be treated as a lossless capacitor in series with an equivalent series resistance (ESR). The dielectric loss angle can be defined as the angle between the impedance of capacitor and the negative reactance.

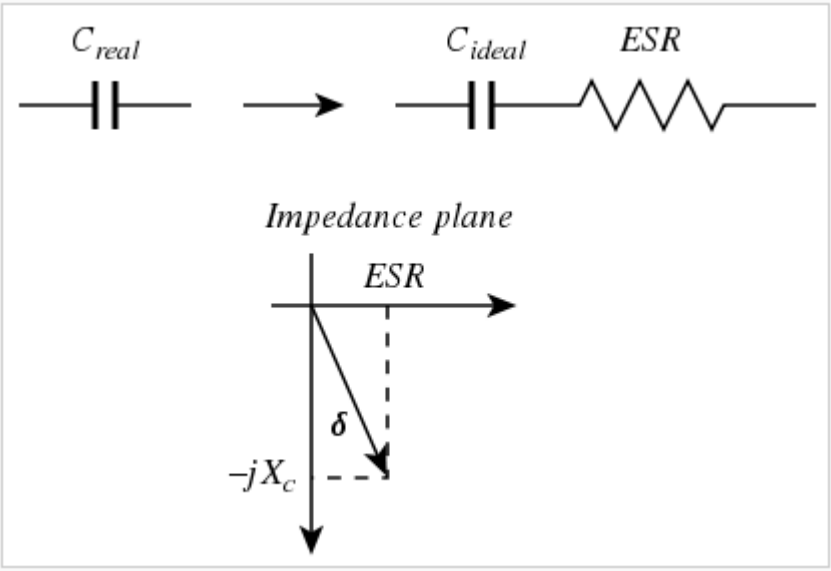

Figure 39 Loss tangent of a real capacitor

5.2.2 Dielectric Polarization Principles

The investigations about dielectric permittivity are based on the dielectric polarization inside the material when an external field is applied to the dielectric materials. When an electric field is applied to a dielectric, instead of flowing through the dielectric material, charges will tend to shift their positions a little bit. This is known as dielectric polarization. Due to such polarization, positive charges will move along the electric field whereas negative charges will move towards the opposite direction. Such movements will create an internal electric field which is opposite to the external field.

Numbers of different dielectric mechanisms have been used to study the reactions of materials to the applied electric field. Figure 40 shows both the real part and imaginary part of the dielectric permittivity spectrum over a wide range of frequencies. The relative permittivity of materials varies with the frequency. In certain frequency range (especially at low frequency), the energy dissipates into materials and results in dielectric loss at lower frequency. The energy loss can be transformed into heat and lead to material ageing which affects the insulating performance of dielectric materials. The temperature itself also has a strong effect on the dielectric permittivity.

The imaginary part of the dielectric permittivity is an intrinsic material property which varies with temperature, pressure and so on. It can be seen from figure 40 that the imaginary part of permittivity has several maximum peaks as frequency increases. Those peaks divide the imaginary permittivity into 4 regions. Each region represents a special polarization mechanism. Each of the different mechanism has its own characteristic frequency in which the energy dissipated due to the corresponding polarization is maximized. Those polarization mechanisms are not able to work under a frequency which is higher than the corresponding maximum peak frequency as they do not have enough time to respond the external field under such high frequency [66].

The four main types of mechanisms are: ionic/space charge relaxation, dipolar or orientation relaxation, atomic polarization and electronic polarization respectively. Those dielectric mechanisms can be classifying into either relaxation or resonance processes.

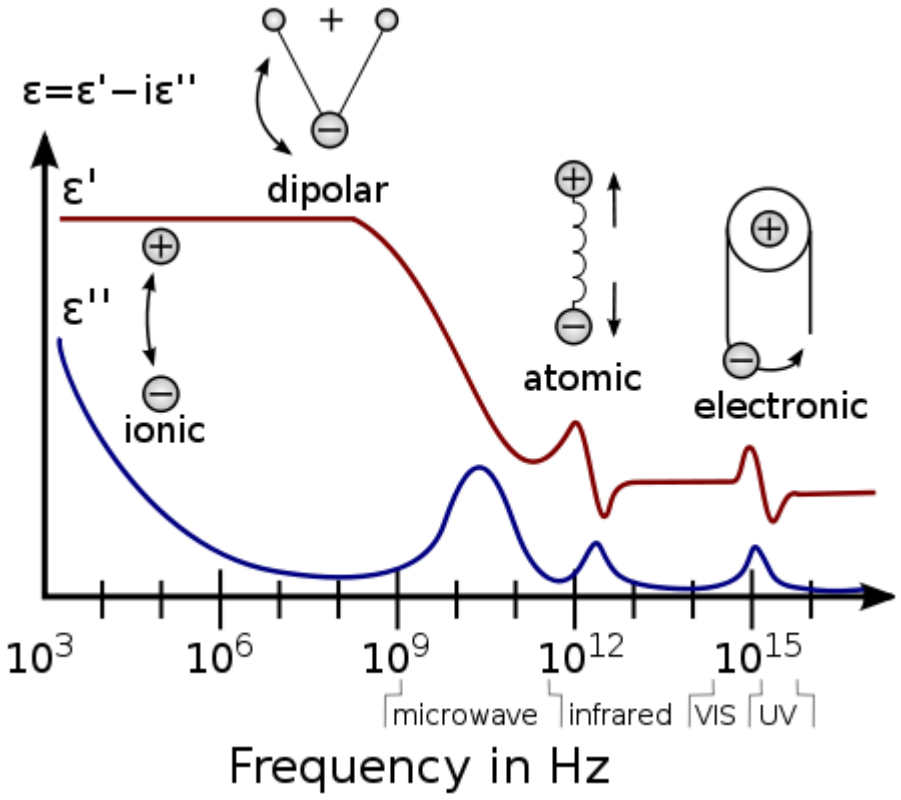

Figure 40 A dielectric permittivity spectrums over a wide range of frequencies [119]

The orientation polarization is the main mechanism under low frequencies range. It can be further divided into dielectric relaxation, ionic relaxation and

dipole relaxation. Generally speaking, the orientation polarization is a slow process in solid dielectric materials as the movement of dipoles is restricted by the potential barriers that are generated by the molecular and lattice structure in the dielectric materials. Therefore it is influenced by the frequency and its polarization effect will be reduced under high frequency. Moreover, some of the dipoles may be locked into orientations and they are not able to respond at all. The orientation polarization under the applied electric field is shown in figure 41.

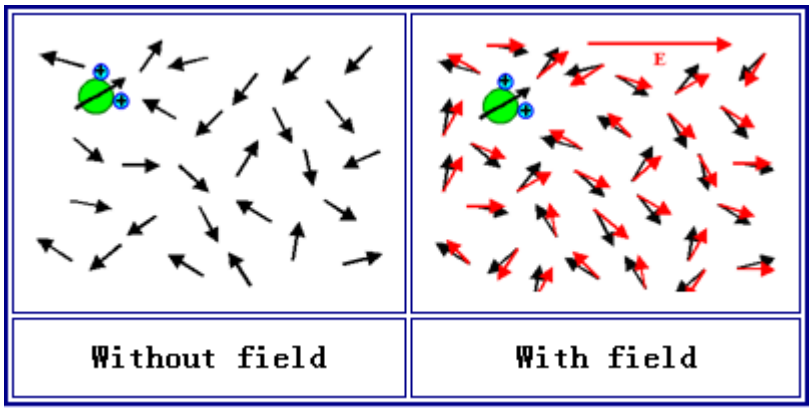

Figure 41 Orientation polarization

The ionic relaxation includes both ionic conductivity and interfacial or space charge polarization. Ionic conductivity is the main mechanism in low frequencies range and the presence of such mechanism only introduces loss into the system. Figure 42 shows the ionic polarization of ion under the applied electric field. The interfacial or space charge polarization occurs when charge carriers have been trapped at the interfaces of these heterogeneous systems [28]. Impurities, cracks and voids may also lead to the accumulation of charge and therefore resulting in interfacial polarization.

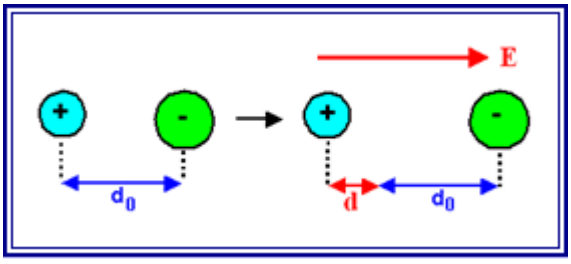

Figure 42 Ionic polarization

Both the atomic polarization and electronic polarization are resonant mechanisms. Resonant mechanisms are much faster than relaxation mechanisms. Atomic polarization is a resonance process where the applied electric field has distorted the electrons arrangements within the molecules. The electronic polarization occurs in the neutral atoms as the applied electric field displaces the nucleus due to the surrounding electrons.

As mentioned above, there are four main types of polarization mechanisms therefore the total polarization of materials will be the sum of all orientation polarization, ionic and interfacial polarization, electronic polarization and atomic polarization. The total polarization P can be written as

$$P = N_0 \alpha E_1 \tag{29}$$

Where N_0 is the number of dipoles per volume and α is the polarisability of the charge and E_l is the local electric field which is the total field as a result of injected charges and other dipoles.

5.2.3 Theory of Dielectric Response

The dielectric behaviours of material under an external applied field has been studied widely. The Debye model which was developed by Peter Debye has been used to estimate the frequency dependent dielectric response [67]. However, as the Debye model assumes that the freedom of molecule movement is limited, it is not possible to apply the model to relaxation with more than one relaxation time. As the dielectric system usually contains more than one type of dipole, the interaction between those dipoles will result in a more complicated situation. The basic Debye model is not suitable to estimate the frequency dependent dielectric response. Expansion of Debye model is developed to describe the experiment results. Both Cole-Cole and Cole Davidson equation have been developed and both of them have relatively good match with the experiment data [68, 69].

Dissado and Hill have also developed a theory which is able to give relatively good predictions compared with the experiment results [59]. In this theory the material is divided into clusters. As the dipole relaxation occurs, the effect will

be transmitted between molecules and therefore across the material. The clusters will gain the relaxation energy from dipoles, which allows the interaction behaviours during the dielectric relaxation. The overall shape of dielectric response will also be affected by the relaxation behaviours of clusters.

Generally speaking, the response that is due to the dipole relaxation which is out of phase with the applied field will result in a dielectric loss peak in the imaginary part of susceptibility, in company with a dielectric increment in the real part of susceptibility. The response that is due to the presence of charge carriers will result in no dielectric loss peak in imaginary part of susceptibility and the real part of susceptibility stays independent with frequency. The response that is due to the presence of partially mobile charge carriers will result in a steep increase in both real and imaginary part of susceptibility.

5.3 Dielectric Spectroscopy Measurements Results

The dielectric permittivity of epoxy/nanocomposites was measured over a wide range of frequency using dielectric spectroscopy (Solatron 1260). During all the measurements, the temperature was maintained at room temperature.

5.3.1 Dielectric Permittivity and Tan Delta Value of Pure Epoxy Resin

Both of the relative permittivity and Tan Delta values of EP0 samples are shown in figure 43. In can be seen from figure 43 (a) that the relative permittivity has slightly higher value at low frequency range. There is a continuous drop in relative permittivity as frequency increases to 1MHz. The results show that the pure epoxy resin is frequency dependent at the measured frequency range (0.1Hz-1MHz). The decrease in real part of permittivity may be due to the charge build up under low frequency range, which is well known as Maxwell-Wagner polarization [27, 70, 71]. The Maxwell-Wagner polarization occurs at the interface between sample and electrode, or inner dielectric boundary layers. In both situations charge carries are blocked at electrodes and dielectric boundary layers, which results in charge separations

and increases the relative permittivity. Generally speaking, this is an ionic relaxation process. The result of polarization reduction due to dipolar groups could also result in a continuous decrease in relative permittivity [57].

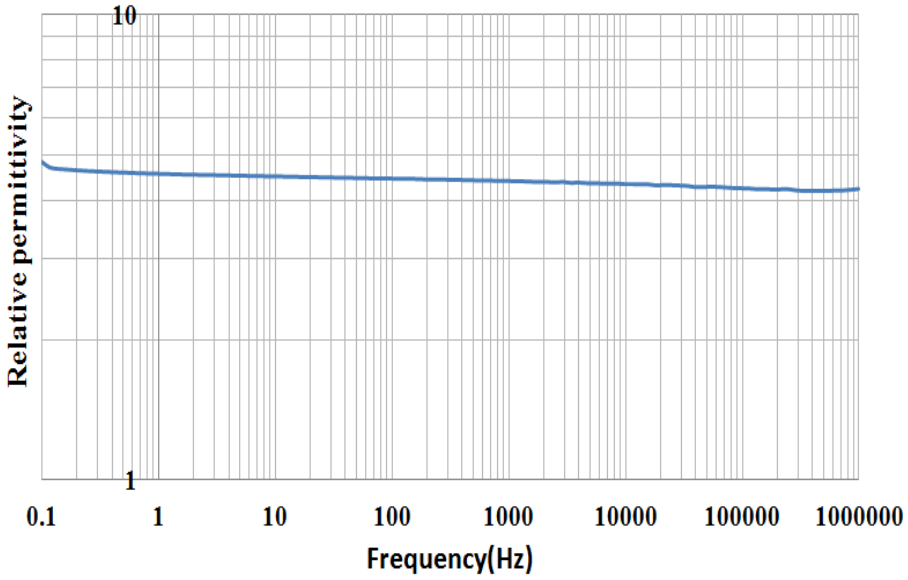

(a) Relative permittivity

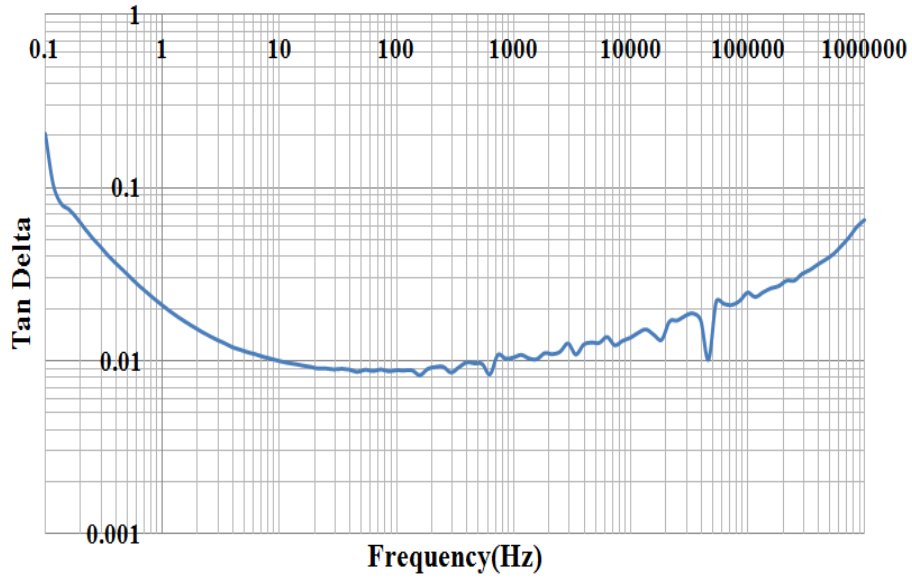

(b) Tan delta value

Figure 43 Relative permittivity and tan delta values of pure epoxy resin sample

The dielectric permittivity tan delta value (also known as loss angle) is used to describe the dielectric materials' ability to dissipate energy. The permitivity of

dielectric materials under time varying fields has both real and image componets. It can be written as equation 22 in chapter 5.2.1. The real part of permittivity ε' is the lossless permittivity that is given by the product of relative permittivity ε_r and permittivity in free space ε_0. The image part of permittivity ε'', on the other hand, represents the energy loss. The tan delta value can be written as equation 24. When an alternating electric field is applied to the sample, the tan delta value can also be defined as:

$$tan\,\delta = \frac{j_a}{j_c} \qquad (30)$$

Where j_a is the active component of current density and j_c is the reactive component of current density that

$$j_a = (r + \frac{\omega^2\tau^2 g}{1+\omega^2\tau^2})E_m e^{j\omega t} \qquad (31)$$

$$j_c = (\omega\varepsilon_0 + \frac{\omega\tau g}{1+\omega^2\tau^2})E_m e^{j\omega t} \qquad (32)$$

Where ω is the phase, r is the conductivity of sample, τ is the relaxation time, E_m is the field strength, t is the time, ε_0 is the permittivity of vacuum and g is the initial conductivity. It can be seen from the above equation that under alternating electric field, the tan delta value of polymer materials depends on not only frequency, but also the conductivity and the relaxation time of large molecular chains. The dielectric loss of polymer materials could be due to both conductivity loss which is caused when the charge carriers travel across the materials under the applied field and orientation polarization of large molecular under the applied field. As the resistivity of epoxy is around 10^{13}-10^{14} Ωm, the conductivity loss of epoxy is small. Moreover, the epoxy resin tends to form large 3D cross-linking network during curing. Such 3D network structure restricts the orientation polarization of large molecule. So the relaxation loss caused by polar groups is the main factor in determining the dielectric loss of epoxy resin as the orientation polarization is mainly caused by the direction of polar groups.

It can be seen from figure 43 (b) that the tan delta value of EP0 sample also has a higher value at low frequency range. It decreases sharply as the frequency increases and reaches a minimum value of 0.009 at 100Hz. Further increase in frequency leads to another increase in tan delta value. The rapid decrease of tan

delta value under low frequency range (below 10Hz) is believed due to both ionic relaxation and dipole relaxation phenomena discussed above. The further increase in tan delta value at higher frequency range (above 100Hz) is believed due to the increase in relaxation loss of epoxy resin's polar groups under high frequency field. The ionic polarization could also occur in higher frequency range and leads to further increase in tan delta value.

5.3.2 Effects of Nano Size Fillers

The relative permittivity of epoxy resin sample loaded with different loading concentration of nano SiO_2 and Al_2O_3 fillers have been shown in figure 44. Generally speaking, the relative permittivity decreases as the frequency increases. As discussed in the dielectric polarization section, the dielectric materials' permittivity is affected by the dielectric polarization inside the materials. In this project, as the frequency range is between 0.1Hz and 1MHz, both the ionic relaxation and dipolar relaxation mechanisms play important roles in deciding materials' permittivity. It is well known that the interfacial or space charge polarization tends to occur at the interfaces. Previous studies show that the epoxy/nanocomposites have a large volume fraction of interfaces therefore the interfacial or space charge polarization is expected to play an important role [72, 73]. The interfacial or space charge polarization occurs when charge carriers have been trapped at the interfaces of these heterogeneous systems. As the frequency of the applied electric field increases, it is more difficult for space charges to be trapped at the interfaces. Therefore, the influence of interfacial or space charge polarizations on the materials' permittivity decreases as the frequency increases. This explains why the relative permittivity decreases as the frequency increases.

The dipolar mechanism also needs to be considered. In a typical epoxy resin system, the permittivity of epoxy is determined by the number of orientable dipoles present in the system and their ability to orient under an applied electric field [74, 75]. As in the epoxy chain, most of the free dipolar functional groups are able to orient under lower frequency of the applied field. The epoxy

composites tend to have higher permittivity in lower frequency range. When the frequency of the applied voltage increases, it will become more difficult for larger dipolar groups to orient themselves. The effect of dipolar groups on the permittivity is reducing continuously as the frequency increasing. Moreover, the increasing of frequency of the applied filed will also result in reducing of SiO_2/Al_2O_3 fillers' inherent permittivity [76]. The combination of both effects results in the reduction of epoxy/nanocomposites' permittivity with increasing frequency.

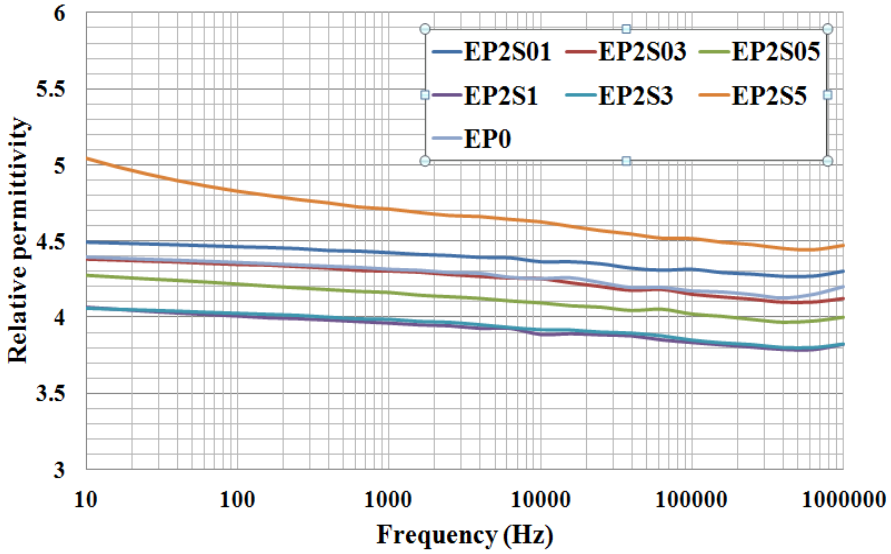

(a) SiO_2

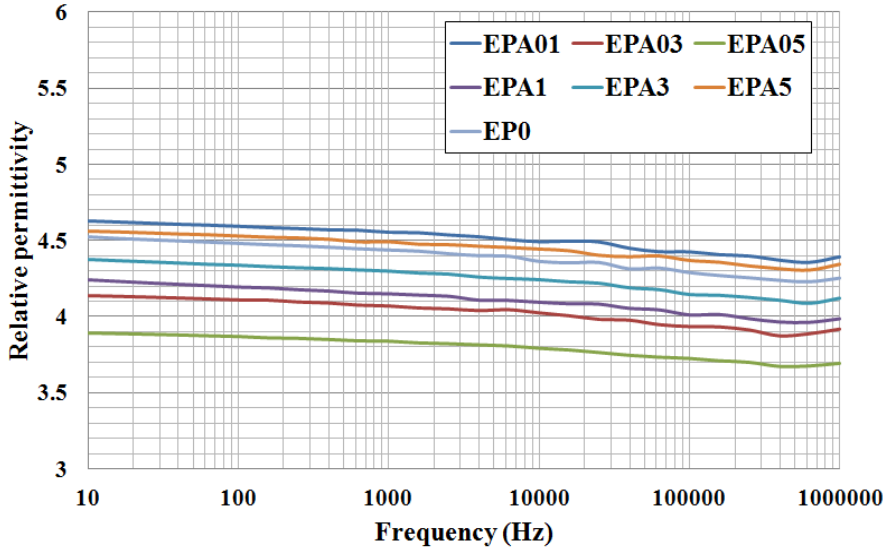

(b) Al_2O_3

Figure 44 Relative permittivity of epoxy resin sample loaded with different loading concentration of nano SiO_2 and Al_2O_3 fillers

5.3.3 Effects of Filler Loading Concentrations

The results in figure 44 show that for all epoxy/nanocomposites loading with SiO_2 and Al_2O_3 nano fillers and with different concentrations, there is a clear reduction in effective permittivity within the measured frequency range. It is known that the effective permittivity of the epoxy/nanocomposites is found to be governed by the polarization associated with epoxy and nano SiO_2/Al_2O_3 particles and it is also strongly influenced by the interfacial polarization at the interface between epoxy and nano particles as well. Therefore, such a reduction in effective permittivity had been observed as the frequency of the measurements will influence the polarization process. It is also known that in a typical resin system, the permittivity of epoxy is determined by the number of orientable dipoles within the system and their ability to orient under an applied electric field [77, 75]. Similarly, the increasing frequency of the applied filed will also result in reduction of SiO_2/Al_2O_3 fillers' inherent permittivity [76, 78]. According to the effective medium theories and mixing rules which are used to work out the permittivity within a polymer-particle heterogeneous system [70], the combination of both effect results in the reduction of epoxy/nanocomposites' permittivity with increasing frequency.

It also can be seen from the graph that when the nano size fillers are added into the base epoxy, the resulting relative permittivity is lower than the unfilled epoxy resin with the loading concentration up to a certain value. Figure 44 (a) shows the relatively permittivity of epoxy resin loaded with different concentrations of nano SiO_2 fillers. It can be seen that the EP2S01 sample has a similar permittivity as the pure resin sample, whereas EP2S5 sample has a higher permittivity. The rest of samples, on the other hand, have lower relative permittivity compared with pure resin sample. Another interesting observation is that the relative permittivity of epoxy/nano- SiO_2 composites seems to decrease as the loading concentration increases. The relative permittivity reaches its lowest value when the loading concentration is between 1% and 3%. Then the permittivity of epoxy-SiO_2 nanocomposites begins to increase as filler concentration increases further more. In figure 44 (b), the relatively permittivity of epoxy resin loaded with different concentrations of nano Al_2O_3

fillers also shows a similar trend. In the case of nano Al_2O_3 filler, only the relative permittivity of epoxy loaded with 0.1wt% nano fillers is slightly greater than the pure epoxy resin sample. Samples with all the other loading concentrations have lower relative permittivity compared with the unfilled sample. However, the relatively permittivity of epoxy/nano- Al_2O_3 composites also decrease to the lowest value and then start to increase as the loading concentration increases. The lowest peak of permittivity occurs between 0.5% and 1%. This observation is surprising as most of the earlier investigations showed that lower loading concentration (even much less than 1%) of nano-size fillers will lead to higher permittivity [15]. Earlier study also stated that the permittivity of epoxy/nanocomposites increases with increasing nano filler concentration in epoxy. However, there are also similar observations in the literature where the nanocomposites' permittivity drops at lower concentration and then increases again as the filler concentration increases to a high value (more than 0.5%) [79]. Such reduction of effective permittivity with increasing nano SiO_2 filler concentration must mean that the polarizations inside the composites are decreased.

The changes of effective permittivity with the presence of nano size filler and their loading concentration may be caused by the following reason. The influence of the filler's inherent permittivity on resulting nanocomposites' permittivity increases as the loading concentration increases. The permittivity of two phase dielectric satisfies the Lichtenecker-Rother mixing rule:

$$Log\ \varepsilon_c = x\ Log\ \varepsilon_1 + y\ Log\ \varepsilon_2 \qquad (47)$$

where, ε_c is the resultant composite permittivity, ε_1 and ε_2 are the permittivity of filler and epoxy and x, y are concentrations of filler and polymer. It is known that the nano size SiO_2 and Al_2O_3 fillers have higher permittivity compared with the net epoxy resin. That could be one of the reasons leading to an increase of effective permittivity with higher loading concentrations. Since the presence of nano size fillers tends to enhance the effective permittivity of resulting composites, the decrease of permittivity in epoxy nanocomposites with lower loading concentration becomes another interesting observation. It is believed that a decreasing in permittivity of epoxy resin/nanocomposites is

only possible to occur when a reduction in electrical polarization has happened within the composites. The interfacial or space charge polarization, which is caused by the space charge accumulation near the interface between base resin system and nano size particles, will affect the effective permittivity of composites. As the interfacial polarization only occurs under lower frequency ranges (up to 10^3 Hz), the presence of interfacial polarization normally leads to a clear variation of permittivity with respect to the measured frequency range. The effect of interfacial polarization on the decrease of permittivity in epoxy nanocomposites with lower loading concentration could be neglected as the measured results in this investigation show that the reduction of effective permittivity with lower nano loading concentration is irrespective to the frequency. Another possibility is the reduction of mobility of the dipolar groups within the composites will reduce the polarization within the composites [73]. The interaction between nano size filler and epoxy chain reduces the mobility of epoxy chain in the bulk material, which will result in a decreasing of the effective permittivity of epoxy/nanocomposites. When a small amount of nano filler is loaded into epoxy, due to the interaction between filler and epoxy chain, the thin immobile nano layers can be formed. Those thin immobile nano layers will restrict the mobility of the epoxy chain [25]. As the loading concentration increases, more immobile nano layer formed and the mobility of epoxy chain decreased continuously, resulting in reduction of nanocomposites' permittivity.

It can be obtained that epoxy-SiO_2 nanocomposite has lower permittivity compared with unfilled epoxy at lower loading concentration. Further increasing on loading concentration of the filler will result in increasing of nanocomposites' permittivity. Fig. 43 (b) also gives similar observations. It also needs to be noticed that epoxy-Al_2O_3 nanocomposites have higher permittivity compared with nanocomposites with nano SiO_2 fillers. This is because nano Al_2O_3 particles have a high permittivity than nano SiO_2 particles. So the type of nano fillers also has a significant influence on nanocomposites' permittivity.

5.3.4 Effects of Filler Size and Filler Type

The influence of filler size on epoxy/nanocomposites' permittivity can be seen from figure 45. The loading concentrations of all composites used in this part are 3wt%. It can be seen from the figure that the composite loaded with micro-size filler seems to have a much higher permittivity compared with all the nanocomposites and pure epoxy resin. The epoxy nanocomposites loaded with 20nm nano SiO_2 filler has the lowest value. The relative permittivity of nano Al_2O_3 filler (with an average diameter of 30nm) is just above the result of the one loaded with 20nm nano SiO_2 filler, and the epoxy loaded with 80nm nano SiO_2 fillers has higher permittivity than epoxy loaded with nano Al_2O_3 filler. Those measurement results show that the size of nano particles has a strong effect on the dielectric permittivity of result composites. A dual layer model has been proposed to help understanding the influence of filler size on the dielectric permittivity of result composites. The details of the model have been discussed in chapter 2.5. The dual layer model shows that the interfacial region between nano fillers and the polymer matrix has a significant effect on the dielectric permittivity of result composites. For the same loading concentrations, the number of nano particles with smaller size is more than the one with larger size. The volume of interfacial region is directly related to the size of nano filler as the size of nano fillers determinate the inter-particle distance and surface area of the nano fillers. Table 11 shows the inter-particle distance and the surface area have been calculated using the equation given by Imai and Tanaka et al [80]. It is clearly that the increase in the size of nano filler will result in a sharp increase inter-particle distance and a huge drop in the surface area of filler. The increase in filler size will result in a smaller volume fraction of interfaces and therefore enhance the interfacial or space charge polarization, as discussed in chapter 2. Also the increase in the dielectric permittivity of epoxy nanocomposites loaded with Al_2O_3 filler could be attributed to the difference in the permittivity of SiO_2 and Al_2O_3 fillers. It is known that the SiO_2 filler has lower permittivity compare with Al_2O_3 filler. The presence of nano Al_2O_3 filler will result in a larger field enhancement compared with SiO_2 filler and lead to a higher permittivity value.

Sample code	Particle type	Particle size (nm)	Inter-particle distance (nm)	Surface area (km^2/m^3)
EP2S3	SiO_2	20	31.6	12.89
EPA3	Al_2O_3	30	47.5	10.30
EP8S3	SiO_2	80	126.6	3.22

Table 11: Inter-particle distance and surface area of nano filler in epoxy nanocomposites

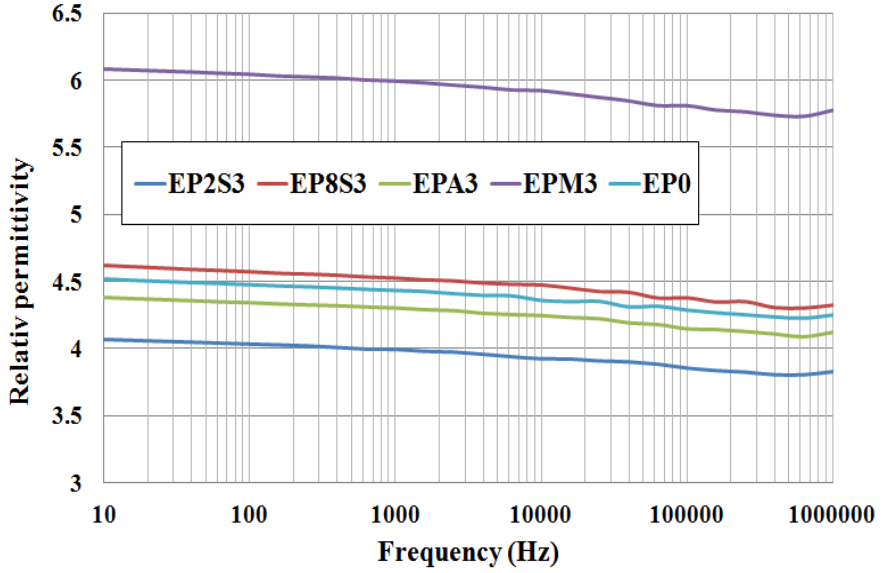

Figure 45 Variations of permittivity with respect to filler size

5.3.5 Tan Delta

The variation of tan delta value in both epoxy- SiO_2 / Al_2O_3 composites is presented in figure 46. The tan delta value of epoxy nanocomposites loaded with nano fillers decreases with the frequency within lower frequency ranges. The tan delta value for both epoxy nanocomposites reaches a minimum value around 100Hz and then begins to increase with the frequency. It can also be observed from figure 46 that the tan delta value of unfilled epoxy is higher than epoxy nanocomposites loaded with nano fillers under lower frequency range (less than 100Hz) at a lower filler loading concentration. When the frequency is higher than 100Hz, there is no significant difference in tan delta value between unfilled epoxy and both epoxy nanocomposites. The presence of nano

size particles seems to have a stronger influence in lower frequency range whereas the tan delta characteristic of net epoxy resin dominates the variation within a frequency range above 100Hz in the measurement range. Such a reduction in tan delta value, especially at a low frequency range, was also observed in other studies [51, 25]. As the electrical conductivity of epoxy composites contribution to its tan delta value, the variation of tan delta value in both net epoxy resin and epoxy nanocomposites in lower frequency range may result in the electrical conductivity of the nanocomposites having been affected by the presence of nano size fillers. As this study was carried out under room temperature, the influence of the relaxation time of the charge carriers on the electrical conductivity of epoxy nanocomposites can be ignored. Thus the number of charge carriers and applied frequency become dominating factors of the electrical conductivity of epoxy nanocomposites. As discussed in chapter 5.3.2, the presence of nano size fillers inside epoxy will restrict the chain mobility and result in reducing electric conductivity as such restriction limited the generation of mobile charge and the movement of charge carriers in polymer dielectrics [25, 74], especially at a lower frequency range where the conductivity will play a more important role. Thus the variation of tan delta value at low frequency range may be due to the influence of inorganic fillers' electrical conductivity. Another interesting observation is that the tan delta value in epoxy nanocomposites loaded with both 5wt% treated and untreated SiO_2 nano fillers are higher than the unfilled resin. At 5wt% filler loading concentration, the number of nano particles is more and the inter-particle distance is less compared with lower filler loading concentration, as shown in table 2. The nano fillers are more likely to attract to each other and the interfacial area around nano particles are likely to overlap. As a result of overlapping, charge carriers travel through the bulk of material much easier through the overlapping region, leading to an increase in the electrical conductivity of nanocomposites [28].

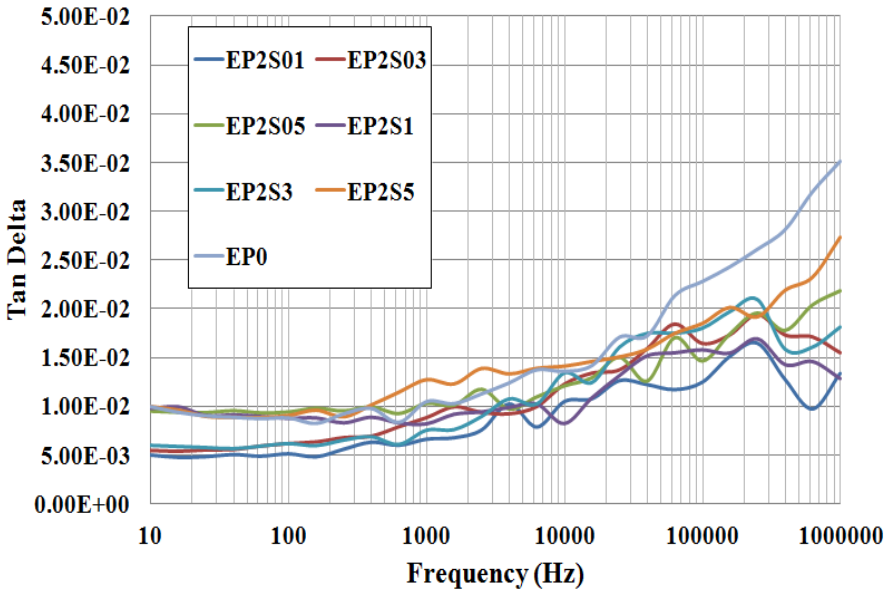

(a) SiO_2

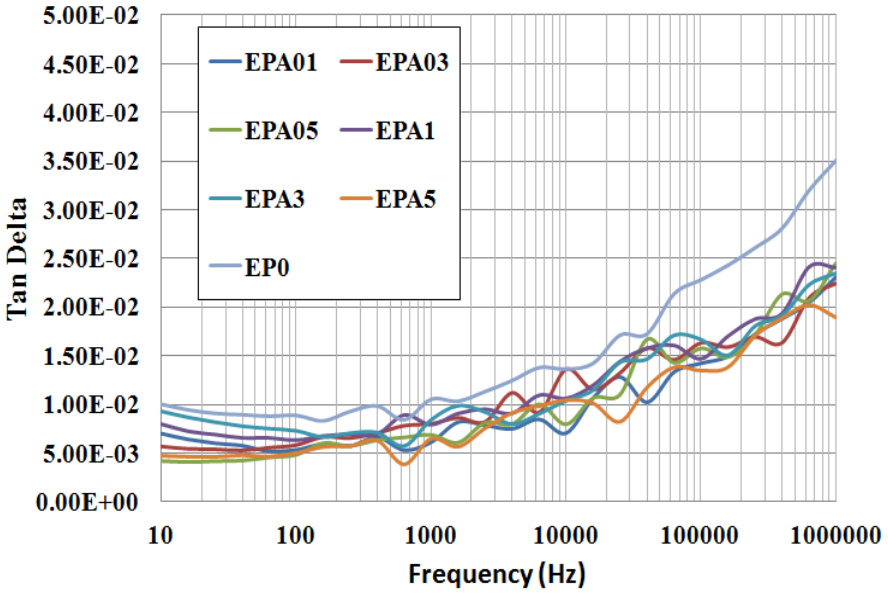

(b) Al_2O_3

Figure 46 Tan Delta value of epoxy resin sample loaded with different loading concentration of nano SiO_2 and Al_2O_3 fillers

6 AC Breakdown of Epoxy Nanocomposites

6.1 Sample under Study

The dielectric breakdown strength of epoxy nanocomposites loaded with different concentration of nano size filler have been studied in this chapter. To help understanding effect of the inter interfacial regions on the dielectric breakdown strength of epoxy nanocomposites, both nano SiO_2 particles with average diameter of 20nm and 80nm have been selected. In addition, unfilled epoxy resin and the epoxy microcomposites loaded with micro size SiO_2 particles are also prepared. The list of samples used in this chapter is shown in table 11.

Sample code	Particle wt%	Size of particle	Type of particle
EP0	0	-	-
EP2S03	0.3	20nm	SiO_2
EP2S05	0.5	20nm	SiO_2
EP2S1	1	20nm	SiO_2
EP2S3	3	20nm	SiO_2
EP2S5	5	20nm	SiO_2
EP8S03	0.3	80nm	SiO_2
EP8S05	0.5	80nm	SiO_2
EP8S1	1	80nm	SiO_2
EP8S3	3	80nm	SiO_2
EP8S5	5	80nm	SiO_2
EPM3	3	50µm	SiO_2
EPM5	5	50µm	SiO_2

Table 11: List of samples under study

6.2 Breakdown Theories

The concept of electrical breakdown is defined as insulators to lose their insulating properties under applied electric field. Such insulation breakdown is usually found in high voltage applications. The maximum voltage can be applied to an insulator before the insulating material failure is called breakdown voltage. It needs to be noticed that the breakdown voltage is not a fix value. This is because the breakdown is statistical in nature, thus the breakdown voltage for individual samples might be difference. When a breakdown value is given, it is normally means the average value of a large set of samples. Breakdown can occur in solid materials, liquids, gases and even in vacuum. There are many mechanisms of electric breakdown, such as electric impact ionization mechanism, thermal breakdown mechanism, avalanche breakdown mechanism, electro-mechanical mechanism and space charge breakdown mechanism etc. Those mechanisms are different from each other. Up to now, it is still unclear which mechanism is correct or if different mechanisms could work under different conditions.

In order to understand and explain the dielectric breakdown behaviours of polymer dielectric materials, the electrical, thermal, mechanical and chemical properties need to be all taken into considerations. But there are still lots of uncertain things even within the simplest polymer system. A comprehensive understanding is required in case of designing an epoxy nanocomposites with given dielectric properties. Although the polymer nanocomposites seems to have a better dielectric properties compared with the microcomposites, there are still lots of work need to be done before its potential can be fully explored.

The process that one charge carrier lose its energy by creating other charge carries is called impact ionization. Von Hippel proposed an electrical ionization model for this mechanism [81, 82]. According to Von Hippel, in polymer dielectric materials, the presence of positive ions in the material is hardly affected by the external applied filed, but the electrons are able to travel through the material if the applied field is higher enough. With a high electrical field, the electrons will move towards the anode and leaves the positive ions

behind. The positive charged ions will disturb the field distribution and lead to an ionization process. The repetition of such ionization process will weaken the insulation properties of material, and finally result in an electrical breakdown. Such breakdown mechanism is called electric impact ionization mechanism. This theory is simple compared with other theories as the theory only assumes that as the applied field is higher enough to let the electrons to travel and have a sufficient possibility to traverse the maximum value of the excitation function [83].

If the electrons have enough energy then they could knock other electrons out from molecules. When the applied field is higher enough, the impact ionization will repeat and result in materials losing their insulating properties. This is known as avalanche breakdown. During an avalanche breakdown, it usually involves a partial discharge (PD) to be initialised and growth until a conduction channel is formed which will result in an electrical breakdown [84]. Moreover, Sharbaugh [85] has developed a model which combines both avalanche and bubble theory together. He believed that both theories could coexist together and created a model to describe both theories in order to get accurate predictions.

In bubble theory, as the presence of bubbles in the dielectric materials, the discharges will damage the insulating properties of the material and lead to the dielectric breakdown. The dielectric breakdown strength will be much lower than it should be. The field inside the material will be reduced as the charged ions tend to be deposited on the cavity wall, which will reduce the discharges in bubbles and result in avalanche breakdown. Moreover, discharges in cavities may also form the tubular channels which will result in electrical tree. Sharbaugh believes that in case of the low pulse duration, the avalanche breakdown mechanism is sufficiently good in describing the materials' dielectric breakdown behaviours. As the pulse duration increases, the dielectric breakdown behaviours are dominated by both avalanche model [84] together the bubble theory [86] which works at high pulse duration.

For many dielectric materials, their insulating properties vary as the change of temperature due to their inherent properties such as crystallisation, dielectric permittivity and loss tangent. When dielectric materials are under an applied electric field, if the heat generated due to both conductivity and loss is higher than the amount of heat that can be dissipated, the temperature of insulating materials will keep increasing, which will finally result in material losing their insulating properties, it is known as thermal breakdown. It needs to be noticed that the breakdown strength of thermal breakdown is much lower than the electrical breakdown. An investigation about the effects of thermal condition on the breakdown strength of polyethylene has been carried out by Nagao [87]. In the study, when film PE samples break down at room temperature, a local joule heat will occur and there are points with high temperature in the film samples. It is observed that the conduction current at those points increases with time, which will result in a dielectric breakdown. Such observations suggest that a thermal process has taken place during breakdown, which refutes the idea that under room temperature, the dielectric breakdown is a pure electronic process [88]. As the local joule heating has been observed, it is suggested that there must be some weakness at the high temperature point in the film sample, which can be result from cracks, cavities or impurities. Nagao assumed that the dielectric molecules will move away from the electrode region under the effects of heating. This will result in a dielectric breakdown as the movement of molecules will thinner the sample at those points. The charging current can be written as

$$I = I_0 exp^{(\frac{-H}{kT})} \qquad (48)$$

Where I is the charging current, H is the activation energy, k is the Boltzmann constant, T is the absolute temperature and I_0 is a constant. It is necessary to notice that the effective magnitude of thermal process on dielectric breakdown is still unknown. For example, Hikita has found that the breakdown strength of PVDF at a temperature range of higher than 50 ^{o}C is decreased [89]. The decrease rate mainly depends on the rate of the applied electric field rather than the rate of thickness. So the ionic conduction was in charge of the breakdown. The thermal effect on the breakdown is still not cleared. One main issue is whether the increase in current is a result from the increase of temperature or

vice verse. At the moment most researches tend to agree that the overheating will result in a current increase [90]. But further investigation is still required before a conclusion can be drawn.

Except the mechanisms described above, other factors may also be involved in the breakdown process. One example is the presence of cracks, cavities and impurities which also have significant effects on materials' breakdown strength. Zeng et. al state that the breakdown is due to the weakness inside the dielectrics, such as cracks and voids. Their investigation results about the ceramic filled with SiC show that higher dielectric breakdown strength had been observed with ceramic samples with SiC fillers. When the SiC filler is dispersed into ceramic samples, they tend to stay inside cracks and cavities. The experiment result shows that the introducing of SiC filler increasing the base ceramic's breakdown significantly. It was concluded those impurities must have a strong effect on base materials' breakdown strength. Moreover, an equation has been developed by Wagner and Maxwell to described the insulating material that contains dispersed conductive particles as impurities,

$$\varepsilon' = \varepsilon'_{\infty}\left(1 + \frac{K}{1+\omega^2\tau^2}\right) \quad (49)$$

$$\varepsilon'' = \frac{k\varepsilon'_{\infty}(k\omega T)}{1+\omega^2\tau^2} \quad (50)$$

Where

$$K = \frac{9f\varepsilon_1'}{2\varepsilon_1'+\varepsilon_2'} \quad (51)$$

$$\tau = \frac{\varepsilon_0(2\varepsilon_1'+\varepsilon_2')}{\sigma_2} \quad (52)$$

$$\varepsilon'_{\infty} = \varepsilon_1'\left[1 + \frac{3f(\varepsilon_2'-\varepsilon_1')}{2\varepsilon_1'+\varepsilon_2'}\right] \quad (53)$$

Where ε_1 is the permittivity of base material, ε_2 is the permittivity of particle filler, σ_2 is the conductivity of particle filler and f is the spheres of volume. Those impurities are believed to be the path where the breakdown tends to occur.

The above is a brief summary of some popular breakdown theories that provide a basic understanding of the dielectric breakdown mechanisms. Currently there

are still many more breakdown theories that can be used to describe the breakdown mechanisms. But it is necessary to notice that at the moment, all current breakdown theories are more or less unable to match the experiment data. So a mixture of breakdown mechanisms is frequently used to explain the experiment results.

6.3 AC Breakdown Results

The Weibull distribution plots for both epoxy resin nanocomposites filled with 20nm and 80nm nano SiO_2 fillers, are shown in figures 47 and 48 respectively. In addition, pure epoxy resin and micro filled epoxy resin composites samples were also tested and the test results are compared with those obtained from epoxy resin nanocomposites. The maximum likelihood estimation (MLE) was used as the parameter estimator for the breakdown data, thus producing the Weibull parameters shown in Table 13 and Table 14 for 20nm and 80nm data respectively.

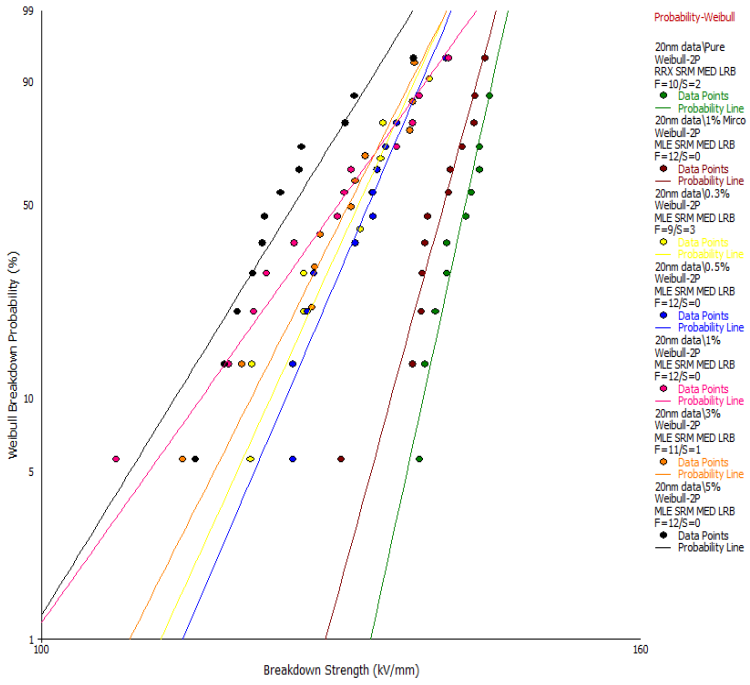

Figure 47 Influence of 20nm SiO_2 loading levels in epoxy resin on breakdown statistics relative to pure and micro-filled epoxy resin

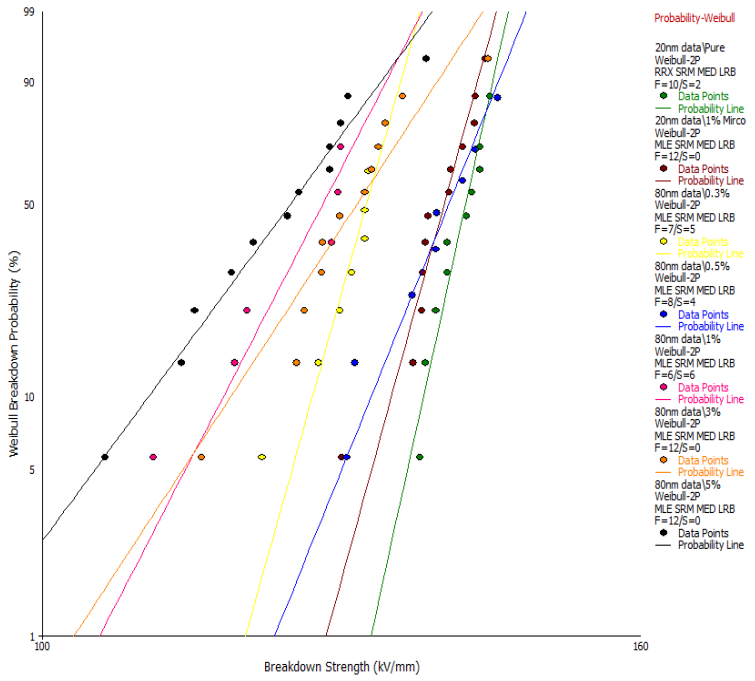

Figure 48 Influence of 80nm SiO_2 loading levels in epoxy resin on breakdown statistics relative to pure and micro-filled epoxy resin

Sample	Scale parameter (η) (kV/mm)	Shape parameter (β)
EP0	140.3	56.7
EPM1	138.2	45.7
EP2S03	129.9	27.3
EP2S05	130.9	29.0
EP2S1	128.9	17.5
EP2S3	129.1	24.6
EP2S5	124.1	20.2

Table 13: Table of Weibull parameters from MLE for all 20nm data

Sample	Scale parameter (η) (kV/mm)	Shape parameter (β)
EP0	140.3	56.7
EPM1	138.2	45.7
EP8S03	130.0	44.5
EP8S05	139.2	30.9
EP8S1	126.5	24.1
EP8S3	130.5	19.0
EP8S5	124.2	16.9

Table 14: Weibull parameters from MLE for all 80nm data

For epoxy nanocomposites with SiO_2 fillers, lower breakdown strengths are observed. It can be seen from the 20nm plot that, comparing with both pure and micro filled epoxy resin, for all epoxy resin nanocomposites, there is a reduction in breakdown strength. As shown in figure 47, the EPM1 sample shows marginally lower breakdown strength (η) and slightly higher scatter (β) compared to the pure sample. The epoxy resin nanocomposites specimens, on the other hand, show a clear reduction in the breakdown strength of at least 10kV/mm, with EP2S5 specimens showing the worst characteristics, being 16.2kV/mm lower than pure epoxy resin samples, at 124.1kV/mm.

As shown in figure 48, the nanocomposites samples loaded with 80nm SiO_2 is very similar to the 20nm ones, as all specimens showing an almost identical reduction in breakdown strength. The EP2S05 sample is only marginally lower than the EP0 sample and EPM1 sample, where as all the other nanocomposites show a clear reduction in the breakdown strength of at least 10kV/mm.

Another interesting observation is the presence of nano size fillers seems reducing the shape parameter. For epoxy resin loaded with 20nm nano SiO_2 fillers, the shape parameter decreases as the loading concentration increases. However, when the shape parameter reaches its lowest point at 1wt% loading concentrations, it starts to increase as further increases of loading concentrations. The shape parameter of epoxy resin loaded with 80nm nano SiO_2 fillers, on the other hand, has a continuous decrease as the loading

concentration increases. As the shape parameter represents the consistence rate of breakdown strength, a higher shape parameter means the composites' breakdown strength is more consistent. Thus the presence of untreated nano size fillers seems to have negative effect on epoxy composites' breakdown stability. This is because the untreated nano size fillers tend to agglomerate together to form large particles. Those large particles may act as impurities that affect the breakdown strength of nanocomposites. So the presence of nano size fillers will affect the consistence of resulting nanocomposites' breakdown strength, especially at higher loading concentration where the nano size fillers have much higher possibility of agglomeration with each other.

In summary, the presence of untreated nano size fillers shows no improvement in epoxy composites' dielectric breakdown strength. Similar results were also observed by Imai et al [80] and Singha et al [15]. Singha et al, observed a significant reduction in breakdown strength when a range of loading levels of epoxy-SiO2 and epoxy-Al_2O_3 composites were ramp tested. The addition of nano-particles to epoxy resin does however significantly reduce the shape parameter (β), a result which is contrary to several other studies, including Singha et al and Hu et al [15, 91].

6.3.1 Effect of Filler Loading Concentration on AC Breakdown Strength

When the nano size fillers are dispersed into the polymer, the morphology of the resulting nanocomposites changes as an interfacial region between nano particles and the polymer matrix has been generated due to the interaction between nano particles and the polymer matrix. As discussed in the previous section, the specific surface is inversely proportional to the diameter of the particle. The percentage of surface atom will increase sharply as the size of fillers decreases to nano scale. The interfacial characteristic between polymer matrix and nano fillers seems to play an important role in the insulation performance of polymer nanocomposites due to the large interfacial area between nano particles and the polymer matrix. The dual layer model can be used to help understanding the interfacial behaviours [77] and it is discussed in

chapter 2. The EP2S03 sample has lower breakdown strength than EP0 sample. In this case the number of nano particles is lower, so the inter-particle distance is larger as shown in table 15. The inter-particle distance and the surface area have been calculated using the equation given by Tanaka et al [25]. Larger inter-particle distance leads to a larger volume fraction of the loosely bound region. Early studies show that the mobile charge carriers could travel easier through the loosely bound region, so those charge carriers could travel through the bulk of polymer nanocomposites much easier under the applied filed [92]. Therefore the final breakdown strength is reduced. Such reduction in breakdown strength could be further enhanced by the inhomogeneously dispersion of nano fillers. As the nano SiO_2 filler has higher dielectric permittivity compared with epoxy resin, a field enhancement will occur near the filler. Also there might be voids and defeats caused during sample preparation process, which will cause further field enhancements. Such filed enhancement could result in partial discharges and reduce the breakdown strength as well. On the other hand, when charge injection taken place in the bulk of the specimens, counter ions will be adsorbed around the nano fillers as a result of electrostatic Coulomb force and Van der Waals force. The presence of such electric double layer will result in a strength inner field at the tightly bound region. When the charge carries are injected into the polymer nanocomposites, the nano fillers can scatter the charge carriers through the bulk of specimens and result in higher breakdown strength. However, the effect of electric double layer on the dielectric breakdown strength of EP2S03 sample can be neglected due to the large inter-particle distance and the small surface area. The combination of effects above causes the reduction of the breakdown strength in epoxy nanocomposites. When the filler loading concentration increase to 0.5wt%, there is a slight increase in the breakdown strength compared with EP2S03 sample. But its breakdown strength is still lower than the breakdown strength of EP0 sample. In case of the EP2S05 sample, the number of nano particles is slightly greater than the EP2S03 sample. Compared with EP2S03 sample, it has shorter inter-particle distance and larger surface area. The effect of electric double layer becomes more important and leads to a slight increase in breakdown strength. Further increase the filler loading concentration will result in a shorter inter-particle distance and larger surface

area as shown in table 15. As a combination effect of large loosely bound region around the nano particles and the diffuse charge layers, a small decrease in breakdown strength has been observed in both EP2S1 and EP2S3 samples. When the filler loading concentration increases to 5wt%, there is a clear reduction of 6kV/mm in breakdown strength compared with EP2S3 sample. As shown in table 15, when the filler loading concentration increases to 5wt%, the number of nano particles becomes much greater. A much smaller inter-particle distance of 29.3nm and a much larger surface area of 17.35 km^2/m^3 have been estimated. With such a small inter-particle distance, the nano particles are more likely to be agglomerated together. Such a reduction might be due to the overlapping of loosely bound region between different nano particles as a result of the reduction in inter-particle distance. Such overlapping of loosely bound region could form conductive paths that allow charge carriers travel through much easier.

Sl. No.	wt%	Inter-particle distance (nm)	Surface area (km^2/m^3)
EP2S03	0.3	114.6	1.02
EP2S05	0.5	92.7	1.70
EP2S1	1	68.4	3.41
EP2S3	3	39.5	10.31
EP2S5	5	29.3	17.35

Table 15: Inter-particle distance and surface area of nano filler in epoxy nanocomposites

6 .3. 2 Effect of Filler Size in AC Breakdown Strength

As discussed in chapter 2, the interfacial region between nano particles and the polymer matrix has a significant effect on the breakdown strength of epoxy nanocomposites. It is necessary to consider the influence of filler size on the breakdown strength of resulting composites. Both nano SiO2 fillers with 20nm and 80nm diameter were filled into epoxy resin and the ac breakdown strength of result epoxy nanocomposites filled were measured. According to the equation given by Tanaka et al [21], the inter-particle distance and surface area of nano filler in epoxy nanocomposites loaded with 20nm and 80nm nano particles has also been calculated, as shown in table 16. It can be observed from the result that the dielectric breakdown strength of in epoxy

nanocomposites loaded with 20nm and 80nm nano particles is similar within the measured loading concentration rage. However, compared with epoxy nanocomposites loaded with 20nm nano fillers, higher shape parameters are observed in epoxy nanocomposites loaded with 80nm nano fillers under lower loading concentration. Compare with epoxy nanocomposites loaded with 20nm nano fillers, the nanocomposites loaded with same concentration of 80nm nano fillers have much larger inter-particle distance therefore resulting in a much smaller surface area, as shown in table 16. The larger particle diameter also results in less number of particles under same loading concentration. Therefore the interfacial region between nano particles and polymer matrix becomes smaller. The reduction of loosely bound region will result in higher breakdown strength, as discussed in chapter 2. Kozako et al show that the partial discharge resistance increase as the filler size decreases [22]. On the other hand, the difficulty of electron transport under the applied field also depends on the probability of electron collision with nano particles. Larger particle diameter will lead to a smaller adsorbed effect to the injected electrons as a result of large inter-particle distance and smaller surface area. Similar breakdown strengths have been observed in nanocomposites loaded with 80nm nano fillers. The large reduction in shape parameter observed in epoxy nanocomposites loaded with 20nm nano fillers is believed due to the agglomeration of filler. As shown in chapter 2, the dispersion of epoxy nanocomposites loaded with untreated nano particles is poor compared with the epoxy nanocomposites loaded with treated nano particles. Therefore there is a possibility that the nano fillers tend to agglomerate with each other. Early studies have already shown that the agglomeration of nano filler has a negative effect on the breakdown strength of result nanocomposites. So the epoxy nanocomposites loaded with 20nm untreated fillers has lower shape parameter compared with unfilled resin within measured range. With large particle diameter, the number of particle is less and the inter-particles distance is larger. So the probability of particle agglomeration is less under lower loading concentrations. The nanocomposites loaded with 80nm untreated fillers has higher shape parameter compared with epoxy nanocomposites loaded with 20nm untreated fillers under lower loading concentration. But when the filler loading concentration is higher than 1wt%, the probability of particle agglomeration in epoxy nanocomposites loaded with

80nm untreated fillers becomes much greater as the inter-particle distance decreases. Thus for epoxy nanocomposites loaded with 20nm and 80nm nano particles, there is no significant difference in shape parameter under higher filler loading concentration. In case of the microcomposites, the number of particles is much less. The inter-particle distance is much larger and the influence of interfacial region can be neglected. Epoxy resin load with 1wt% micro size filler only has a small reduction compared with the unfilled resin. The reduction in both breakdown strength and shape parameter is believed to be due to the field enhancement caused by higher permittivity of the inorganic filler and the presence of voids and defects.

Sl. No.	wt%	Average particle diameter (nm)	Interparticle distance (nm)	Surface area (km^2/m^3)
EP2S03	0.3	20	114.6	1.02
EP8S03		80	366.9	0.31
EP2S05	0.5	20	92.7	1.70
EP8S05		80	296.8	0.53
EP2S1	1	20	68.4	3.41
EP8S1		80	218.8	1.06
EP2S3	3	20	39.5	10.31
EP8S3		80	126.6	3.22
EP2S5	5	20	29.3	17.35
EP8S5		80	93.7	5.42

Table 16: Inter-particle distance and surface area of nano filler in epoxy nanocomposites loaded with 20nm and 80nm nano particles

7 Space Charge Behaviours of Epoxy Nanocomposites

7.1 Sample under Study

In this chapter a comparative study on the space charge behaviours of epoxy nanocomposites has been carried out. Epoxy nanocomposites thin films loaded with different concentrations of nano SiO_2 and Al_2O_3 particles have been selected for the study. In addition, pure epoxy resin samples were also prepared and tested. The thickness of the samples used in the space charge measurement in this chapter is 150 μm. The details of samples are given in table 17.

Sample code	Particle wt%	Size of particle	Type of particle
EP0	0	-	-
EP2S01	0.1	20nm	SiO_2
EP2S03	0.3	20nm	SiO_2
EP2S05	0.5	20nm	SiO_2
EP2S1	1	20nm	SiO_2
EP2S3	3	20nm	SiO_2
EP2S5	5	20nm	SiO_2
EPA01	0.1	30nm	Al_2O_3
EPA03	0.3	30nm	Al_2O_3
EPA05	0.5	30nm	Al_2O_3
EPA1	1	30nm	Al_2O_3
EPA3	3	30nm	Al_2O_3
EPA5	5	30nm	Al_2O_3
EPM1	1	50μm	SiO_2
EPM5	5	50μm	SiO_2

Table 17: List of sample under study

The process of the PEA measurements can be split into two parts. The first part includes volts on and the volts off measurements. The volts on measurements are taken while the voltage is applied to the sample whereas the volts off measurements are taken as the applied voltage is removed. Decay measurements, on the other hand, are taken after the charge processes, and the voltage has been removed permanently. Before the measurements, a reference measurement also needs to be taken. For all samples, the voltage for reference measurement is set to 1.5kV. The applied voltage during the volts on measurements is 6kV, and the sample thickness is 200μm. Thus the applied electric field was 30kV/mm. Moreover, for the clarity, only selected data from volts off and decay measurements are presented in the result.

7.2 Charge Injection, Transport and Trapping

Epoxy resin is not supposed to conduct current as it is insulator. However, under sufficient high electrical field, electrical charges are able to be injected into the bulk of epoxy from the external electrodes and those charges may also travel across the bulk under the external electric field. In this case the electrical properties of epoxy resin may be changed. Such change is not only due to high applied field but also temperatures, electrode-polymer interface and so on. For example, early researches show that many phenomena observed from polymer insulator such as space charge limitation and ohmic currents, electron and hole injection and ionization can be result from the electrode-polymer interface [93]. Early research also found that mechanisms used to describe conduction and charge transportation within conductors and semiconductor does not work for polymer insulators. Instead, charge trapping, tunnelling and hopping conduction dominates charge transportation in polymer insulators [94, 95, 93, 96]. To help understanding breakdown and aging mechanisms in insulators, it is important to understanding the charge transportation in polymer insulators.

7.2.1 Charge Injection

When a sufficient high electric field is applied to the polymer insulators, electric charges (electrons and holes) will be injected into the bulk of polymer from the external electrodes. In this case, electric charges need to overcome a physical potential barrier between external electrode and polymer insulator [94]. Such potential barrier can be affected by the electrode-polymer interface conditions. Early investigations show that the electrode-polymer interface is complicated [96, 34]. Two main mechanisms have been developed to describe the charge injections into polymer bulk through electrode-polymer interface. They are known as Schottky injection and Fowler Nordheim injection.

The Schottky injection is one of the methods to describe how electrons are injected into polymer bulk through the electrode-polymer interface if the electrons have sufficient energy to overcome the potential barrier [96, 94]. In this theory it is assumed that when electric charges are injected into polymer bulk, an electrostatic attraction will be generated between the electrode and injected charges, as the electrode is positively charge due to losing electrons. Such electrostatic attraction will result in a change in potential barriers as a result of electron potential energy.

The current density *J* can be given by the following equation [97]

$$J = \frac{4\pi e m {k_B}^2 T^2}{h^3} \left[exp \left(\frac{-\phi + \frac{e}{2}\sqrt{\frac{eE}{\pi\varepsilon}}}{k_R T} \right) \right] \quad (54)$$

And it can be further summarized into the following equation

$$J = AT^2 exp\ (-\frac{\phi - \beta_s\sqrt{E}}{kT}) \quad (55)$$

$$\beta_s = \sqrt{\frac{e^3}{4\pi\varepsilon_0\varepsilon_r}}$$

Where *J* is the current density, *A* is the Richard-Dushman constant, ε_0 is the permittivity of free space, ε_r is the relative permittivity of dielectric materials and *E* is the electric field across the electrode-polymer dielectric interface

In the case of sufficient high applied electric field, the width of potential barrier can be reduced to very thin. In such situations, the classical mechanisms are no longer valid. Instead, the quantum tunnelling effect will play an important role [96]. It means that particles will exhibit a particle-wave duality and as an effect of quantum mechanical effect, electrons do not need to have enough energy in order to overcome the potential barrier and get into the polymer bulk rather than tunnel through the thin barrier. The Fowler Nordheim injection is used to describe such phenomenon.

In this case the current density *J* can be written as the following equation [97]

$$J = A(T, \phi)E^2 exp\,[\frac{B(\phi)}{E}] \qquad (56)$$

Where $A(T,\phi)$ and $B(\phi)$ is based on the magnitude of potential barriers and also the temperature.

7.2.2 Charge Transport

When the external applied electric field is low, the Ohm's law can be simply applied to describe the voltage-current characteristic. In such situations, the conduction is known as "Ohmic conduction" in which the electric charge carriers are travelled through the material bulk with velocity that is proportional to the external applied field. In this case the current density *J* is proportional to the applied field *E* and the following equation is introduced

$$J = ne\mu E \qquad (57)$$

Where the conductivity σ is

$$\sigma = n\mu e \qquad (58)$$

But in case of the polymer dielectric materials, the electrons and holes are unlikely to move freely inside polymer bulk under lower applied electric field. Instead, those charge carriers that have enough energy are more likely to be trapped in traps (charge trapping process is described in the following section) within material bulk. The trap-limited mobility is commonly used to describe such phenomenon. Blythe has proved this model on PE and it looks that the model can also be used on other amorphous solids as well [98]. Under low field, the charge carriers' mobility can be summarised by Arrhenius Law

$$\mu = \mu_0 exp\ (\frac{-E_a}{kT}) \quad (59)$$

Where k is the dependence rate of constant of chemical reaction on temperature T and Ea is the active energy. With sufficient high electric field, the voltage-current characteristics do not obey Ohm's law any more. Instead, the current density begins to increase super-linearly as the applied electric field increases. Both Space Charge Limited Current (SCLC) mechanism and Poole Frenkel mechanism can be used to describe the voltage-current characteristics.

Usually the SCLC can be found in thin films. A schematic diagram of current density against voltage in case of SCLC is shown in figure 49. When a voltage is supplied to the polymer dielectric materials from external electrodes, the electrons travels through the bulk of materials under Ohm's law. A space charge (SC) region will build up under the charge injection process. If the external applied field is higher enough, the SC field will begin to limit the flow of current. In this situation the Ohmic conduction is replaced by trap-limited SCLC. Under the trap-limited SCLC, the current density can be affected by charge injection from electrodes, mobility of carriers and polymer dielectric materials' trapping properties. By assuming the charges are highly injected from electrodes and the space charge distribution is uniform, the charge density J can be written as the following equation

$$J = \theta \frac{9\varepsilon_0 \varepsilon_r \mu V^2}{8d^3} \quad (60)$$

where θ is the ratio of electrons in the conduction band and traps, μ is the mobility of charge carriers, V is the applied voltage from electrodes and d is the thickness of the polymer dielectric materials [34]. When the applied voltage increases, at a certain point the Fermi energy level exceeds the potential barrier of traps, there will be a sudden jump in current density. This is known as the trap-filled limit. If the voltage increases furthermore, a new SCLC will be generated and this is the trap free SCLC.

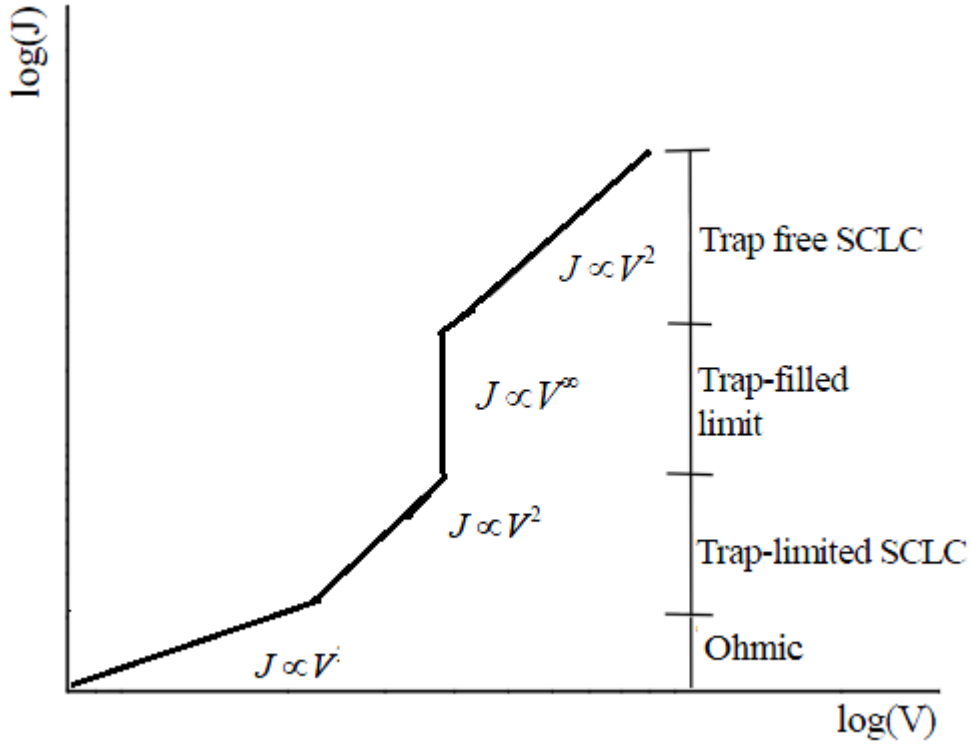

Figure 49 Current density vs. voltage in case of SCLC (ideal case)

The Poole Frenkel mechanism is similar to the Schottky injection mechanism which occurs at the electrode-materials interface but it is a bulk effect [96]. Assuming electrons have been trapped in donor state (details can be seen at the following section), it requires certain energy to overcome the positional barriers in order to escape from the trap. With an external electric field applied, the potential barrier will be reduced and the reduction is proportional to the square root of the field. In this case the conductivity can be written as

$$\sigma = \sigma_0 exp\ (\frac{\beta_{PF}\sqrt{E}}{2kT}) \quad (61)$$

Where

$$\beta_{PF} = \sqrt{\frac{e^3}{\pi\varepsilon_0\varepsilon_r}} \quad (62)$$

And σ_0 is a constant.

It can be seen from the above equation that Poole Frenkel mechanism is highly influenced by the temperature *T*. According to this mechanism, it is unlikely to generate free electrons at room temperature.

7.2. 3 Charge Trapping

For polymer dielectric materials, it is hard for charges to move in the material bulk under ordinary conduction mechanisms due to their extremely low conductivity. Polymer molecules are joined by covalent bond to form molecule chains which is known as polymer chains. The band mechanisms can be introduced. Those chains are also joined by Van der Waals attractions which mean that no valance band exists between polymer chains. Such phenomena limit the movement of charge and the generation of mobile charges within polymer dielectrics. Moreover, the charges inside polymer bulk can be further limited by the presence of traps inside the polymer dielectric bulk. Physical attributes such as polarised states, broken bonds within the crystalline structure, dislocations foreign particles, cross-linking impurities and additives that result in localised states are known as traps. Traps can be described as a potential barrier that blocks the charge carriers to move in the conduction or valance band [99]. Acceptor is used to describe those traps for electrons whereas donor is used to describe those traps for holes [100]. Charges can stay inside traps from seconds to a long time (e.g. 1 second to 1 week). Enough energy is required for charges to overcome such potential barriers in order to leave the traps, which is known as detrap. Charges are also able to move from one trap to a nearby trap due to hopping and tunnelling, which depends on the distance between those two traps [94, 93].

Generally speaking, traps can be divided into deep traps and shallow traps. Deep traps are normally located at 0.8 to 1.4 eV below the conduction band where as shallow traps are located at 0.1 to 0.3 eV below the conduction band. When an external field is applied to the polymer dielectric materials, all charge carries begin to move under the same force but with different velocity. This is known as fast and slow moving charges. The fast moving charges are those free mobile charges and also charges that are trapped in the shallow traps, whereas the charges trapped in the deep traps are normally slow moving charges. Basically, the deep traps tend to trap charges with longer time as it requires high energy to overcome the potential barrier. Those deeply trapped

charges are likely to form space charge and therefore increase the net space charge significantly.

7.3 Space Charge and Measurement Method

7.3.1 Concept of Space Charge

The effect of space charge within solid dielectrics has been studied relentlessly due to its significant affects on solid dielectrics. Space charge is a surplus of charge carries (include electrons, ions and holes) distributed over a region of space. These electric charges are moving around inside the materials and being trapped. Trapped charges may result in space charge limited current (SCLC) which could lead to electrical breakdown or ageing under sufficient high electric field [100]. Space charge usually occurs in dielectric materials and it is one of the major factors that determine materials' dielectric behaviours, such as breakdown strength [101]. Earlier studies also showed that the presence of nano fillers in epoxy resin affects the space charges accumulation in epoxy resin. Epoxy nanocomposites seem to accumulate less charge compared with filler-free epoxy resin. It was also observed that epoxy nanocomposites have faster charge dynamics, especially for negative charges.

The presence of space charge may be due to charge injection from electrode or be generated within the solid dielectrics. The reason of space charge formation can be classified into the following mechanisms:

1. Charge injection from external electrodes
2. The orientation of dipole movements inside dielectric materials results from applied electric field
3. Ionisation of impurities inside the dielectric materials results from the applied electric field

The electron injection from the cathode and electron extraction (hole injection) from the anode are the dominated mechanism for charge emission in most

polymer dielectric materials. It can be also described as electron injection from the cathode and hole injection from the anode, which is widely used to describe charge carriers inside polymer dielectric materials. In case of charge injections from external electrodes, the electrons and holes travel across the polymer-electrode interface and get into the bulk of dielectrics. The defects on material surface, the impurities may affect the charge injection as the charge injection highly depends on the interface condition between electrode and polymer dielectrics [100, 102, 103, 104].

When an external electric field is applied to the polymer dielectrics, the dipoles inside polymer dielectrics will be orientated under the applied electric field. This is known as dipole polarization or orientation polarization. The mechanism of such movements and its effect on the dielectric behaviours of the material has already been discussed in chapter 2.3. The orientation of dipole movements will result in a space charge accumulation over a range of space inside polymer dielectric materials. The ionisation of possible chemical species within the bulk of dielectric materials, such as cross-linking residues and impurities, is another reason for space charge accumulation inside the bulk of dielectric materials [104]. The applied voltage and temperature also have significant effects on the space charge formation under high voltage applications. Therefore, the observation of space charge distributions may changes even within the same sample [100, 104].

The space charge density as a combination of both current density and inhomogeneous resistivity over a range of space can be summarized as below:

$$\zeta(x) = J\varepsilon\frac{d\rho(x)}{dx} \qquad (63)$$

Where ζ is the space charge density, J is the current density, ε is the absolute permittivity where $\varepsilon=\varepsilon_r*\varepsilon_0$ and ρ is the electrical resistivity [105].

7.3.2 Homocharge and Heterocharge

In the concept of space charge formation, homo charge and hetero charge are frequently used to describe the space charges' polarities. Homocharge is space

charge that has the same polarity to the nearby electrode, whereas heterocharge is space charge that has the opposite polarity. Figure 50 shows an example of both homocharge and heterocharge. The presence of space charge inside polymer dielectric material bulk will influence the local electric field inside polymer bulk, therefore the net space charge distribution inside polymer dielectric materials is important as the change of local electric field inside polymer insulator affects the breakdown strength of material and it also becomes difficult to predict the lifetime of polymer insulators.

Charge injections from electrodes will generate homocharges near the electrodes. Such charges are expected to increase the electric stress in the sample bulk but reduce the electric stress at the electrode interface. Heterocharges could be caused due to the ionization of small molecules and these charges are expected to have opposite effect on electric stress inside polymer sample compared with homocharge.

It is also necessary to notice in the later discussion that, as the PEA technique used in this project only measures the net charge distribution, both the presence of homocharges and heterocharges might be cancelling out each other. It means that even both types of charges exist inside the sample, only the one with higher amount could be seen. Thus homocharges and heterocharges is actual means the net charge of an unbalance of both positive and negative charges.

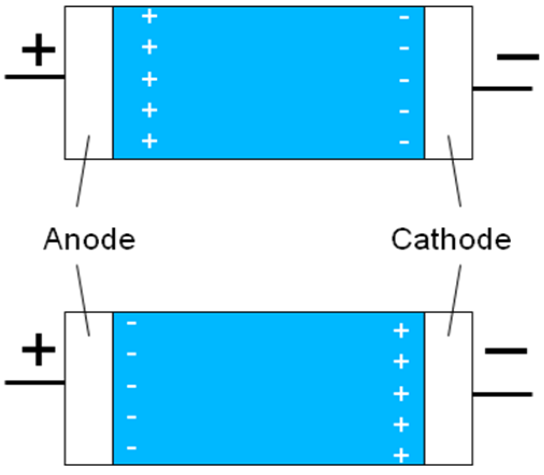

Figure 50 Homocharge and heterocharge

7.4 Space Charge Measurements Results

The process of the PEA measurements can be split into two parts. The first part is volts on and the volts off measurements. The volts on measurements are taken while the voltage is applied to the sample whereas the volts off measurements are taken as the applied voltage is temporarily removed. Decay measurements, on the other hand, are taken after the charge processes, and the voltage has been removed permanently. Both volts on measurements and volts off measurements last for two hours. The decay measurement lasts for one hour. Before the measurements, a reference measurement also needs to be taken. For epoxy resin samples, the voltage for reference measurement is set to 2kV. The applied voltage during the volts on measurements is 6kV, and the sample thickness is 200 µm. Thus the applied electric field was 30kv/mm. The readings are taken by using the software called "easy data" at 15 seconds, 30 seconds, 1 minute, 2 minutes, 3 minutes, 4 minutes, 5minutes, 10 minutes, 20minutes, 30 minutes, 45 minutes, 60 minutes, 90 minutes and 120 minutes for both volts on and volts off measurements. For the clarity, only selected data are presented in the results. The readings for the decay measurements are only for the first 60 minutes.

Space charge formation in dielectric material is closely related to the applied electric stress. Figure 51 is a typical diagram of space charge measurement result. When a sufficient high field is applied to the material, space charge starts to occur.

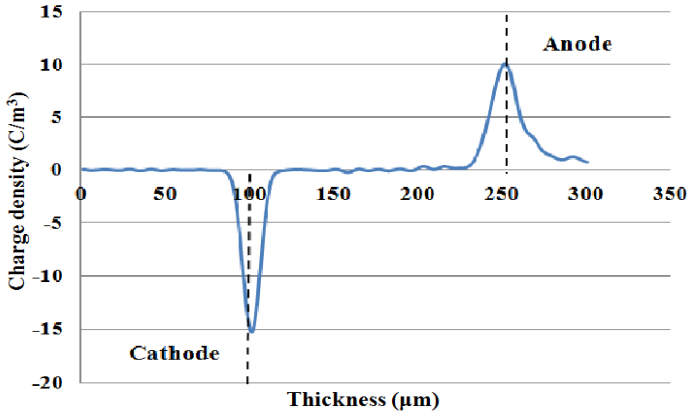

Figure 51 Typical waveform of space charge measurement

7.4.1 Effects of Nano Filler

The minimum applied field required for space charge to occur is known as the 'threshold field'. The simple and easiest way to identify the 'threshold field' is to perform a ramp test. In this test, the voltage is increased quickly and the peak voltages at the two electrodes are recorded. In the absence of space charge, the peak voltage versus the applied voltage should have a linear relationship. On the other hand, the peak voltage deviates from the linear line in the presence of space charge. The form of deviation varies depending on the nature of space charge. It bends downwards if charge injection from the electrode occurs (homocharge) and upwards in the case of formation of heterocharge. In the present tests, PEA measurements were carried out 1 minute after the voltage was increased from 0 kV to 8 kV at a step of 0.5 kV. The results are shown in figure 52 for all five samples.

The ramp testing results are shown in table 18. It can be seen that there are some differences in the 'threshold voltage' at which the peak voltage starts to deviate from the linear line. Since they all bend inwards, indicating charge injection from the electrodes. Compared with the EP0 sample, the EP2S1 sample has slightly higher threshold field before the space charge starts to accumulate. A further increase in filler loading concentration will result in a reduction in the threshold field.

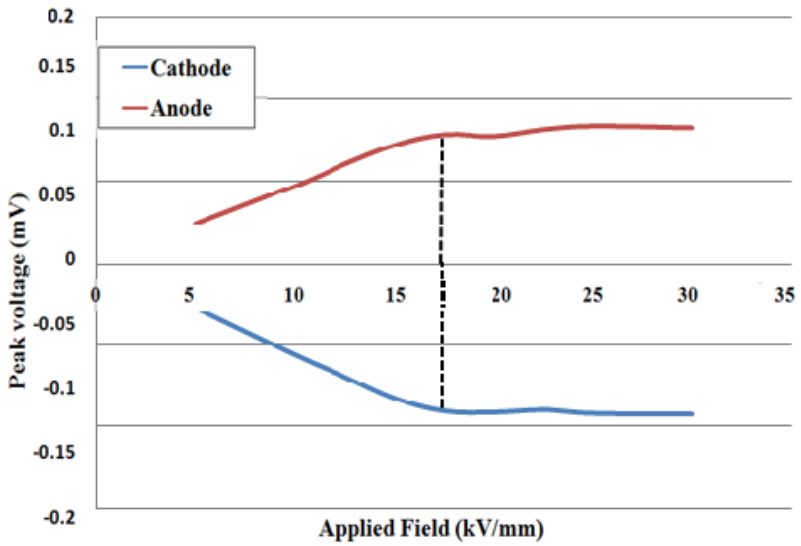

(a) Unfilled Resin

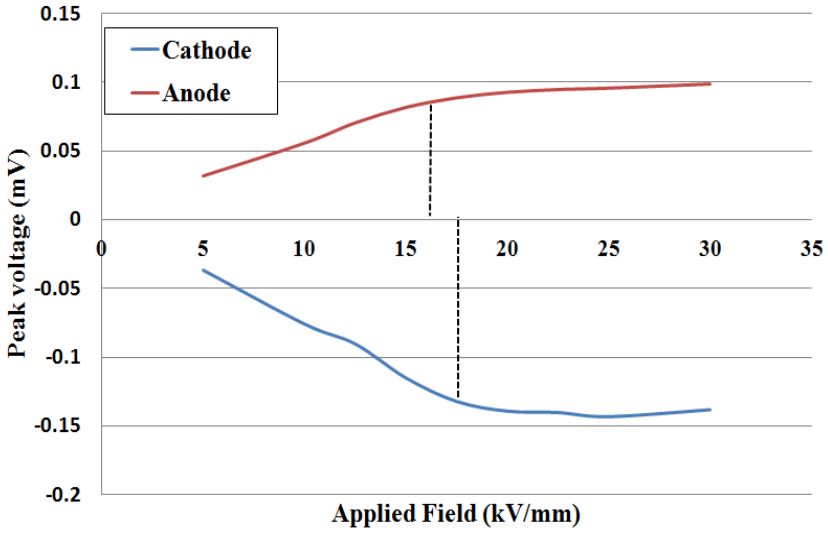

(b) EP2S1

Figure 52 Threshold fields of both unfilled resin and epoxy-SiO_2 nanocomposites

Sample code	Threshold field at Cathode (kV/mm)	Threshold field at anode (kV/mm)	Peak voltage at cathode (mV)	Peak voltage at anode (mV)
EP0	16.3	16.2	-0.09	0.078
EP2S1	18.7	16.4	-0.139	0.088
EP2S3	17.3	15.1	-0.185	0.108
EP2S5	16.1	14.9	-0.251	0.122
EPM5	17.4	16.0	-0.26	0.21

Table 18: Threshold field of epoxy composites

7.4.2 Effects of Filler Loading Concentration

The "volts-off" space charge accumulation of specimens with different nano SiO_2 filler concentrations is shown in figure 53. It can be seen from figure 53 (a), a large amount of homocharges is observed for EP0 sample，especially near the cathode side. As the duration of the applied voltage increases, the amount of charge in the specimen increases as well. The homocharge usually occurs when the injected charges are trapped to the interface between base epoxy and nano fillers under the applied field. Charges are dictated by

homocharges, which means that the charge injection takes place from both electrodes [106]. The heterocharges which is caused by ionization process may also present in the specimen. However, as the PEA system only measures the net charges, it might be covered by the charge injection. Compared with the unfilled samples, Figure 53 (b) shows a similar charge distribution in EP2S1 sample. However, it is noticed that EP2S1 sample has a slower initial charge build-up rate. The magnitude of charges in EP2S1 sample is slightly less than that in the EP0 sample. The reason for such decreasing in the magnitude of space charge is either the presence of nano filler has hindered the charge injection or more heterocharges are generated due to the ionization process. According to the multi core model of nanocomposites which is present by Tanaka [14], when the nano particles were introduced into the base epoxy resin, shallow trap band is created [107] in the loosely bound layer, either distribute or replace the original trap band, especially at higher loading concentrations. The presence of shallow trap band results in higher mobility of charge carriers, and hence causes less space charge accumulation. So lower charge injection rate should be observed in epoxy nanocomposites. There is a possibility for interfacial region to overlap with each other due to the small inter-particle distance between nearby nano particles, especially at a higher loading concentration. The overlapping region could act as a conductive path so the charge carriers can travel through the bulk of materials easier. Such high conduction could also reduce the charge injection from the electrodes. On the other hand, due to the presence of the nano SiO_2 fillers, the heterocharges generated by ionization process should also increase, leading to more heterocharges close to the electrodes. The small amount of heterocharges will cancel out with some of the injected charges. The net charges observation from the PEA system shows a small decrease in the magnitude of space charges. As shown in figure 53 (c), when the filler concentration increases to 3%, space charge distribution is very different. There is a positive peak close to the cathode as a result of heterocharges accumulation. A small amount of heterocharges are also observed adjacent to the anode. There are also some positive charges accumulated in the middle of the sample bulk. The presence of heterocharge accumulation adjacent to both electrodes is believed to be due to the increasing concentration of nano filler which results in more heterocharges

formation. According to the multi-core model proposed by Tanaka, the first and second layer could act as deep traps. Therefore the area of first and second layer increases at the filler loading concentration increases and results in space charge accumulation in the bulk of the sample. In is known that the nano particles could be charged either positive or negative under the applied field. As a result an electrical double layer with opposite polarity is formed near the charged particles. Such electrical double layer will either enhance the electron injection and restrict the hole inject or inverse due to its polarity. The presence of positive charges in the bulk of the materials could be a result of such electrical double layer. Similar results were also observed for both epoxy and LDPE samples loaded with higher concentration of nano fillers [108, 109]. When more filler are added into the epoxy sample, more heterocharges are accumulated adjacent to the cathode and the charge peaks inside the middle of sample become clearer, as shown in figure 53 (d).

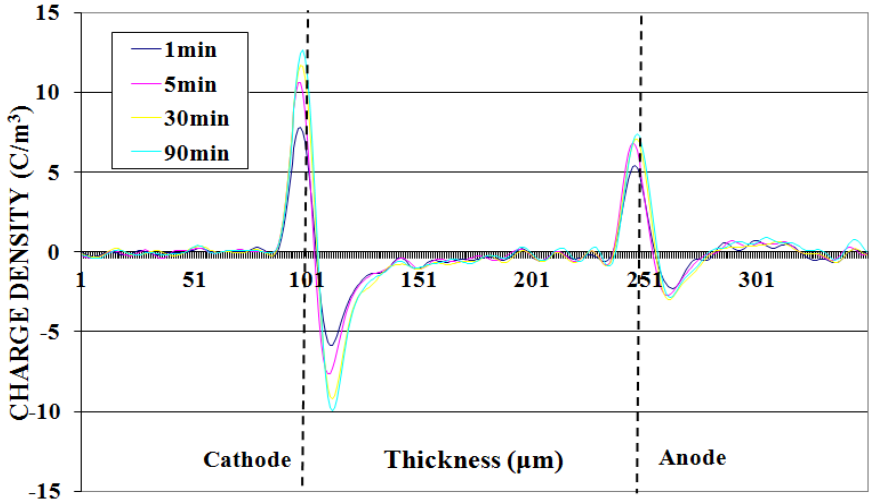

(a)EP0

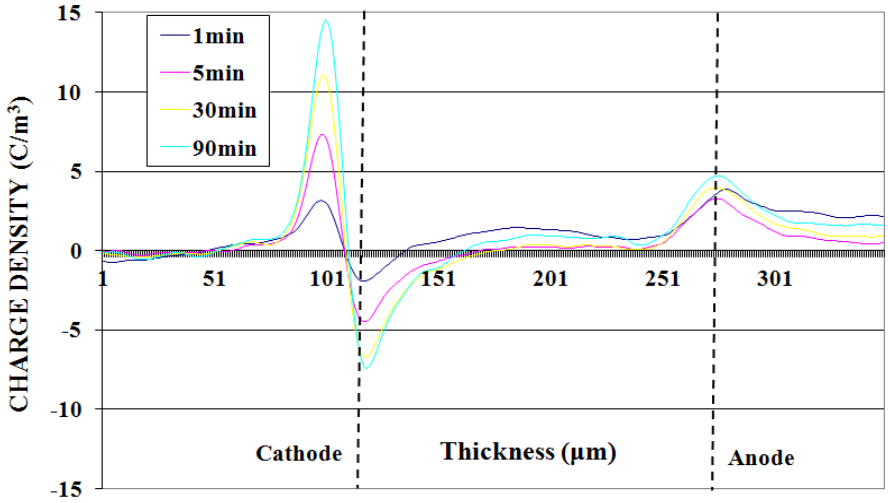

(b) EP2S1

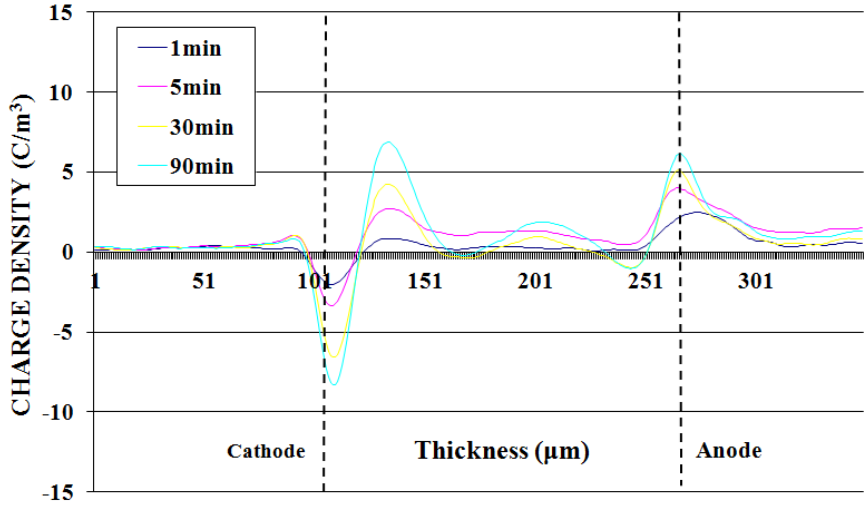

(c) EP2S3

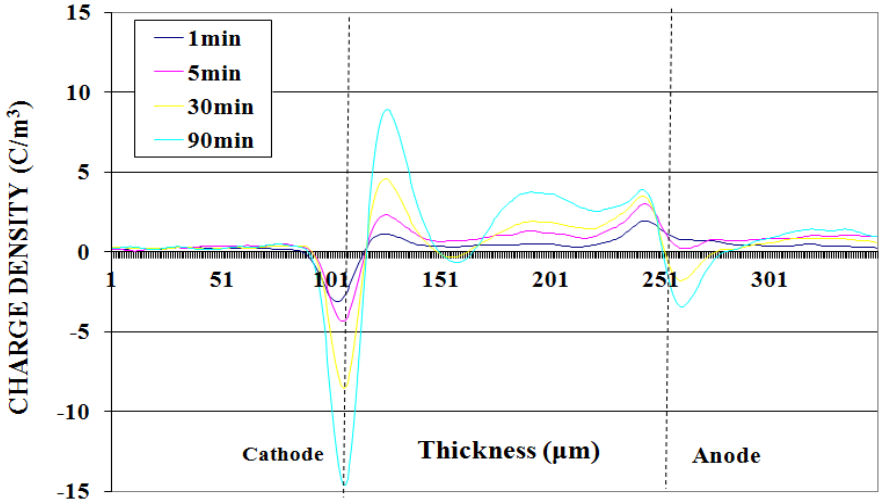

(d) EP2S5

Figure 53 Charge build-up in epoxy-SiO_2 nanocomposites at 6KV

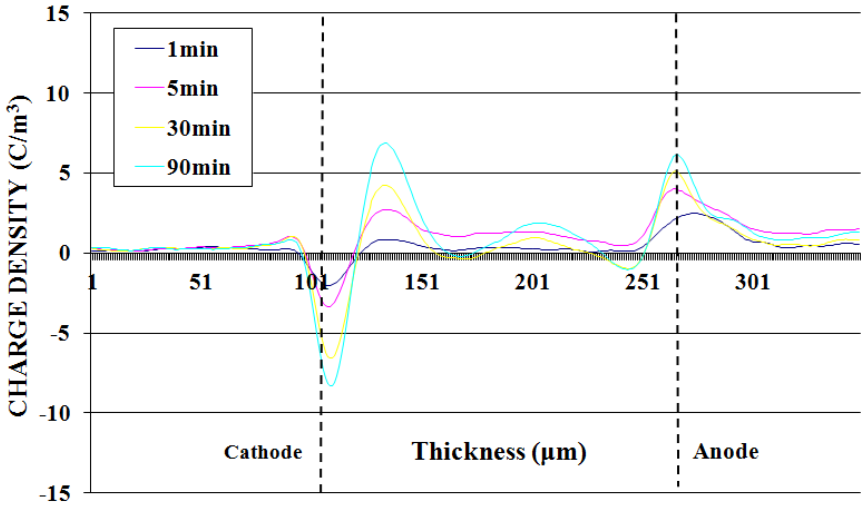

(a) SiO_2

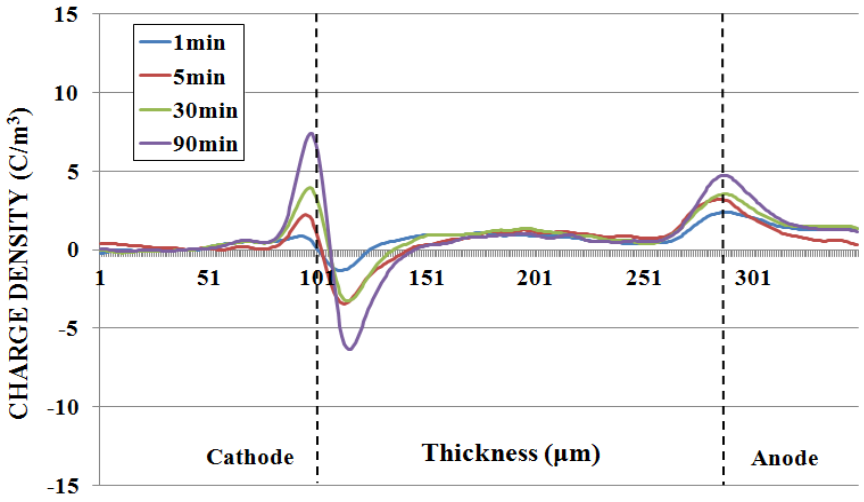

(b) Al_2O_3

Figure 54 Charge build -up in 3wt% epoxy-SiO_2/Al_2O_3 nanocomposites at 6kV

Figure 54 shows the observation of space charge accumulation in both epoxy-SiO_2/Al_2O_3 nanocomposites with 3% filler concentrations. It can be seen clearly that charges are dictated by homocharge in epoxy-Al_2O_3 nanocomposites, whereas in epoxy-SiO_2 composites, charges are dominated by heterocharges. But there is a small amount of positive charge presence in the middle of both samples. Generally speaking, the space charge built-up of epoxy resin loaded with 3wt% nano Al_2O_3 fillers is similar to epoxy resin loaded with 1wt% nano SiO_2/ filler. The difference in charge formation between two nanocomposites is believed to be caused by the amount of heterocharges accumulated adjacent to the electrodes. Compared with Al_2O_3 particles, the same amount of SiO_2 particles seems to have a better enhancement on the ionization process in nanocomposites. The reason for such

a difference observation may be due to the higher permittivity of nano Al_2O_3 fillers. The difference in particle size may also influence the results.

7.4.3 Space Charge Decay

Figure 55 shows the decay measurement results from the epoxy resin loading with nano size SiO_2 fillers. It can be seen from figure 55 (a) that once the applied voltage is removed, the charge inside the EP0 sample drops very fast. In about one minute's time, almost 75% of charge is decayed. Moreover, after 15 minutes decay, there is almost no charge remaining inside the sample. Figure 55 (b) shows the decay results of EP2S1 sample. It is clear that with 1wt% nano silicon filler, the charge decay rate inside the epoxy sample has reduced significantly. But after 30 minutes decay, there is not much charge left inside the sample. However, the results from EP2S3 give a very different decay performance. It can be seen from figure 55 (c) that the charge decay rate of epoxy resin sample loaded with 3wt% nano silicon fillers is very slow. Most of charge decay happens within the first minute. Even after 30 minutes decay time, only a small amount of charge inside the sample has been decayed. According to the multi-core model, most of the charges are trapped in the deep traps inside the first and second layer. Moreover, for EP2S5, after the charge decay in the first minute, it is hard to see any decay within 30 minutes time. Overall, the presence of nano size silicon fillers seems to cause deep traps inside the epoxy samples and trapped charges after the applied voltage have been removed. The increase in the amount of nano silicon filler inside the epoxy resin sample has a significant effect on the charge decay performance.

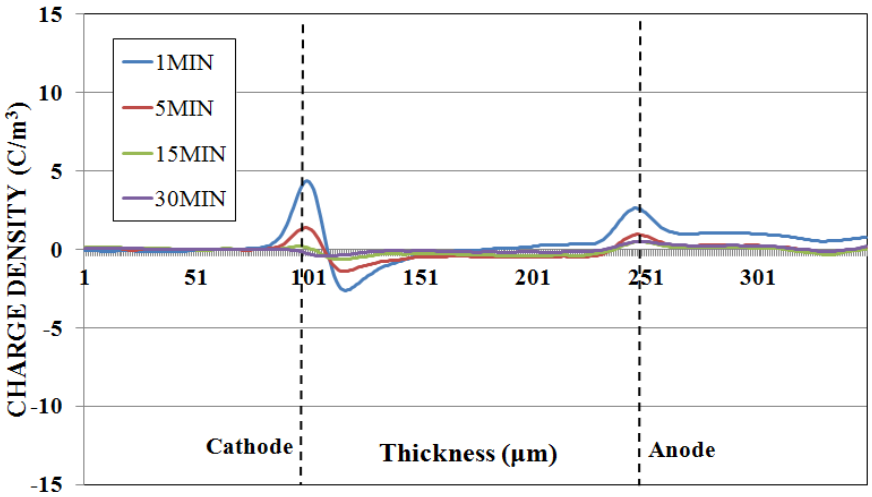

(a)Unfilled

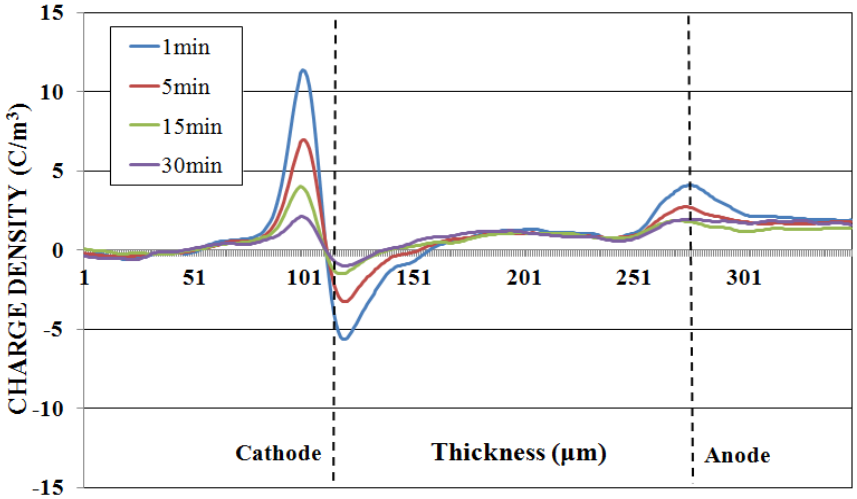

(b) 1wt%

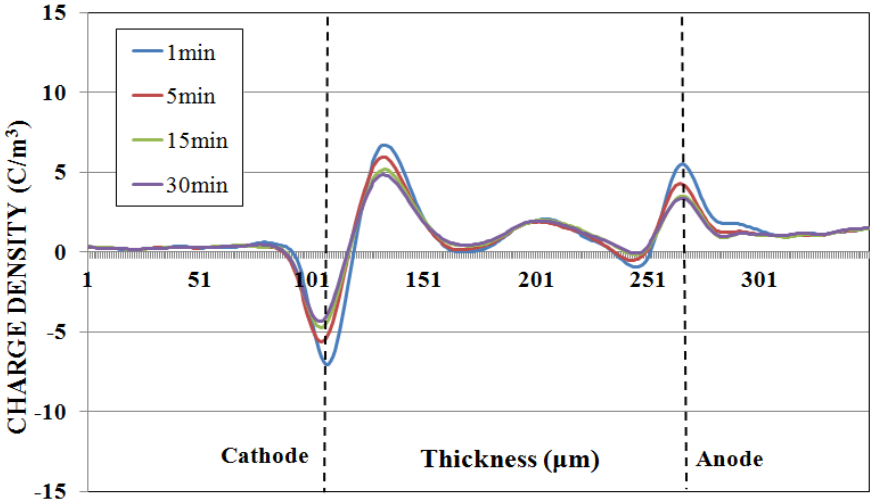

(c) 3wt%

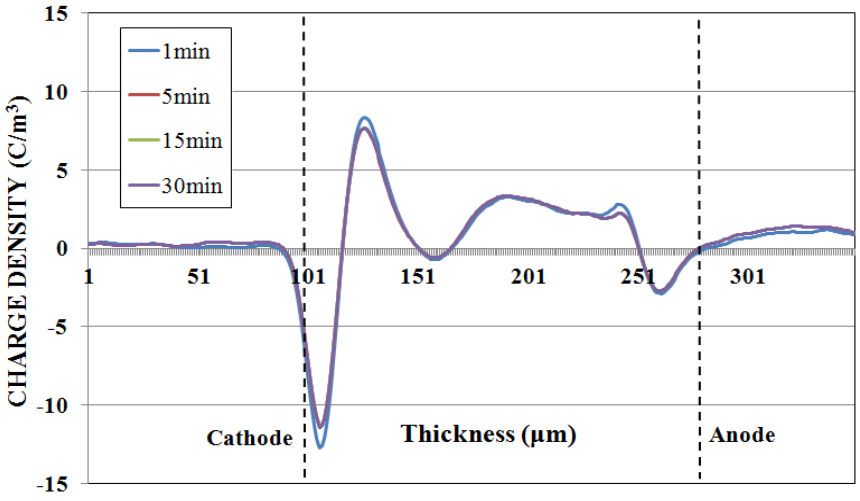

(d) 5wt%

Figure 55 Charge decay in epoxy-SiO_2 nanocomposites at 6KV

The total charge decay for epoxy resin loaded with nano size SiO_2 fillers is shown in figure 56. The amount of total charge trapped inside the sample can be worked out by integration of the charge density between two electrodes, as shown in equation 65 [120]. It can be seen from the figure that for all three epoxy nanocomposite samples loaded with different concentration of fillers, the amount of total charges trapped inside the bulk samples drops rapidly at the first 1 or 2 minutes. Then the decay rate suddenly slows down. As discussed before, according to the multi-core model, the first and second layer act as deep traps whereas the third layer acts as shallow traps. Those fast decayed charges are mainly trapped in the shallow traps at the third layer, whereas some other charges were trapped deeply at the first and second layers.

$$Q = \int_{x_{cathode}}^{x_{anode}} P(x)dx \qquad (65)$$

where P(x) is the density of space charge along x directions.

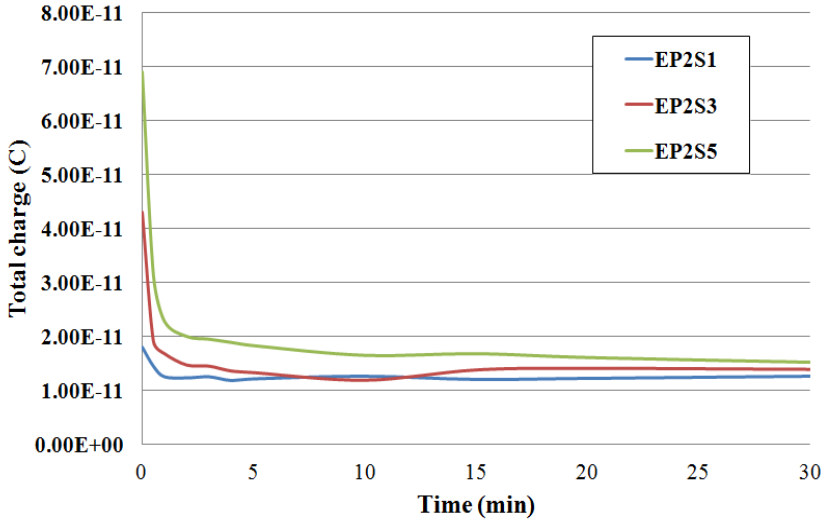

Figure 56 Total charge decay in epoxy-SiO_2 nanocomposites

The total charge decay curve could be analysed by using two exponential functions that represented both fast decayed charges and deeply trapped charges. The equation can be written as:

$$Q = A_1 e^{-\frac{t}{\tau_1}} + A_2 e^{-\frac{t}{\tau_2}}$$

Where A_1 and A_2 are constant numbers that represent the initial amount of shallow trapped charges and deeply trapped charges respectively, τ_1 and τ_2 are the charge decay speeds of shallow trapped charges and deeply trapped charges respectively. Matlab program has been used to calculate the four variable A_1, A_2, τ_1 and τ_2 numbers and the results are shown in table 19.

	A_1	τ_1	A_2	τ_2
EP2S1	5.9029	0.46	12.2426	909.1
EP2S3	28.7763	0.31	14.1563	769.2
EP2S5	46.3332	0.35	21.3124	68.0

Table 19: Parameters for space charge decay results

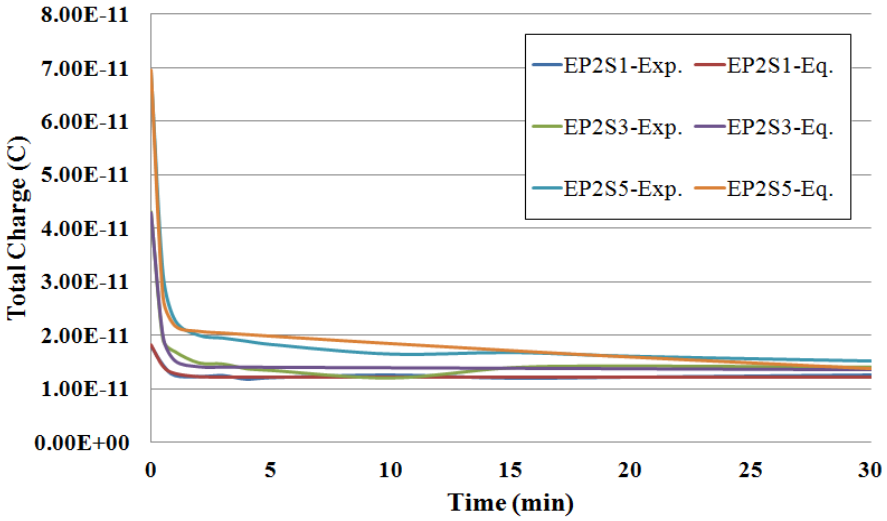

Figure 57 Total charge decay curve in epoxy-SiO_2 nanocomposites from experiments and equations

It can be obtained from table 19 that both the initial amount of shallow trapped charges and deeply trapped charges increase with filler loading concentration. This is because the increase in filler loading concentration will result in larger interfacial region. As a result more charges have been trapped at the interfacial region. Compared with EP2S1 sample, the EP2S3 sample has lower τ_1 value. This is due to the increase in volume of third leading to a fast charge decay rate. However, as the filler loading concentration further increases to 5wt%, the value of τ_1 starts to increase. In this case the inter-particle distance between nearby nano particles are short enough so that the third layer are more likely to overlap with nearby layers and finally leads to a reduction in the volume of third layer, as discussed before. Comparative curves between the experiment results and equations are given in figure 57.

The electrical field distortion due to the accumulation of space charge is shown in figure 58. One clear observation is the electrical field inside both EP0 and EPM5 samples show a big distortion due to the presence of space charge. However, the epoxy nanocomposites samples only have slight field distortion. Therefore it is obvious that the presence of nano particles seems to affect the space charge formation inside the nanocomposites. Compared with unfilled resin, the amount of space charge is less in epoxy nanocomposites. The results from the threshold field of space charge formation also indicate that the

formation of space charge in epoxy nanocomposites require higher threshold field.

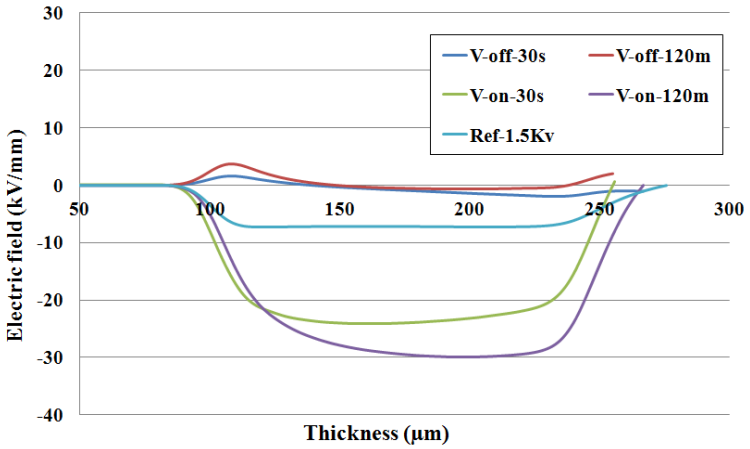

(a) EP0

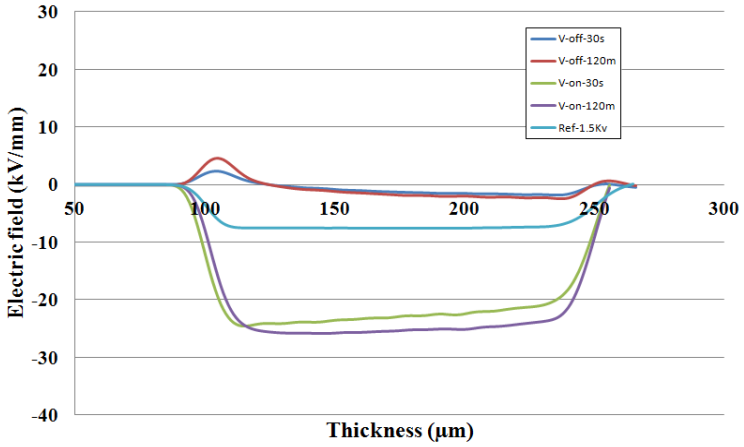

(b) EP2S1

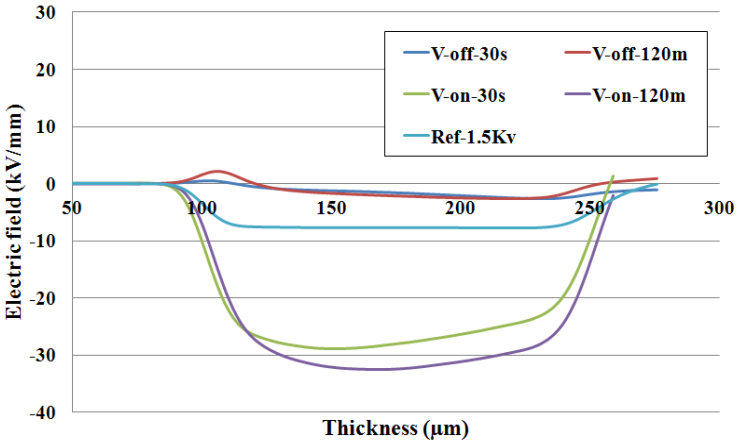

(c) EPM5

Figure 58 Field distortions of both unfilled resin and epoxy-SiO_2 nanocomposites

8 Surface Treatments and Water Absorption

8.1 Surface Treatments of Nano Particles

Early studies on polymer nanocomposites show that in order to achieve better dielectric properties, it is necessary to avoid nano size filler agglomeration. Inorganic nano size filler such as silica has extremely large surface area covered by silanol groups. Such hydrophilic surface does not have good compatibility with polymers such as epoxy resin. Moreover, those inorganic nano particles that contain hydrophilic surface tend to agglomerate with each other easily through hydrogen bonding to form large agglomerations. The agglomeration of nano particles can form another network through the polymer matrix and therefore affect the structure and properties of resulting nanocomposites. To avoid such a situation, it is necessary to reduce the degree of nano particle agglomeration. The mechanical methods such as high speed shearing and ultrasonic shearing are not effective enough to break those agglomerations as the bond force between nano particles is stronger than the shear force. The chemical treatment of nano particle surface is therefore introduced to reduce agglomeration and achieve better dispersion of filler.

8.1.1 Sample under Study

In this section a comparative study on the effect of surface treatment on the dielectric permittivity, AC breakdown behaviours, space charge behaviours and glass transition temperature of resulting epoxy nanocomposites has been carried out. To help understanding the effect of surface treatment on the dielectric properties of epoxy nanocomposites, composites loaded with both treated and untreated nano SiO_2 fillers have been prepared. A filler loading concentration of 1, 3 and 5 weight percent have been selected to give a comparative study of the resulting epoxy nanocomposites. The list of sample used is shown in table 20.

Sample code	Particle wt%	Surface treatment	Type of particle
EP0	0	-	-
EP2S1	1	N	SiO_2
EP2S3	3	N	SiO_2
EP2S5	5	N	SiO_2
T-EP2S1	1	Y	SiO_2
T-EP2S3	3	Y	SiO_2
T-EP2S5	5	Y	SiO_2

Table 20: List of sample under study

8.1.2 Glass Transition Temperature

The glass transition temperature for epoxy resin loaded with different loading concentration of both treated and untreated nano SiO_2 particles has been measured and the results are shown in figure 59 and the values are given in table 21. It can be seen that the surface-treatment of nano fillers has a clear effect on the T_g of resulting nanocomposites. It is known that the dispersion and surface characteristic of nano size fillers will affect the relaxation of molecule chains and the polymer chain movement. If the silane is used as a coupling agent to make a surface modification on nano size fillers, the T_g of resulting composites is slightly different compared with the composites loading with non-treated fillers. The T_g of both EP2S1 and T-EP2S1 samples is similar. This is probably because at a loading concentration of 1wt%, the agglomerations of nano particles are not significant as the number of nano particles is less. However, as the filler loading concentration increases, T-EP2S3 and T-EP2S5 samples have higher T_g compared with the EP2S3 and EP2S5 samples. The T_g of epoxy nanocomposites loaded with treated nano fillers has a slower decease rate with the increase of loading concentration compared with the epoxy nanocomposites loaded with non-treated nano fillers. When silane is used as a coupling agent to modify the nano fillers, tight bond can be formed between epoxy molecular and inorganic nano size fillers. The

reduction in the decease rate is believed due to the restriction of surface treated nano filler on polymer molecular chain movement which will result in the increases of T_g.

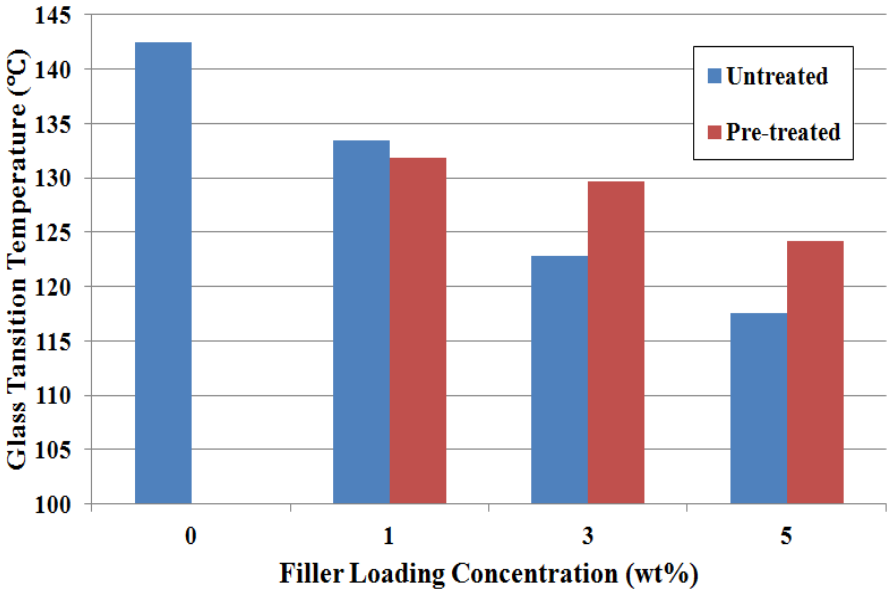

Figure 59 Glass transition temperatures of epoxy nanocomposites with and without surface treatment

Sample code	Particle wt%	Surface treatment	Tg (℃) ±2℃
EP0	0	-	142.5
EP2S1	1	N	133.4
EP2S 3	3	N	122.8
EP2S 5	5	N	117.5
T-EP2S1	1	Y	131.8
T-EP2S3	3	Y	129.7
T-EP2S5	5	Y	124.2

Table 21: Glass transition temperature of samples

8.1.3 Dielectric Spectroscopy Results

The variations of dielectric permittivity as a function of frequency for epoxy nanocomposites with both treated and untreated SiO_2 nano fillers and with

different concentrations are shown in figure 60. It is observed from the measurement results that effective permittivity of epoxy nanocomposites is strongly affected by the presence of inorganic nano fillers and their surface characteristics. It can be seen from figure 60 (a) that the EP2S1 sample has lower dielectric permittivity than EP0 sample in the measured frequency range. When the filler loading concentration increases to 3wt%, the relative permittivity of EP2S3 sample is similar compared with EP2S1 sample. Further increase in the filler loading concentration to 5wt% leads to an increase in permittivity. Compared with EP0 ample, EP2S5 sample has higher effective permittivity within the measured frequency range. Similar trend of dielectric permittivity behaviour has been observed in epoxy nanocomposites loaded with treated SiO_2 nano fillers. The effective permittivity of epoxy nanocomposites loaded with treated SiO_2 nano fillers is slightly lower compared with those loaded with untreated SiO_2 nano fillers.

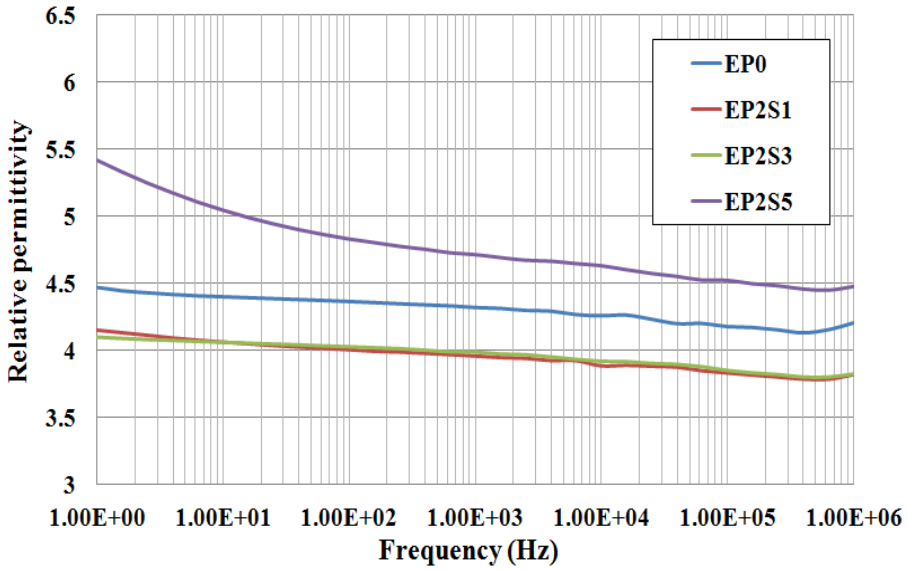

(a) Without surface treatment

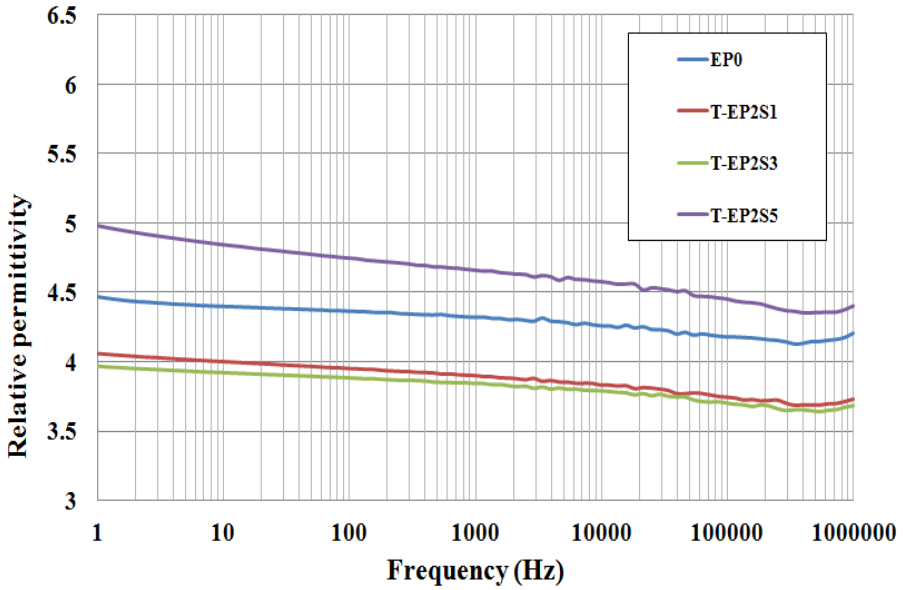

(b) With surface treatment

Figure 60 Variations of permittivity of epoxy-SiO_2 nanocomposites with respect to frequency

The difference in permittivity is a result of the reduction of mobility of the dipolar groups within the composites which will reduce the polarization within the composites [110]. When the nano fillers are introduced into the polymer materials, an interaction region between polymer matrix and nano fillers is formed. The dual layer model proposed by Santanu and Thomas [15] can be applied to explain the dielectric permittivity behaviours observed and it is discussed in chapter 5. In epoxy nanocomposites loaded with 1wt% nano fillers, the presence of tightly bound region will restrict the mobility of epoxy chain and the motion of free dipolar functional groups within the epoxy chain in the bulk material [25]. Moreover, both the tightly bound layer and loosely bound layer contribute to the decreases in local density and therefore result in lower permittivity. When the filler loading concentration increases, the volume fraction increases and leads to a further reduction in permittivity. When the silane is used as a coupling agent, the molecular movement is restricted through OH radicals due to silane coupling. The surface treatment of nano fillers also leads to a better particle dispersion rate in the base polymer materials and results in a contribution to the volume fraction. Therefore the epoxy nanocomposites loaded with treated nano fillers has slightly lower permittivity compared with those loaded with untreated nano fillers.

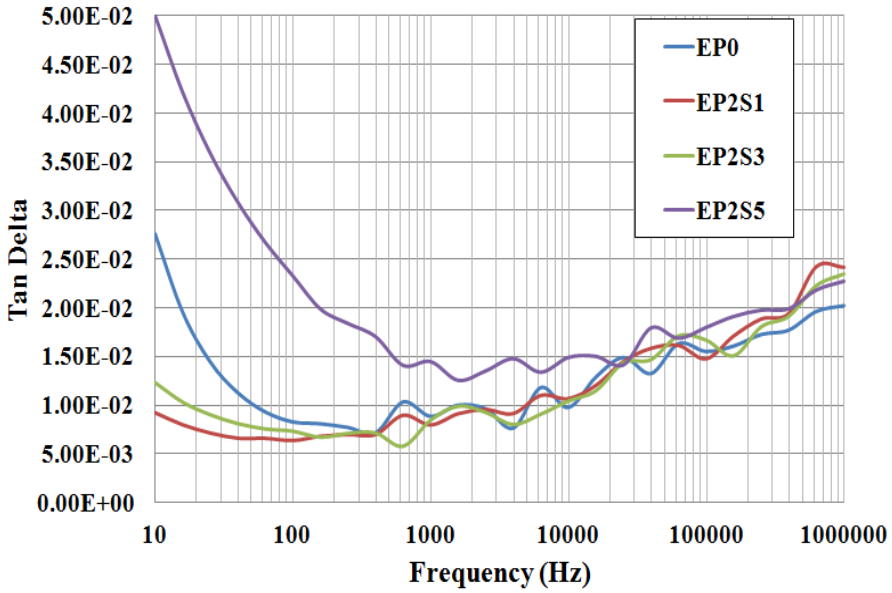

(a) Without surface treatment

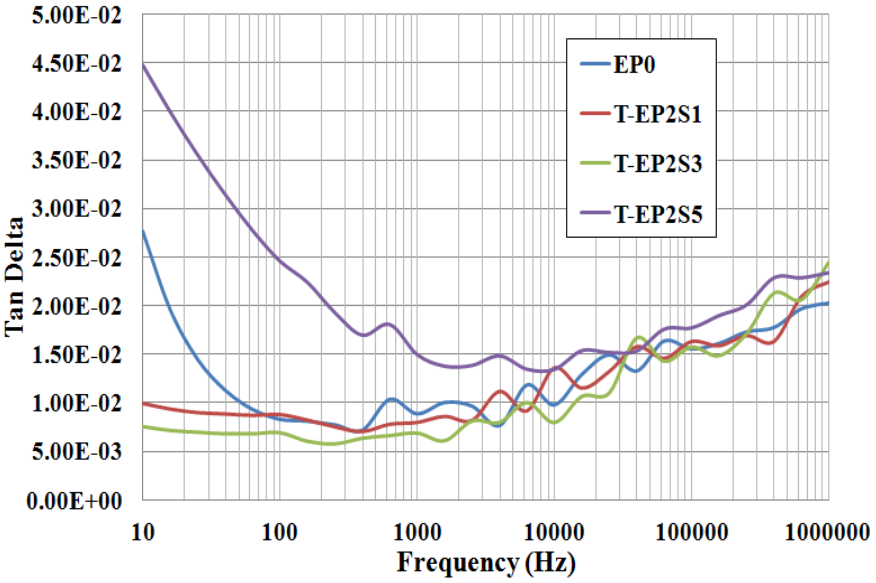

(b) With surface treatment

Figure 61 Variations of dielectric loss of epoxy-SiO_2 nanocomposites with respect to frequency

The variation of tan delta value in epoxy nanocomposites with both treated and untreated SiO_2 nano fillers and with different concentrations is presented in figure 61. As the surface treatment of nano particles affects the particle dispersion, the overlapping in epoxy nanocomposites loaded with treated nano fillers is less compared with epoxy nanocomposites loaded with untreated nano fillers. Epoxy nanocomposites loaded with treated nano fillers have lower electrical conductivity compared with nanocomposites loaded with untreated

nano fillers at same loading concentration and result in lower tan delta value as discussed in chapter 5.3.

8.1.4 AC Breakdown Results

The ac breakdown strength of unfilled epoxy resin and epoxy nanocomposites filled nano SiO2 fillers with and without surface treatment with filler loading of 1, 3 and 5wt% were measured and the results is shown in figure 62. The two parameter Weibull distribution is used to analyse the ac breakdown results, thus producing the Weibull parameters shown in Table 22. The results show that there is a reduction in breakdown strength for all epoxy nanocomposites loaded with untreated fillers. The breakdown strength of EP2S1 sample is lower compared with the breakdown strength of EP0 sample. However, when the filler loading concentration increases to 3wt%, there is a small increase in breakdown strength compared with EP2S1 specimens. But if the filler loading concentration further increases to 5wr%, the breakdown strength of EP2S5 specimens starts to decrease again. Unlike the epoxy nanocomposites loaded with untreated nano fillers, epoxy nanocomposites loaded with treated nano fillers has better breakdown strength compared with the unfilled epoxy, as shown in Fig. 62 (b). It can be clearly observed that the breakdown strength of T-EP2S1 sample is slightly higher compared with the EP0 specimens. When the loading concentration increases to 3wt%, there is a further increase in both shape and scale parameters. However the breakdown strength starts to reduce with further increase in the filler loading concentration to 5wt%. It has been reported by Preetha et al that a similar trend of breakdown strength behaviour has been observed in epoxy nanocomposites loaded with nano Al_2O_3 fillers [111]

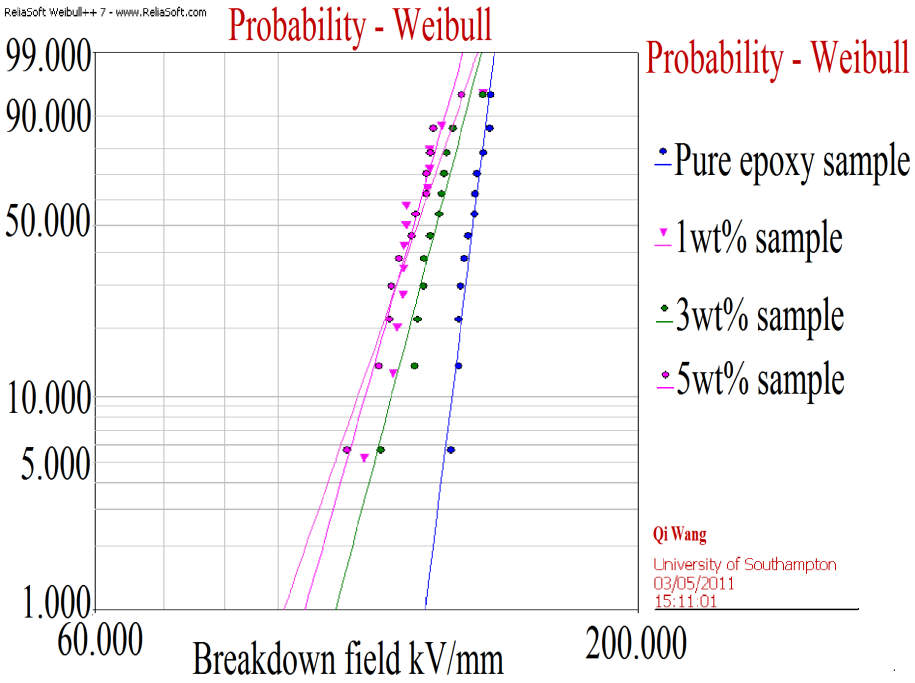

(a) Without surface treatment

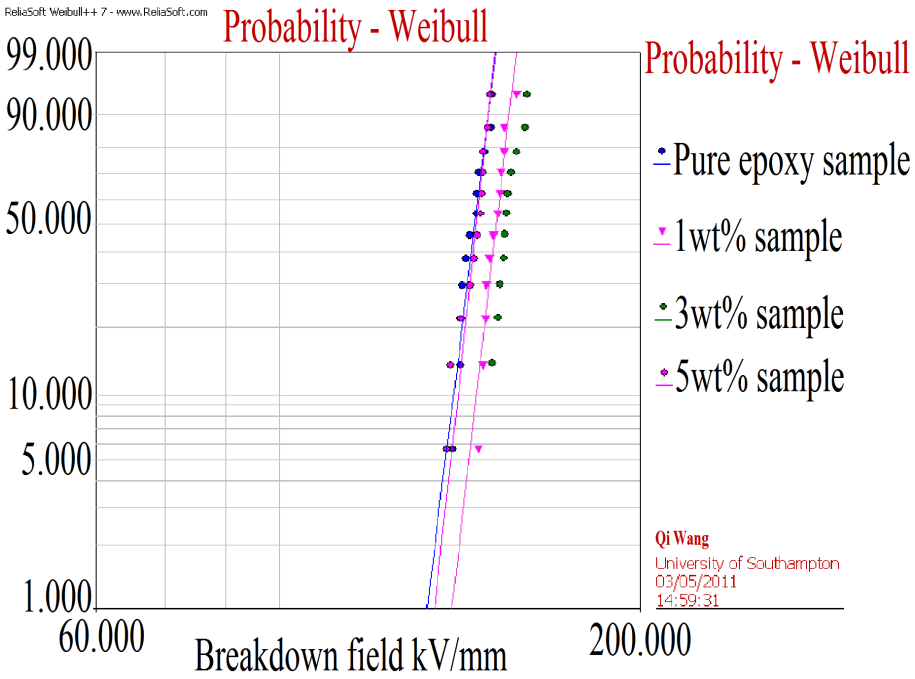

(b) With surface treatment

Figure 62 Breakdown strength of epoxy nanocomposites

Sample	Scale parameter (η) (kV/mm)	Shape parameter (β)
EP0	140.0	39.9
EP2S1	126.0	14.3
EP2S3	130.5	19.0
EP2S5	124.3	17.5
T-EP2S1	146.9	42.7
T-EP2S3	151.4	43.0
T-EP2S5	140.5	45.6

Table 22: Weibull parameters from MLE for epoxy nanocomposites loaded with both treated and non-treated nano size filler

The above results show that the surface treatment of nano fillers has a significant effect on the breakdown behaviour of resulting nanocomposites. Early studies have already shown that there is an interfacial region between polymer matrix and nano fillers which is formed due to the interaction between polymer matrix and nano fillers. Thus the interfacial characteristic between polymer matrix and nano fillers seems to play an important role in the insulation performance of polymer nanocomposites.

Compared with EP0 specimens, the T-EP2S1 sample has higher breakdown strength. Surface treated nano fillers can dispersed more homogenously in base resin. For epoxy nanocomposites loaded with treated nano fillers, the nano fillers inside the polymer can be treated as isolated particles under lower loading concentrations. Also after surface treatment, the silane will attach on the surface of nano fillers to form chemical bounds. This will lead to a decreases of surface tension of nano fillers and therefore enhance the interfacial adhesion between epoxy resin and inorganic nano filler. Thus it is able to reduce the voids in epoxy nanocomposites loaded with surface treated nano fillers and result in an increase of breakdown strength. With 3wt% loading concentration, the breakdown strength of T-EP2S3 samples increase slightly as the interfacial area play a more important role. However, further increase the filler loading concentration to 5wt% will also cause overlapping of loosely bound region and finally result in a reduction in breakdown strength.

8.1.5 Space Charge Results

The "volts-off" space charge accumulation of specimens with treated nano SiO_2 filler is shown in figure 63. It can be seen from figure 63 (a), there is a small amount of homocharge accumulated near the cathode in T-EP2S1 sample. As the duration of the applied voltage increases, the homocharge was replaced by heterocharge. There is little charge accumulated in the bulk of the sample. Compared with the charge build up results from EP2S1 samples in chapter 4.5, no significant change has been observed but the T-EP2S1 sample seems to have a bit more heterocharges near the cathode where as a small amount of positive charge accumulated in the bulk of EP2S1 sample. There is an increases amount of heterocharges accumulated near the cathode in T-EP2S3 sample. Unlike the results of EP2S3 sample, only a small amount of charge has been observed in the bulk of T-EP2S3 samples. Further increase in the filler loading concentration results in a similar observation where heterocharges accumulated near both electrodes and a small amount of positive charge accumulates in the bulk of the sample. It seems that the surface treatment of nano particles has a negative effect on the formation of electrical double layer. Moreover, the treated nano particles have less possibility to agglomerate with nearby particles. So the interfacial region of nanocomposites loaded with treated nano particles is larger than the one loaded with untreated nano particles, especially at higher loading concentrations. The large interfacial overlapping region could act as a conductive path and leads to high conductivity and fast neutralization. Consequently no significant amount of charge accumulated in the bulk of the sample.

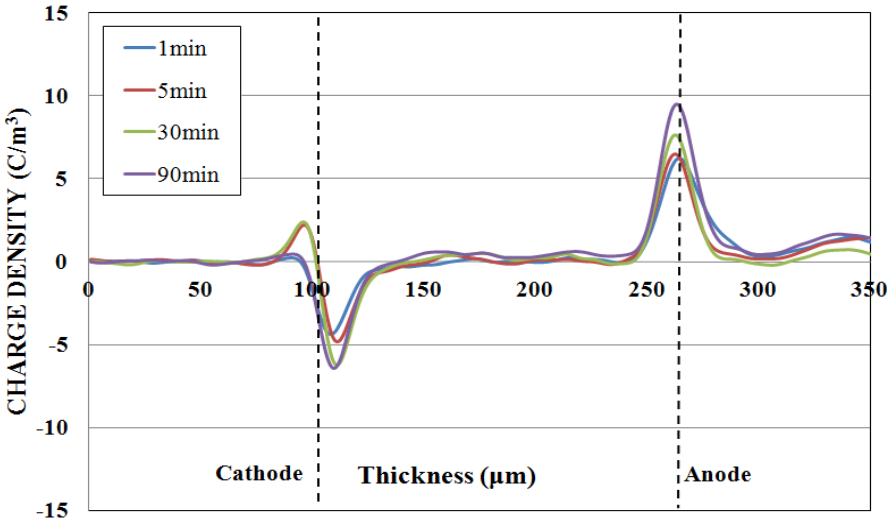

(b) 1wt%

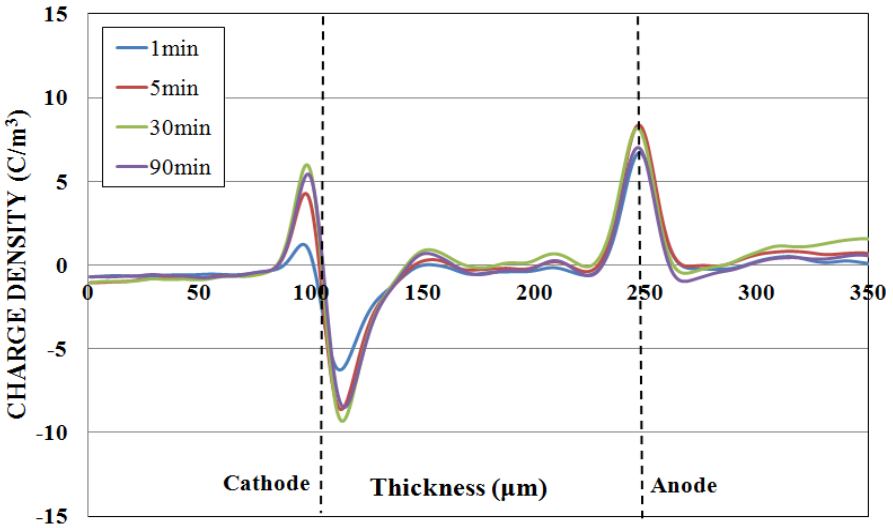

(c) 3wt%

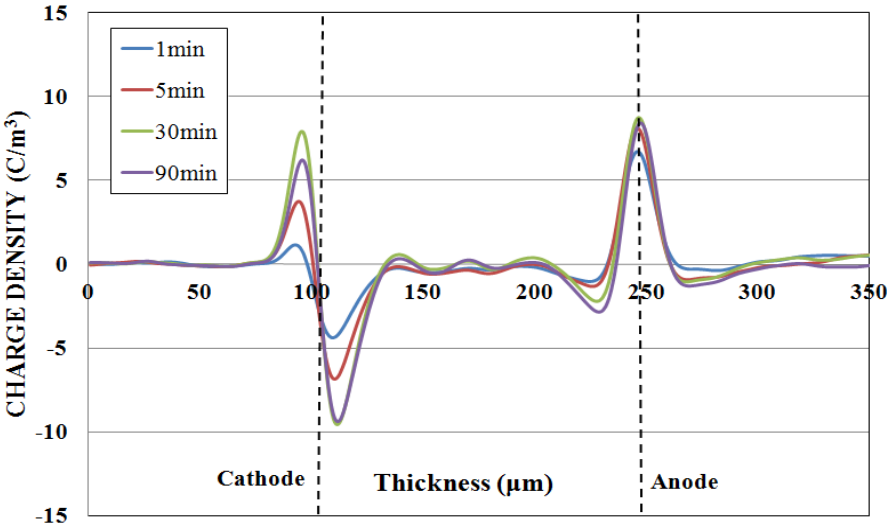

(d) 5wt%

Figure 63 Charge build-up in epoxy nanocomposites loaded with treated SiO_2 filler

8.2 Water Absorption of Epoxy Nanocomposites

8.2.1 Sample under Study

The effect of water absorption on the dielectric permittivity and AC breakdown strength has been studied in this chapter. Space charge behaviours and glass transition temperature of resulting epoxy nanocomposites has been carried out. Epoxy nanocomposites in both dried and saturated conditions have been prepared for the test. A filler loading concentrations of 1, 3 and 5 weight percent have been selected to give a comparative study of the resulting epoxy nanocomposites and the list of sample used in this study is shown in table 23.

Sample code	Particle wt%	Water absorption condition	Amount of water absorb (wt%)	Type of particle
EP0	0	-	0	-
D-EP2S1	1	Dried	0	SiO_2
D-EP2S3	3	Dried	0	SiO_2
D-EP2S5	5	Dried	0	SiO_2
S-EP2S1	1	Saturated	2.12	SiO_2
S-EP2S3	3	Saturated	2.48	SiO_2
S-EP2S5	5	Saturated	2.83	SiO_2

Table 23: List of sample under study

8.2.2 Glass Transition Temperature Results

Figure 64 shows the T_g of the epoxy nanocomposites in both dried and saturated conditions and the detailed results is shown in table 24. It can be seen that the saturated epoxy nanocomposites have lower T_g compared with the dried ones. Moreover, as the loading concentration increases, the decrease rate of T_g does not change. For epoxy nanocomposites loaded with 1wt% nano SiO_2 fillers, the difference of T_g between dried and saturated sample is 19.7℃,

where as for 5wt% samples, there is a difference of 19.3℃. The studies show that the water absorbed by epoxy nanocomposites tend to accumulated at the interface between polymer molecular and the inorganic nano size fillers [112]. The water absorption of epoxy nanocomposites is enhanced by the presence of nano size fillers as a result of hydration. The bound water will disrupt the Van der Waals force between molecular chains and the hydrogen bonds as well. In such case the chain mobility will be increased, result in a lower T_g.

Sample code	**Particle wt%**	**Water absorption condition**	**Tg (℃) ±2℃**
D-ED0	0	Dried	142.5
S-EP0	0	Saturated	128.3
D-EP2S1	1	Dried	133.4
D-EP2S3	3	Dried	122.8
D-EP2S5	5	Dried	117.5
S-EP2S1	1	Saturated	113.7
S-EP2S3	3	Saturated	107.0
S-EP2S5	5	Saturated	98.2

Table 24: Glass transition temperature of samples

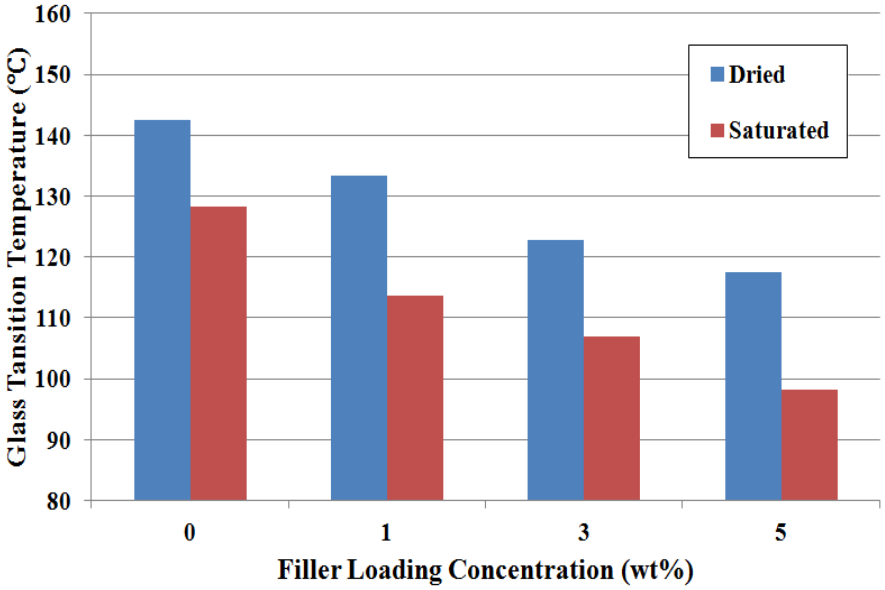

Figure 64 Glass transition temperatures of epoxy nanocomposites under dried and saturated condition

8.2.3 Dielectric Spectroscopy Results

The variations of dielectric permittivity as a function of frequency for both dried and saturated epoxy nanocomposites loaded with SiO_2 nano fillers and with different loading concentrations are shown in figure 65. It is observed from the measurement results that effective permittivity of epoxy nanocomposites is strongly affected by the water absorptions. It can be seen from figure 65 (a) that the variation of relative permittivity in saturated epoxy nanocomposites have similar tends compared with the relative permittivity in dried epoxy nanocomposites for all filler loading concentrations. The permittivity of S-EP2S1 sample is lower than the permittivity in S-EP0 sample in the measured frequency range. Another clear observation is, compared with dried epoxy nanocomposites, the dielectric permittivity of saturated epoxy nanocomposites increases at low frequency range (less than 10Hz) for all filler loading concentrations. When the filler loading concentration increases to 3wt%, the S-EP2S3 sample has slightly higher relative permittivity compared with the EPD3 sample, especially in lower frequency range. A higher permittivity was also observed in S-EP2S5 sample in comparison with D-EP2S5 sample. The increase in relative permittivity at low frequency range is

due to the polarization at the electrode as a result of both accumulations of charge carries and chain migrations. The presence of water molecular leads to chain scission in epoxy resin and results in higher chain migration. Thus it is easier for epoxy chain to migrate in saturated sample compared with dried samples.

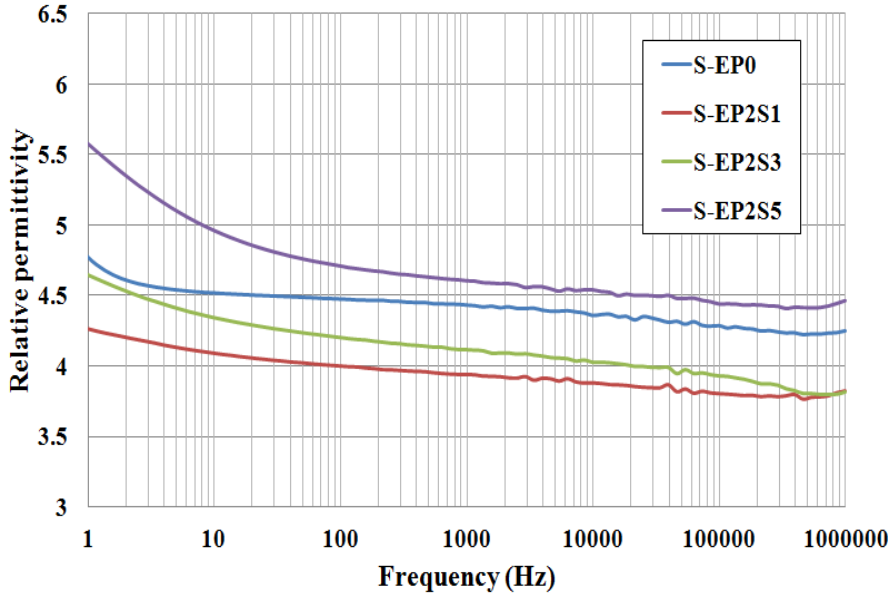

(a) Saturated

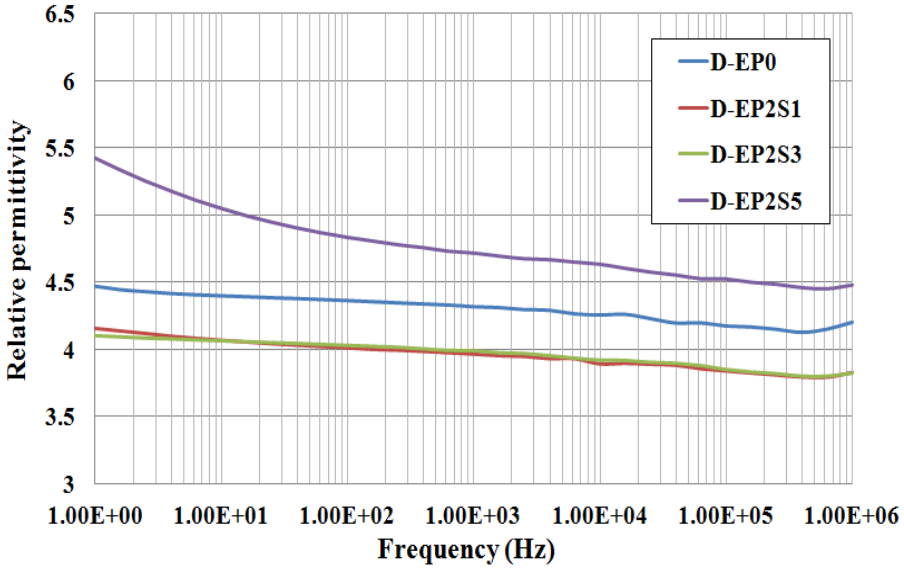

(b) Dried

Figure 65 Variations of permittivity of both saturated and dried epoxy-SiO_2 nanocomposites

The permittivity increases in lower frequency range is believed to be a result of water absorption as it is appeared in any saturated samples, as shown in figure 65(b). When the water is absorbed into epoxy matrix, water molecules could either stay in the free volume holes as "free water" or interact with adjacent bond side and are bonded with polymer matrix with hydrogen bond [113, 114, 115] to form bound water. It is known that the free water has a hopping time of 7×10^{-10} s [116], so it is unlikely to cause the relaxation process at such a low frequency range. The increases in permittivity in lower frequency range should be due to the presence of bound water. The study about water-epoxy interaction by Jelincski also supports such conclusion [117].

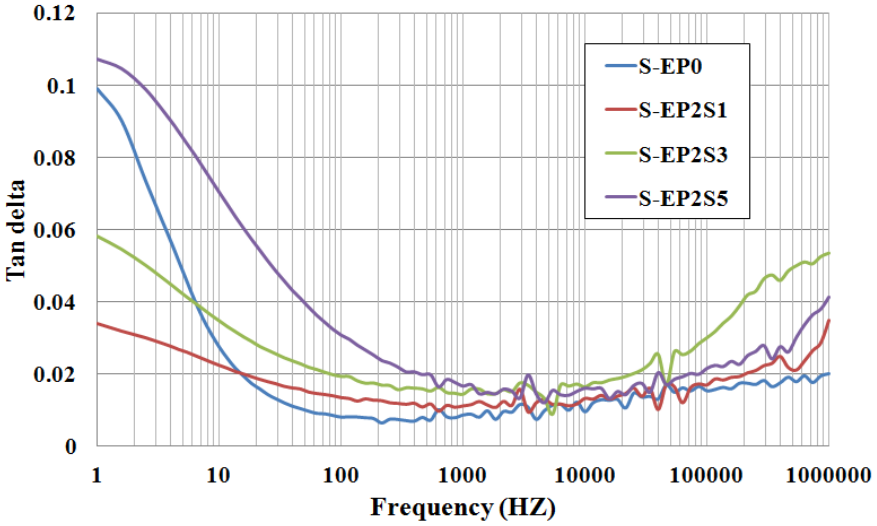

(a) Saturated

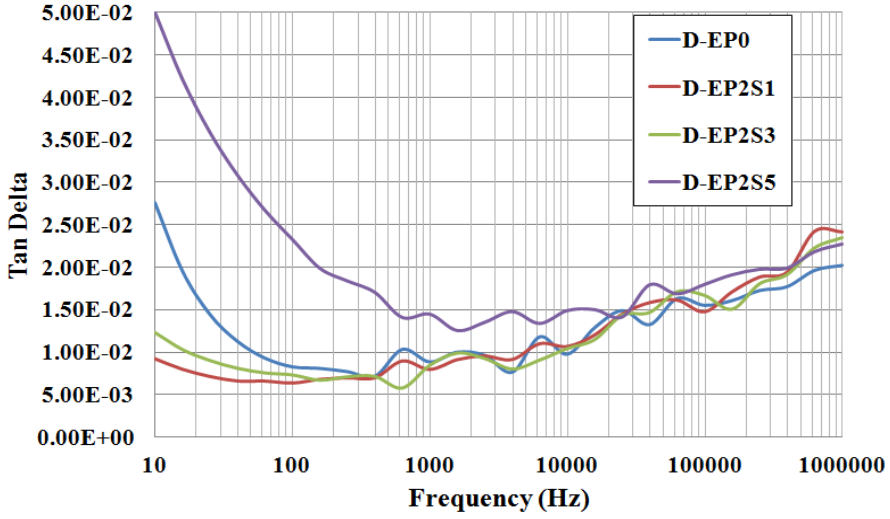

(b) Dried

Figure 66 Variations of tan delta value of both saturated and dried epoxy-SiO_2 nanocomposites

The variations of tan delta value as a function of frequency for both dried and saturated epoxy nanocomposites loaded with SiO_2 nano fillers and with different loading concentrations are shown in figure 66. It can be seen that there is an increase in tan delta value for all saturated samples compared with the dried ones, especially in lower frequency range. The rapid increase in tan delta value in lower frequency range due to the presence of water inside the sample shows a conductive effect inside the saturated samples due to the presence of water, which leads to higher conductive current in lower frequency range.

8.2.4 AC Breakdown Results

The ac breakdown strength of unfilled epoxy resin and both dried and saturated epoxy nanocomposites loaded with SiO_2 nano filler with loading concentration of 1, 3 and 5wt% were measured and the results is shown in figure 67. The two parameter Weibull distribution was used to analyse the ac breakdown results, thus producing the Weibull parameters shown in Table 25. The analysing results show that there is a large reduction in breakdown strength for saturated epoxy nanocomposites samples compared with dried epoxy nanocomposites samples. The breakdown strength of S-EP0 sample is much lower compared with the breakdown strength of D-EP0 sample. Moreover, the breakdown strength of all saturated epoxy nanocomposites samples are much lower compared with the dried samples loaded with same filler loading concentration, as shown in table 25. It can be clearly observed that the breakdown strength of all saturated epoxy nanocomposites samples is almost half of the dried epoxy nanocomposites samples. The breakdown strength of S-EP2S1 sample is also lower compared with the breakdown strength of S-EP0 sample. When the loading concentration increases to 3wt%, the breakdown strength of S-EP2S3 sample is similar compared with S-EP2S1 sample. However the breakdown strength starts to reduce with further increase in the filler loading concentration to 5wt%.

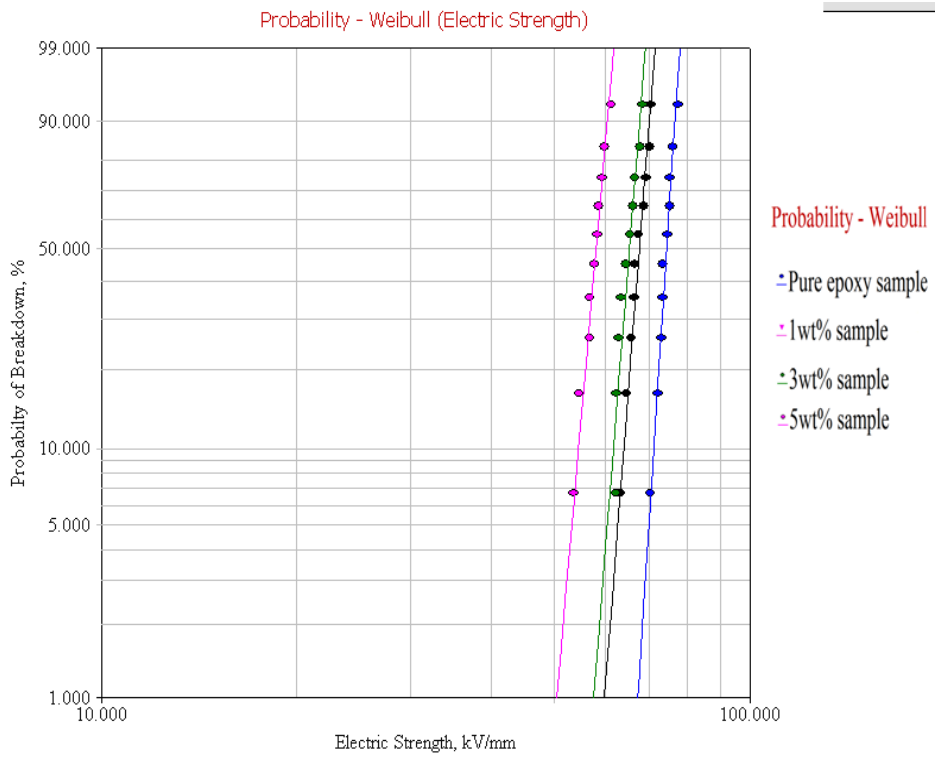

Figure 67 Breakdown strength of saturated epoxy nanocomposite samples

Sample	Scale parameter (η) (kV/mm)	Shape parameter (β)
D-EP0	140.0	39.9
D-EP2S1	126.0	14.3
D-EP2S3	130.5	19.0
D-EP2S5	124.3	17.5
S-EP0	75.1	41.3
S-EP2S1	68.3	34.1
S-EP2S3	66.0	33.1
S-EP2S5	58.4	30.2

Table 25: Weibull parameters from MLE for both dried and saturated epoxy nanocomposite samples

The above results indicate that the presence of water in epoxy nanocomposites has a significant effect on the breakdown behaviour of resulting nanocomposites. Early researches have already pointed out that the rapid decrease in breakdown strength is due to the presence of water in the epoxy resin that helps the charges to conduct across the sample and leads to early

breakdown. In epoxy nanocomposites, the waters tend to form a layer surrounding the nano particles. In saturated condition, the content of water is high enough so the water layers surrounding the nano particles may overlap with each other to form a conductive path for charge carriers to travel through the bulk of the materials. As a result the S-EP2S1 sample has lower breakdown strength compared with S-EP0 sample. Increase in filler loading concentration will reduce the inter-particle distance and result in a higher possibility for water layers surrounding the nano particles to overlap with nearby layers. So a further decrease in breakdown strength has been observed in S-EP2S5 sample.

8.2.5 Space Charge Results

The space charge measurement results of both dried and saturated pure epoxy resin sample and epoxy nanocomposites loaded with SiO_2 nano filler is shown in figure 68. Compare with the dried samples, a large amount of heterocharge has been observed, especially at the anode side. Presence of water in the epoxy resin is able to help charge to conduction in the sample. In case of the saturated samples, the high content of water leads to formation of water layers surrounding the nano particles may overlap with nearby particles to form a conductive path for charge carriers to travel through the bulk of the materials. It is possible that such increase in heterocharge accumulation is due to the migration of both positive and negative charge carriers inside the epoxy nanocomposite sample as a effect of water layer which surrounding the nano particles. Similar observations has also been reported elsewhere where heterocharge formation has been observed in epoxy resin samples loaded with filler by a boiling treatment in water at 100℃ for 8 hours [118].

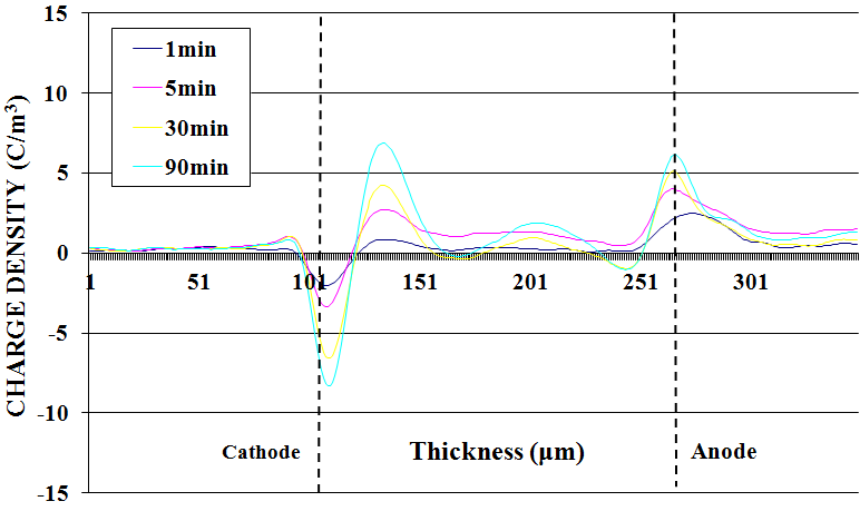

(a) Dried

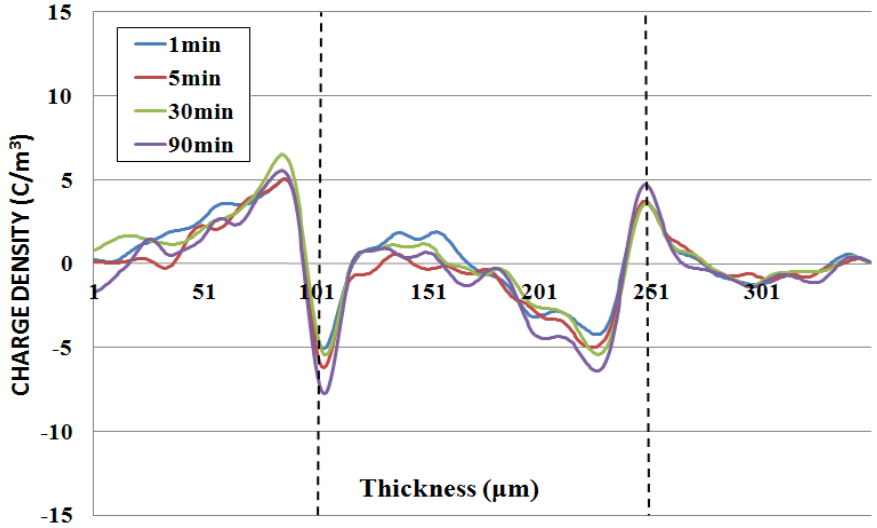

(b) Saturated

Figure 68 Charge build-up in both dried and saturated S-EP2S3 sample

9 Conclusions and Further Works

9.1 Conclusions

In this project, the dielectric properties of epoxy nanocomposites have been investigated to give a better understanding of the insulating performance of epoxy nanocomposites. Factors that affect the dielectric properties of epoxy nanocomposites such as surface treatment of nano particles and water absorption have also been studied. A commercial set of Bisphenol-A type epoxy resin is used in this study. Both nano particles with and without surface treatment have been used. The results show that the interface region between nano particle and polymer materials seems to be a key factor in determining the dielectric properties of epoxy nanocomposites in this project.

The permittivity for both epoxy-SiO_2/Al_2O_3 nanocomposites decreases at lower concentration (less than 1%). The relative permittivity of nanocomposites appears to have a minimum value with a threshold filler concentration (1wt% for nano SiO_2 and 0.5wt% for nano Al_2O_3). When the filler content is above the threshold value, the permittivity of nanocomposites begins to increase with filler concentration. The epoxy-Al_2O_3 nanocomposite has a higher permittivity than epoxy-SiO_2 nanocomposites as the Al_2O_3 particles have a higher inherent permittivity. Moreover, the increase in filler size will lead to a larger permittivity as well. The variation of dielectric permittivity is mainly due to the presence of large specific surface area of the nano particles. The interfacial region tends to restrict the chain mobility and therefore result in a reduction in permittivity. The glass transition temperature of epoxy nanocomposites at low filler loading concentrations also shows that the chain mobility has been restricted.

The presence of interfacial region around nano filler could overlap with each other and act as a conductive path to allow charge carriers travel through the bulk of nanocomposites much easier, especially at higher filler loading concentration. As a result, high conductivity and fast neutralisation has been

obtained and charge injection inside the sample has been reduced. Moreover, the presence of nano particles seems to enhance the ionization process inside the sample, especially with higher filler concentrations (large than 1wt %). The isolated interface region could also act as traps. The filler type also has an effect on space charge accumulations. It can also be observed that higher content of nano size filler (5wt% for SiO_2) will lead to more complicated charge accumulation. The large interfacial area of epoxy nanocomposites also results in a reduction in the breakdown strength of epoxy resin nanocomposites. Moreover, there is a significant reduction in the shape parameter (β) as well. This unexpected result can be attributed to a number of factors.

The effect of surface functionalization on nano size fillers by using silane as a coupling agent has also been tested and the result shows that the surface treatment of nano fillers does not have significant effects on the result composites' dielectric permittivity. The loss tan delta value of epoxy nanocomposites is slightly smaller than the one without surface treatment in lower frequency range (less than 100 Hz). However, both epoxy nanocomposites have similar loss tangent performance above 100 Hz. The breakdown strength of epoxy nanocomposites loaded with surface treated nano fillers, on the other hand, have high breakdown strength and consistence compare with the non-surface treated ones. Moreover, the epoxy nanocomposites loaded with surface treated nano fillers show slightly higher T_g when the loading concentration is high.

The influence of water on the glass transition temperature, dielectric behaviours and AC breakdown has also been investigated. The results of both dielectric spectroscopy and DSC measurements show that the hydration bonded formed between water molecular and nano particles. The presence of those hydration bound leads to the reduction in both dielectric permittivity and glass transition temperature. An extremely large reduction in breakdown strength is observed with saturated epoxy nanocomposite samples. It is believed that the reduction is due to the hydration water in the epoxy resin helps the charges to conduct across the sample and leads to early breakdown.

9.2 Further Work

Further researches may be required in but not limited to the following areas:

9.2.1 Sample Preparation Techniques

The manufacture processes of epoxy nanocomposites are the most important part in the investigation as the dispersion rate are one of the key factors that determining the overall insulating performance of the result nanocomposites. In this study, even the surface functionalised nano particles still have a possibility to agglomerate with nearby particles, especially at higher filler loading concentration. The dispersion of nano size filler is the key factor that affects the dielectric properties of resulting epoxy nanocomposites. In order to achieve better insulating performance, it is necessary to develop better sample preparation technical with uniform particle dispersion. At the current stage, it seems that it is not able to avoid nano particle agglomerations when preparing epoxy nanocomposites by using solution blending methods via mechanical mixture and ultrasonic wave, especially at higher filler loading concentration. So it is a good idea to try preparing nano particles directly inside the epoxy using sol-gel methods.

9.2.2 Characterisation of Interface

The experiment results that the interfacial region between epoxy and nano particles seems to have a significant effect on the overall performance of the epoxy nanocomposites. However, the commonly used microscopy techniques (SEM and TEM) are not able to provide enough information about the sample surface and interface. It is a good idea to use the Atomic force microscopy (AFM) for further analyse as it is able to provide three-dimensional surface profile with higher resolution than SEM.

9.2.3 Comprehensive Study on Other Insulating Materials and Nano Particles

The research in this project is focused on the epoxy resin sample only. It is valuable to do some comprehensive study using other material samples such as LDPE and XLPE. Moreover, as the epoxy microcomposites are widely used in

industrial applications nowadays due to their excellent mechanical properties, it is also useful to look at the insulating performance of epoxy loaded with both micro size fillers and nano size fillers.

9.2.4 Long Term Ageing Test

Although ageing testing on composites has already been studied widely, it is still better to do some ageing test on the current samples. The ageing measurement results under various conditions could give a better understanding of the aging theory. As the interfacial characteristic between epoxy and nano particles are the key factor in determining the dielectric properties of polymer nanocomposites, it is also helpful to observe interface degradation to give a better understanding of the ageing behaviour of polymer nanocomposites.

9.2.5 Mechanism and Modeling Work

The conduction mechanism in polymer nanocomposites is still not clear. Although there are several models can be used to describe the interface characteristic of the interfacial region between epoxy and nano particles and the conduction phenomenon, but none of the model could give a precise prediction in all the measurement results. Therefore it is necessary to work further on the polymer nanocomposites model and mechanism. Moreover, it is also necessary to start doing some simulation work based on the current experiment results, which will give a better understanding about epoxy nanocomposites.

Appendix A
SEM Data Analyses

	Particle diameter (nm)		
	Set 1	Set 2	Set 3
Particle 1	37	72	170
Particle 2	65	60	70
Particle 3	78	64	140
Particle 4	38	83	88
Particle 5	46	65	126
Particle 6	284	94	63
Particle 7	86	376	161
Particle 8	62	74	73
Particle 9	43	36	460
Particle 10	371	58	85
Particle 11	73	46	80
Particle 12	84	93	57
Particle 13	42	135	65
Particle 14	90	86	77
Particle 15	127	113	68
Particle 16	66	62	58
Particle 17	138	82	194
Particle 18	54	44	235
Particle 19	70	93	84
Particle 20	47	286	45
Particle 21	86	40	321
Particle 22	176	85	62
Particle 23	94	73	90
Particle 24	122	108	95
Particle 25	57	58	104
Particle 26	73	211	129
Particle 27	70	68	80
Particle 28	243	43	70
Particle 29	74	85	66
Particle 30	68	74	83
Average diameter	98.8	95.5	116.6
Standard deviation	75.3	72.0	87.4

Table 26: Average diameter and standard deviation of epoxy nanocomposites loaded with surface-treated nano fillers

	Particle diameter (nm)	
	Set 1	Set 2
Particle 1	472	704
Particle 2	210	375
Particle 3	92	586
Particle 4	186	109
Particle 5	263	84
Particle 6	302	183
Particle 7	72	107
Particle 8	91	241
Particle 9	636	153
Particle 10	147	324
Particle 11	84	516
Particle 12	112	67
Particle 13	174	102
Particle 14	78	83
Particle 15	63	126
Particle 16	85	125
Particle 17	153	75
Particle 18	98	209
Particle 19	142	184
Particle 20	463	62
Particle 21	157	290
Particle 22	88	426
Particle 23	102	283
Particle 24	80	127
Particle 25	163	142
Particle 26	144	75
Particle 27	103	94
Particle 28	372	208
Particle 29	518	173
Particle 30	284	95
Average diameter	197.8	213.6
Standard deviation	148.9	163.6

Table 27: Average diameter and standard deviation of epoxy nanocomposites loaded with non-treated nano fillers

Bibliography

[1] J. Hedrick, I. Yilgor, G. Wilkes and J. McGrath, "Toughening of Epoxy Resins with Ductile Glassy Thermoplastics. I. Hydroxyl Functional Polysulfones," *Polymer Bulletin,* vol. 13, pp. 201-208, 1985.

[2] C. Gao, "Effects of Nanometer Material and Their Application," *Journal of Jiangsu University of Science and Technology,* vol. 22, no. 06, pp. 63-70, 2001.

[3] C. Cheng, "Nanostructured material's special effects and its applications," *Journal of Anhui Institute of Architecture,* no. 04, pp. 43-47, 2005.

[4] T. Lewis, "Interfaces are the dominant feature of dielectrics at the nanometric level," *IEEE Journals & Magazines* , vol. 11, pp. 739 - 753 , 2004.

[5] J. Nelson, "Role of the interface in determining the dielectric properties of nanocomposites," *Annual Report Conference on Electrical Insulation and Dielectric Phenomena,* pp. 314 - 317, 2004.

[6] C. Zhang, "The Dielectric Behaviour of the Interface in Polymer Nanocomposites," *IEEE International Conference on Solid Dielectrics,* pp. 423 - 427, 2007.

[7] G. Tesoro, Epoxy Resins: Chemistry and Technology (Second ed.), New York: Marcel Dekker Inc., 1987.

[8] Z. Yu, "Application of Natural Powder Quartz in Epoxy Encapsulation Materials," *Non-Metallic Mines,* vol. 25, pp. 42-48, 2002.

[9] S. Chun and M. Lee, "Mulifunctional naphthalene containing epoxy resins and their modification by hydrosilation for electronic application[J]," *Polymer Bulletion,* vol. 40, pp. 623-630, 1998.

[10] T. Mochi, "Phase structure and thermomechanical properties of primary and tertiatry amine-cured epoxy/silica hybrids[J]," *Journal of Polymer Science：Part B：Polymer Physics,* vol. 39, pp. 1071-1084, 2001.

[11] M. Okazaki, M. Murota and Y. Kawaguchi, "Curing of epoxy resin by ultrafine silica modified by grafting of hyperbranched polyamidoamine using dendrimer synthesis methodology [J]," *Journal of Applied Polymer Science,* vol. 80, pp. 573-579, 2001.

[12] R. Roy and S. Komarneni, "Multi-Phasic Ceramic Composites made by Sol-Gel Technique," in *MRS Spring Meeting.*, 1984.

[13] P. Ajayan, L. Schadler and P. Braun, Nanocomposite science and technology, Wiley-VCH, 2003.

[14] T. Tanaka, "Dielectric Nanocomposites with Insulating Properties," *IEEE Transactions on Dielectrics and Electrical Insulation,* vol. 12, pp. 914-928 , 2005.

[15] S. Singha and M. Thomas, "Dielectric Properties of Epoxy

Nanocomposites," *IEEE Transactions on Dielectrics and Electrical Insulation,* vol. 15, pp. 416-428, 2008.

[16] K. Klabunde, Nanoscale Materials in Chemistry, John Wiley & Sons, 2001.

[17] C. Gurumurthy and C. Hui, "Controlling interfacial interpenetration and fracture properties of polyimide/epoxy interfaces," *Journal of Adhesion,* vol. 82, pp. 239-266, 2006.

[18] P. Maity, S. Kasisomayajula, V. Parameswaran and N. Basu, "improvement in surface degradation properties of polymer composites due to pre-processed nanometric alumina fillers," *Dielectrics and Electrical Insulation, IEEE Transactions on,* vol. 15, pp. 63-72, 2008.

[19] X. Huang, Y. Zheng, P. Jiang and Y. Yin, "Influence of nanoparticle surface treatment on the electrical properties of cycloaliphatic epoxy nanocomposites," *Dielectrics and Electrical Insulation, IEEE Transactions on,* vol. 17, pp. 635-643, 2010.

[20] Y. Sun, Z. Zhang and C. Wong, "Fundamental research on surface modification of nano-size silica for underfill applications," *Advanced Packaging Materials: Processes, Properties and Interfaces, 2004. Proceedings. 9th International Symposium on,* pp. 132-138, 2004.

[21] T. Tanaka, M. Kozako, N. Fuse and Y. Ohki, "Proposal of a multi-core model for polymer nanocomposite dielectrics," *Dielectrics and Electrical Insulation, IEEE Transactions on,* vol. 12, pp. 669-681, 2005.

[22] M. Kozako, S. Kuge, T. Imai, T. Ozaki, T. Shimizu and T. Tanaka, "Surface erosion due to partial discharges on several kinds of epoxy," *Electrical Insulation and Dielectric Phenomena, 2005. CEIDP '05. 2005 Annual Report Conference on,* pp. 162-165, 2005.

[23] M. I. Baraton, F. Chancel and L. Merhari, "In-situ deter mination of grafting on nanosized ceramic," *Nanostruct Mater,* p. 319–322, 1997.

[24] J. Fothergill, "Ageing, space charge and nanodielectrics: ten things we don't know about dielectrics," *IEEE International Conference on Solid Dielectrics,* pp. 1-10, 2007.

[25] G. Tsagaropoulos and A. Eisenberg, "Dynamic mechanical study of the factors affecting the two glass transition behavior of filled polymers. Similarities and differences with random ionomers," *Macromolecules,* vol. 28, p. 6067–6077, 1995.

[26] F. Starr1, T. Schrøder1 and S. Glotz, "Effects of a nanoscopic," *Phys. Rev.,* vol. 64, pp. 113-124, 2001.

[27] A. Volkov and A. Prokhorov, "Broadband Dielectric Spectroscopy of Solids," *Radiophysics and Quantum Electronics,* vol. 46, p. 657–665, 2003.

[28] F. Kremer, A. Schonhals and W. Luck, Broadband Dielectric Spectroscopy, Springer-Verlag, 2002.

[29] M. Reading, An investigation into the structure and properties of polyethylene oxide nanocomposites, Phd thesis, 2010.

[30] L. Ying, M. Yasuda and T. Takada, "Pulsed electroacoustic method for measurement of charge accumulation in solid dielectrics," *Dielectrics and Electrical Insulation, IEEE Transactions on,* vol. 1, pp. 188-195,

1994.

[31] P. Salovaara and K. Kannus, “Increasing the dielectric breakdown strength of polypropylene using polyaniline additive,” *Energy and Power System,* pp. 127-135, 2006.

[32] W. Weibull, “A statistical distribution function of wide applicability,” *Journal of Applied Mechanics,* vol. 18, pp. 293-297, 1951.

[33] H. Pham and C. Lai, “On recent generalizations of the weibull distribution,” *Reliability, IEEE Transactions on,* vol. 56, pp. 454-458, 2007.

[34] L. Dissado and J. Fothergill, Electrical degradation and breakdown in polymers, Peter Peregrinus, 1992, pp. 601-607.

[35] ReliaSoft, Life data analysis reference, 2005.

[36] R. Abernethy, The new Weibull handbook, 2004.

[37] D. Cox and D. Hinkley, Theoretical Statistics, Chapman & Hall, 1974.

[38] L. Bao, F. Yee and Y. Lee, “Moisture absorption and hygrothermal aging in a bismaleimide resin,” *Polymer,* vol. 17, pp. 7327-7333, 2001.

[39] P. Bonniau and A. Bunsell, “A comparative study of water absorption theories applied to glass epoxy composites,” *Journal of Composite Materials,* vol. 15, pp. 273-293, 1981.

[40] G. Xiao and M. Shanahan, “Water absorption and desorption in an epoxy resin with degradation,” *Journal of Polymer Science Part B: Polymer Physics,* vol. 35, pp. 2659-2670, 1997.

[41] A. Kinloch, M. Little and J. Watts, “The role of interphase in the environmental failure of adhesive joints,” *Acta Mater,* vol. 48, pp. 4543-4553, 2000.

[42] A. Kinloch, Durability of structural adhesives, Applied Science, 1983.

[43] R. Oiml, The scale of relative humidity of air certified against saturated salt solution, 1996.

[44] M. Knoll, “ufladepotentiel und Sekundäremission elektronenbestrahlter Körper,” *Zeitschrift für technische Physi,* vol. 16, pp. 467-475, 1935.

[45] J. Fried, Polymer science and technology, London: Prentice-Hall International Editions, 1995.

[46] User Handbook, Information for user of METTLER TOLLDO thermal analysis system, 1997.

[47] B. Wunderlich, Thermal Analysis, New York: Academic Press, 1990.

[48] C. Goupil and P. Norman, The use of Differential Scanning Calorimetry(DSC) in the prediction of metal composition and polymer characterisation, 1996.

[49] J. McNaughton and C. Mortimer, Differential scanning calorimetry, Norwalk: Perkin-Elmer Corporation.

[50] M. Liška and J. Antalík, “Enthalpy relaxation in glasses: regression analysis of integral DSC data,” *Journal of Thermal Analysis and Calorimetry*, vol. 67, pp. 213-222, 2004.

[51] W. Starr, T. Schrøder and S. Glotzer, “Effects of a nanoscopic filler on the structure and dynamics of a simulated polymer melt and the

relationship to ultrathin films," *Phys. Rev. E,* vol. 64, p. 1802–1805, 2001.

[52] A. Mayes, "Softer at the boundary," *Nature Materials,* vol. 4, pp. 651-652, 2005.

[53] T. Lewis, "Interfaces and nanodielectrics are synonymous," *Solid Dielectrics, 2004. Proceedings of the 2004 IEEE International Conference on,* vol. 2, pp. 792-795, 2004.

[54] J. Nelson and Y. Hu, "The impact of nanocomposite formulations on electrical voltage endurance," *Solid Dielectrics, Proceedings of the 2004 IEEE International Conference on,* vol. 2, pp. 832-835, 2004.

[55] B. Ash, L. Schadle and R. Siegel, "Glass transition behavior of Alumina/polymethylmethacrylate nanocomposites," *Materials Letters,* vol. 55, pp. 83-87, 2002.

[56] "Dielectric behavior at microwave frequencies of an epoxy resin during crosslinking," *Journsl of Applied Polymer Science,* vol. 1, pp. 1583-1900, 1993.

[57] A. Jonscher, Dielectric relaxation in solids, Chelsea Dielectric Press, 1983.

[58] L. Dissado and R. Hill, "Non-Exponential decay in Dielectrics and Dynamics of Correlated Systems," *Nature,* no. 279, pp. 685-689, 1979.

[59] L. Dissado and R. Hill, "A new approach to the structure of imperfect materials and their relaxation spectroscopy," in *Proceedings of the Royal Society*, London, 1983.

[60] L. Dissado and R. Hill, "Anomalous low -frequency dispersion," *J. chemical Society, Faraday Transactions,* vol. 80, pp. 291-319, 1984.

[61] L. Dissado and R. Hill, "Invariant behaviour for the response of simple fractal circuits," *J. Physics :Condense Matter,* vol. 3, pp. 9773-9790, 1991.

[62] Q. Craig, Dielectric analysis of pharmaceutical systems, Taylor & Francis, 1995.

[63] M. Frechette, M. Trudeau, H. Alamdari and S. Boily, "Introductory remarks on nanodielectrics," *IEEE Transactions on Dielectric and Electrical Insulation,* vol. 11, no. 5, 2004.

[64] J. Marinez, M. Boulouz, C. Mayoux and C. Lacabanne, "Thermally stimulated creep for the study of ageing insulating polymers under electrical field," *IEEE International Symposium on Electrical Insulation,* p. 62–65, 1992.

[65] F. Schönhals, Broadband Dielectric Spectroscopy, Springer, 2003.

[66] A. Harrop, Dielectrics, London Butteworths, 1972.

[67] P. Debye, Polar molecules, London: The Chemical Catalog Co. Dover Publications, 1945.

[68] K. Cole and R. Cole, "Dispersion and adsorption in dielectrics," *J. Chem. Rev.,* vol. 9, p. 341–352, 1941.

[69] D. Davidson and R. Cole, "ielectric relaxation in Glycerol, Propylene Glycol, and n-Propanol," *J. Chem. Phys.,* vol. 19, p. 1484–1490, 1951.

[70] C. Brosseau, P. Queffelec and P. Talbot, "Microwave characterization of

filled polymers," *J. Appl. Phys.,* vol. 89, pp. 4532-4540, 2001.

[71] J. Nelson and Y. Hu, "The impact of nanocomposite formulations on electrical voltage endurance," *ICSD,* pp. 832-835, 2004.

[72] S. Singha, "Reduction of permittivity in epoxy nanocomposites at low nano-filler loadings," *Electrical Insulation and Dielectric Phenomena, Annual Report Conference on,* pp. 726-729, 2008.

[73] S. Singha and M. Thomas, "Permittivity and tan delta characteristics of epoxy nanocomposites in the frequency range of 1 MHz-1 GHz," *EEE Transactions on Dielectrics and Electrical Insulation,* vol. 15, pp. 2-11, 2008.

[74] J. Eloundou, "Dipolar relaxations in an epoxy–amine system," *European Polymer J.,* vol. 38, pp. 431-438, 2002.

[75] L. Zhang, H. Zhang, G. Wang, C. Mo and Y. Zhang, "Dielectric behavior of nano-TiO2 bulks," *Phys. Stat. Sol.,* vol. 157, pp. 483-491, 1996.

[76] J. Nelson and J. Fothergill, "Internal charge behavior of nanocomposites," *Nanotechnology,* vol. 15, pp. 586-595, 2004.

[77] J. Eloundou, "Dipolar relaxations in an epoxy–amine system," *European Polymer J.,* vol. 38, pp. 431-438, 2002.

[78] J. Santos, D. Garcia and J. Eiras, "Dielectric characterization ofmaterials at microwave frequency range," *Materials Research,* vol. 6, pp. 97-101, 2002.

[79] H. Shi, N. Gao, H. Jin, G. Zhang and Z. Peng, "Investigation of the effects of nano-filler on dielectric properties of epoxy based composites," *Properties and Applications of Dielectric Materials, IEEE 9th International Conference on the,* pp. 804-807, 2009.

[80] T. Imai, F. Sawa, T. Ozaki, Y. Inoue, T. Shimizu and T. Tanaka, "Comparison of insulation breakdown properties of epoxy nanocomposites under homogeneous and divergent electric fields," *IEEE Conf. Electr. Insul. Dielectr. Phenomena,* pp. 306-309, 2006.

[81] V. Hippel, "Electric Breakdown of Solid and Liquid Insulators‖," *J. Appl. Phys.,* vol. 8, pp. 815-832, 1937.

[82] V. Hippel, "Der mechanismus des elektrischen durchschlages in festen isolatoren‖," *Zeitschrift fur Physik,* vol. 67, pp. 707-724, 1931.

[83] V. Hippel, "Elektrische festigkeit und kristallbau‖," *Zeitschrift fur Physik,* vol. 75, pp. 145-170, 1932.

[84] E. Forster, "Research in the dynamics of electrical breakdown in liquid dielectrics," *IEEE Trans. Elec. Insul.,* Vols. E1-15, pp. 182-185, 1980.

[85] A. Sharbaugh, J. Devins and S. Rzad, "Review of past work on liquid breakdown," *IEEE Trans. Elec. Insul.,* Vols. E1-15(3), pp. 167-170, 1980.

[86] P. Watson and A. Sharbaugh, "High-field conduction currents in liquid n-hexane under microsecond pulse conditions," *J. Electrochem. Soc.,* vol. 107, pp. 516-521, 1960.

[87] M. Nagao, T. Kimura, Y. Mizuno, M. Kosaki and M. Ieda, "Detection of joule heating before dielectric breakdown in polyethylene films," *IEEE Trans. Elec. Insul.,* vol. 25, pp. 715-722, 1990.

[88] M. Hikita, S. Tajima, I. Kanno, G. Sawa and M. Ieda, “New approach to breakdown study by measuring pre-breakdown current in insulating materials,” *J. Appl. Phys.*, vol. 23, pp. 886-888, 1984.

[89] M. Hikita, M. Nagao, G. Sawa and M. Ieda, “Dielectric breakdown and electrical conduction of poly(vinylidene-fluoride) in high temperature region,” *J. Phys.*, vol. 13, pp. 661-666, 1980.

[90] R. Buehl and V. Hippel, “The electrical breakdown strength of ionic crystals as a function of temperature,” *Physical Review*, vol. 56, pp. 941-947, 1939.

[91] Y. Hu, R. Smith, J. Nelson and L. Schadler, “Some mechanistic understanding of the impulse strength of nanocomposites,” *IEEE Conf. Electr. Insul. Dielectr. Phenomena*, pp. 31-34, 2006.

[92] T. Tanaka, “Interpretation of several key phenomena peculiar to nano dielectrics in terms of a multi-core model,” *Electrical Insulation and Dielectric Phenomena, IEEE Conference on*, pp. 298-301, 2006.

[93] M. Ieda, “Electrical conduction and carrier traps in polymeric materials,” *IEEE Trans. E. I.*, Vols. EI-19, pp. 162-178, 1984.

[94] T. Lewis, “The micro-physics of charge in solid dielectrics,” in *Space Charge in Solid Dielectrics*, 1998.

[95] K. Kojima, Y. Takai and M. Ieda, “Electronic conduction in polyethylene naphthalate at high electric fields,” *J. Appl. Phys.*, vol. 59, pp. 2655-2659, 1986.

[96] T. Lewis, “Electrical effect at interfaces and surfaces,” *IEEE Transactions on Electrical Insulation.*, Vols. EI-21(3), pp. 289-295, 1986.

[97] C. Mayoux, “Aging of polymeric materials in power cables,” *IEEE Trans. Diel. E. I.*, vol. 4, pp. 665-673, 1997.

[98] A. Blythe and D. Bloor, Electrical properties of polymers, Cambridge University Press, 2005.

[99] F. Zakopoulos, “A report on the modelling of space charge dynamics,” University of Southampton, 2002.

[100] J. Fothergill and L. Dissado, “Space Charge in Solid Dielectrics,” The Dielectrics Society, 1998.

[101] Q. Craig, “Dielectric analysis of pharmaceutical systems,” Taylor & Francis, 1995.

[102] T. Mizutani, H. Semi and K. Kaneko, “Space charge behaviour in low-density polyethylene,” *IEEE Transactions on Dielectrics and Electrical Insulation*, vol. 7, no. 4, p. 503–508, 2000.

[103] T. Lewis, “Charge transporte in polymers,” *IEEE Proc. Electr. Insul. And Diel.*, p. 533–561, 1976.

[104] T. Mizutani, “Space charge measurement techniques and space charge in polyethylene,” *IEEE Trans. DEI*, vol. 1, p. 923–933, 1994.

[105] S. Boggs, “A rational consideration of space charge,” *DEIS*, vol. 20, no. 4, 2004.

[106] D. Fabiani, G. Montanari, A. Dardano, G. Guastavino, L. Testa and M. Sangermano, “Space charge dynamics in nanostructured epoxy resin,”

Electrical Insulation and Dielectric Phenomena, Annual Report Conference on, pp. 710-713, 2008.

[107] G. Montanari, D. Faviani, F. Palmieri, D. Kaempfer, R. Thomann and R. Mülhaupt, "Modification of electrical propertiesand performance of EVA and PP insulation throughNanostructure by organophilic silicates," *IEEE Trans. Dielectr. Electr. Insul.,* vol. 11, pp. 754-762, 2004.

[108] L. Fothergill, J. Nelson and M. Fu, "Dielectric properties of epoxy nanocomposites containing TiO2, Al2O3 and ZnO fillers," *Electrical Insulation and Dielectric Phenomena, Annual Report Conference on,* pp. 406- 409, 2004.

[109] G. Chen, C. Zhang and G. Stevens, "Space charge in LLDPE loaded with nanoparticles," *Electrical Insulation and Dielectric Phenomena, Annual Report - Conference on,* pp. 275-278, 2007.

[110] M. Roy, J. Nelson, R. MacCrone and L. Schadler, "Candidate mechanisms controlling the electrical characteristics of silica/XLPE nanodielectrics," *J. Mater. Sci.,* vol. 42, pp. 3789-3799, 2007.

[111] P. Preetha and M. Thomas, "AC breakdown characteristics of epoxy nanocomposites," *Dielectrics and Electrical Insulation, IEEE Transactions on,* vol. 18, no. 5, pp. 1526-1534, 2011.

[112] C. Zhou, M. Fu, J. Fothergill and S. Rowe, "Influence of absorbed water on the dielectric properties and glass-transition temperature of silica-filled epoxy nanocomposites," *Electrical Insulation and Dielectric Phenomena, IEEE Conference on,* pp. 321-324, 2006.

[113] A. Buchman and R. Bryant, "Molded carbon–carbon composites based on microcomposite technology," *Applied Composite Materials,* vol. 6, p. 309–326, 1999.

[114] R. Hill and L. Dissado, "The temperature dependence of relaxation processes," *J. Phys. C: Solid State Phys.,* vol. 15, p. 5171–5193, 1982.

[115] I. Maxwell and R. Pethrick, "Dielectric studies of water in epoxy resins," *Journal of Applied Polymer Science,* vol. 28, p. 2363, 1983.

[116] R. Cooke and I. Kuntz, "roperties of water in biological-systems," *Annu. Rev. Biophys. Bioeng.,* vol. 4, p. 95–126, 1974.

[117] L. Jelinski, J. Dunmais, A. Cholli, T. Ellis and F. Karasz, "Nature of the water-epoxy interaction," *Macromolecules,* vol. 18, p. 1091–1095, 1985.

[118] T. Lizuka, H. TaKai, K. Fukimaga and T. Maeno, "Measurement of space charge distribution in epoxy resin after aater absorption treatment," *IEEE CEIDP,* pp. 41-44, 1997.

[119] Application Note 1217-1, "Basics of measuring the dielectric properties of materials," *Hewlett Packard literature number 5091-3300E,* 1992

[120] Gallot-Lavall ée, O., & Teyssedre, G. (2005). The pulsed electro-acoustic technique in research on dielectrics for electri engineering. *RS - RIGE , 8*, 749-772.

[121] Sibond Inc. (2003). Silane Coupling Agents. China.